

**EFFECT OF ULTRAVIOLET EXPOSURE ON THE
DURABILITY OF POLYCARBONATE**

by

Stephen B. Clay

Thesis submitted to the Faculty of the
Virginia Polytechnic Institute and State University
in partial fulfillment of the requirements for the degree of

Master of Science

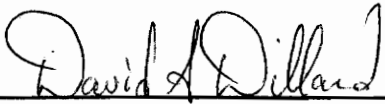
in

Engineering Mechanics

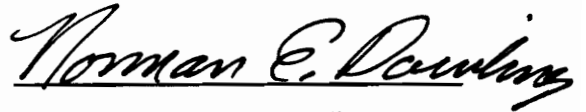
APPROVED:



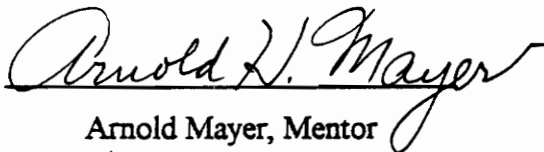
Robert A. Heller, Chairman



David A. Dillard



Norman E. Dowling



Arnold Mayer, Mentor

August 1995

Blacksburg, Virginia

C.2

LD
5655
V855
1995
C539
C.2

Effect of Ultraviolet Exposure on the Durability
of Polycarbonate

by

Stephen B. Clay
Dr. Robert A. Heller, Chairman
Engineering Mechanics

ABSTRACT

Polycarbonate is commonly used in windshield-canopy structures for military aircraft since it is transparent and possesses excellent toughness characteristics at temperatures well below its glass transition region. It is believed that ultraviolet radiation present in sunlight causes polycarbonate to degrade. This is a serious problem since the majority of the military aircraft in the United States spend their entire service lives outdoors.

This study was conducted in connection with the United States Air Force to analyze the photodegradation of polycarbonate caused by ultraviolet radiation. First, aircraft grade polycarbonate plates were exposed to continuous ultraviolet light in a QUV laboratory weathering chamber for durations of three, seven, ten, and twenty weeks. The material changes were then characterized by several mechanical, viscoelastic, and chemical experiments. The feasibility and sensitivity of each test method was determined, and the amount of polymer degradation was measured.

The results from uniaxial tension and dynamic mechanical (DMA) tests indicated a significant reduction in strength and ductility and an increase in stiffness. Polycarbonate also experienced a decrease in impact resistance of approximately 42% at intermediate exposure levels followed by a slight increase for the longest exposure durations. Micro-

indentation experiments showed about a 27% increase in hardness for surfaces directly exposed to ultraviolet light while the hardness of the surfaces indirectly exposed was insensitive to ultraviolet exposure. A 30% weight loss was also seen after only seven weeks of exposure.

A few conclusions were made about the causes of photodegradation along with recommendations for future work in the area of ultraviolet exposure of thermoplastic materials.

ACKNOWLEDGEMENTS

I would first like to thank Dr. Robert A. Heller, my faculty advisor, for his guidance and advice throughout this project. He has taught me more over the past two years than I could have possibly learned from books or classwork. He always had time to answer questions and give suggestions.

I would also like to thank Dr. David A. Dillard, Dr. Norman E. Dowling and Dr. Arnold Mayer for actively serving on my advisory committee. Dr. Arnold Mayer also served as my mentor in the United States Air Force.

A special thanks goes to Rick Smith for his patience and excellent technical support at Wright Lab in Dayton, Ohio. I am also grateful to Bob McCarty, Maj. Becky Wagner, Malcolm Kelley, and Ralph Speelman at Wright Patterson Air Force Base, Ohio. I would like to thank the Air Force Palace Knight program for all of the financial support and funding made available for this project.

I also appreciate the advice and answers from Dr. Tom C. Ward in the area of polymer chemistry.

I would like to thank the ESM machine shop as well as Bob Simonds in the mechanical testing laboratory for their technical support in specimen alterations, machine operations, and film developing.

Hari Parvatareddy and Jeff Paine are two colleagues that deserve thanks for instruction and advice in testing techniques and many other things.

I would also like to thank Amy Lentz in the chemistry department for conducting the GPC tests.

I am also thankful for Sophie Hon for helping when a deadline was fast approaching.

Finally, I would like to thank God, my family in West Virginia, and my wife Terry for the love and encouragement which they are always willing to share and for the sacrifices that had to be made during the past two years.

TABLE OF CONTENTS

CHAPTER 1 INTRODUCTION	1
CHAPTER 2 EXPOSURE OF POLYCARBONATE TO ULTRAVIOLET RADIATION	6
INTRODUCTION	6
Natural Versus Artificial Weathering	7
Artificial Weathering Chambers	8
EXPERIMENTAL DETAILS	11
CHAPTER 3 EFFECT OF ULTRAVIOLET EXPOSURE ON THE VISCOELASTIC MODULI AND THE GLASS TRANSITION TEMPERATURE OF POLYCARBONATE	24
INTRODUCTION	24
Dynamic Mechanical Analysis	24
Dynamic Mechanical Analyzer	27
Glass Transition Temperature	29
EXPERIMENTAL DETAILS	30
RESULTS AND DISCUSSION	32
CHAPTER 4 EFFECT OF ULTRAVIOLET EXPOSURE ON THE STRENGTH AND DUCTILITY OF POLYCARBONATE	46
INTRODUCTION	46
Strength	46
Ductility	47

Surface Effects	48
EXPERIMENTAL DETAILS	49
RESULTS AND DISCUSSION	50
Strength and Stiffness	50
Ductility	52
CHAPTER 5 EFFECT OF ULTRAVIOLET EXPOSURE ON THE MOLECULAR WEIGHT OF POLYCARBONATE	66
INTRODUCTION	66
Gel Permeation Chromatography	68
EXPERIMENTAL DETAILS	69
RESULTS AND DISCUSSION	69
CHAPTER 6 EFFECT OF ULTRAVIOLET EXPOSURE ON THE HARDNESS OF POLYCARBONATE	75
INTRODUCTION	75
Hardness Testing	75
EXPERIMENTAL DETAILS	77
RESULTS AND DISCUSSION	78
CHAPTER 7 EFFECT OF ULTRAVIOLET EXPOSURE ON THE IMPACT TOUGHNESS OF POLYCARBONATE	88
INTRODUCTION	88
Wave Propagation	90

Impact Failure	91
Impact Testing	92
EXPERIMENTAL DETAILS	92
RESULTS AND DISCUSSION	96
CHAPTER 8 CONCLUSIONS AND RECOMMENDATIONS	115
CONCLUSIONS	115
RECOMMENDATIONS FOR FUTURE WORK	116
VITA	118

LIST OF FIGURES

FIGURE 2.1 Photo-Fries rearrangement of polycarbonate	19
FIGURE 2.2 The Spectral Power Distribution (SPD) of the Four Types of Lamps for use in the QUV Weathering Device	20
FIGURE 2.3 The Spectral Power Distribution of the UVB-313 and the FS-40 Fluorescent Lamps Compared to Natural Sunlight	21
FIGURE 2.4 Overall View of the QUV Weathering Apparatus	22
FIGURE 2.5 Cross-Sectional View of the QUV Weathering Apparatus	23
FIGURE 3.1 Voigt and Maxwell elements	37
FIGURE 3.2 Simple dynamic relationships between stress and strain, illustrating the role of the phase angle	38
FIGURE 3.3 Dynamic mechanical analyzer mode of vibration	39
FIGURE 3.4 Glass transition temperature of polycarbonate versus weeks of exposure to ultraviolet radiation obtained from dynamic mechanical analysis at heating rates of 1°C per minute and 5°C per minute	40

FIGURE 3.5 Storage modulus, loss modulus, and loss tangent (at a frequency of 1 Hz) versus temperature for polycarbonate as recorded by the DuPont DMA 983 41

FIGURE 3.6 Log of storage modulus (at a frequency of 1 Hz) versus temperature for unexposed polycarbonate and polycarbonate exposed to ultraviolet radiation for ten and twenty weeks 42

FIGURE 3.7 Log of storage modulus (at a frequency of 1 Hz) of polycarbonate at a temperature of 35°C versus weeks of exposure to ultraviolet light 43

FIGURE 3.8 Log of loss modulus (at a frequency of 1 Hz) versus temperature for unexposed polycarbonate and polycarbonate exposed to ultraviolet radiation for ten and twenty weeks 44

FIGURE 3.9 Glass transition temperature of polycarbonate (at a heating rate of 1°C/min) versus weeks of ultraviolet exposure 45

FIGURE 4.1 Tension specimen geometry 56

FIGURE 4.2 Engineering tensile strength at yield versus weeks of ultraviolet exposure 57

FIGURE 4.3 True stress at fracture of polycarbonate tension specimens 58

FIGURE 4.4 Linear portion of engineering stress versus extensometer strain of unexposed polycarbonate for determination of Young’s modulus 59

FIGURE 4.5 Engineering stress-displacement diagrams for polycarbonate material exposed to ultraviolet radiation for 0, 3, 7, 10, and 20 weeks	60
FIGURE 4.6 Percent elongation of polycarbonate tension specimens versus weeks of ultraviolet exposure	61
FIGURE 4.7 Percent reduction of area of polycarbonate tension specimens versus weeks of ultraviolet exposure	62
FIGURE 4.8 Micrograph of surface of polycarbonate tension specimens after exposure periods of 3 weeks and 7 weeks	63
FIGURE 4.9 Micrograph of surface of polycarbonate tension specimens after exposure durations of 10 weeks and 20 weeks	64
FIGURE 4.10 Micrograph of edge of polycarbonate tension specimens after exposure durations of 10 and 20 weeks	65
FIGURE 5.1 Relative molecular weight averages of polycarbonate as determined by gel permeation chromatography for surfaces indirectly and directly exposed to ultraviolet radiation for durations of 0, 3, and 7 weeks	74
FIGURE 6.1 The Knoop microhardness diamond pyramidal indenter and the Knoop micro-indentation	84
FIGURE 6.2 Comparison of Knoop and Vickers indentations using 100 gram load on hard steel	85

FIGURE 6.3 TUKON microhardness tester set-up	86
FIGURE 6.4 Knoop hardness value (H_K) versus exposure time of the indirectly and directly exposed surfaces	87
FIGURE 7.1 Drop dart impact test two-piece specimen clamp and test specimen	103
FIGURE 7.2 Load and energy of polycarbonate during drop-weight impact testing versus time as recorded by the Dynatup 730 drop-weight impact tester	104
FIGURE 7.3 Mean failure energy versus exposure time	105
FIGURE 7.4 Maximum load of polycarbonate during impact contact versus weeks of exposure to ultraviolet radiation	106
FIGURE 7.5 Maximum deflection of polycarbonate during impact contact versus weeks of exposure to ultraviolet radiation	107
FIGURE 7.6 Contact load of polycarbonate with striker versus deflection during impact contact	108
FIGURE 7.7 Stress-strain diagram of unexposed polycarbonate	109
FIGURE 7.8 Stress-strain diagram of polycarbonate exposed to ultraviolet radiation for three weeks	110

FIGURE 7.9 Stress-strain diagram of polycarbonate exposed to ultraviolet radiation for seven weeks	111
FIGURE 7.10 Stress-strain diagram of polycarbonate exposed to ultraviolet radiation for ten weeks	112
FIGURE 7.11 Stress-strain diagram of polycarbonate exposed to ultraviolet radiation for twenty weeks	113
FIGURE 7.12 Mean fracture energy and calculated impact energy versus weeks of ultraviolet exposure	114

LIST OF TABLES

TABLE 2.1 Threshold UV Wavelengths for Breaking Various Bonds	17
TABLE 2.2 QUV Weathering Apparatus	18
TABLE 3.1 DuPont Instruments 983 Dynamic Mechanical Analyzer (DMA) . . .	36
TABLE 6.1 Tukon microhardness tester	82
TABLE 6.2 Knoop hardness values	83

CHAPTER 1

INTRODUCTION

Polycarbonate, $[C_6H_4C(CH_3)_2C_6H_4OCO_2]_n$ [1], is a transparent, high toughness thermoplastic which makes it an excellent material for aircraft transparencies, visors, vandal-resistant glazing, riot shields, and street lamp diffusers [2, 3]. The presence of the carbonate group in the chemical structure could be one reason for the excellent toughness characteristics well below the glass transition temperature of polycarbonate [4].

This study is being conducted in connection with the United States Air Force and will therefore concentrate on the problems associated with present day military aircraft windshield-canopy structures. One of the major problems that exists is low service life which is usually determined by surface scratches or crazes that impair the vision of the pilot [5]. Another problem that arises during the service of the transparency is birdstrike. The most important mechanical property during birdstrike is impact resistance. Both the surface characteristics and the impact resistance of the transparency are altered during outdoor exposure to weathering elements. The focus of this paper is to study the effect that ultraviolet light has on the durability of the military aircraft transparency.

Polycarbonate, like many other polymers, experiences degradation due to the weathering elements in the environment which include sunlight, high temperature, moisture, wind, dust, and pollutants [2, 6]. The weathering process is due to a combination of exposure to the above elements as well as other destructive factors which may be present. The overall effects of weathering is evident when comparing the average transparency lifetime in the United States to the average lifetime in Europe. In the United States, military aircraft are kept in an outdoor environment year round, and the average service life of a windshield-canopy structure is two years. In Europe, military aircraft are kept in hangars when not in flight and sometimes reach a service life of up to ten years [5].

In most of the weathering studies the researchers attempt to look at one or two elements of the environment separately to see how each one affects the properties of the polymer. Many studies have been conducted in which a polymer is exposed to high temperature to increase the rate of physical aging [7-9]. Physical aging decreases the amount of free volume available to the polymer material system which causes degradation to the mechanical properties of the material [10].

Other studies have attributed polymer degradation to the temperature gradient across the thickness of a polymeric article. Compressive residual stresses are present near the wall of an injection molded specimen due to the faster cooling rate caused by exposure to the lower temperature of the wall of the mold. These compressive stresses generally give the material a higher toughness since cracks are less likely to grow in these areas. It has been shown that a high temperature gradient across the thickness of an injection molded specimen causes the compressive residual stresses to decrease and in some cases become tensile which promotes crack growth and drastically reduces the toughness of the material [11-13].

It has also been shown that the presence of moisture in the material causes the mechanical properties of a polymer to degrade. This degradation has been attributed to a reduction in the residual stresses induced by the injection molding process and to the development of disc-shaped flaws in the material which can be as large as two millimeters in diameter [13].

To thoroughly investigate the mechanisms of degradation that occur during outdoor weathering all of the above mentioned elements should be considered. However, the remainder of this paper will concentrate only on the changes in the mechanical properties of polycarbonate caused by photodegradation due to exposure to ultraviolet light. A series of mechanical and dynamic tests were performed to evaluate the amounts of degradation that occurred at various levels of exposure.

Chapter 2 is entitled Exposure of Polycarbonate to Ultraviolet Radiation and describes how the ultraviolet portion of sunlight chemically affects the polymer chain.

Accelerated artificial weathering in the laboratory is compared to natural weathering in an outdoor environment, and the mode of exposure to ultraviolet radiation of the polycarbonate coupons is described.

Chapter 3 is entitled Effect of Ultraviolet Exposure on the Viscoelastic Moduli and the Glass Transition Temperature of Polycarbonate and discusses some viscoelastic properties of polymers and describes how these properties can be obtained with the use of dynamic mechanical testing. The details of the dynamic mechanical analyzer are also described along with the results obtained from fixed frequency tests in the Dupont 983 Dynamic Mechanical Analyzer.

Chapter 4 is entitled Effect of Ultraviolet Exposure on the Strength and Ductility of Polycarbonate. The theory and results of uniaxial tension testing are discussed. The true stress is considered the measure of strength while percent elongation and percent reduction of area are used to quantify the ductility.

Chapter 5 is entitled Effect of Ultraviolet Exposure on The Molecular Weight of Polycarbonate. The changes in the molecular weight of polycarbonate after exposure to ultraviolet light are discussed and analyzed. Also the theory and description of molecular weight by gel permeation chromatography (GPC) are given.

Chapter 6 is entitled Effect of Ultraviolet Exposure on the Hardness of Polycarbonate. The hardness of the material was determined by the Knoop microindentation technique and the changes in hardness caused by exposure to ultraviolet radiation is discussed. Also the theory and description of the microhardness test is given.

Chapter 7 is entitled Effect of Ultraviolet Exposure on the Toughness of Polycarbonate. The toughness of the material was characterized by the impact toughness obtained by drop dart impact tests. Impact theory and the description of the test set-up are given along with the test results.

Chapter 8 is entitled Conclusions and Recommendations and summarizes the conclusions drawn from the results of this study and gives recommendations for future work in the area of ultraviolet exposure of thermoplastic materials.

REFERENCES

1. R. E. Wetton, "Dynamic Mechanical Thermal Analysis of Polymers and Related Systems", *Developments in Polymer Characterisation - 5*, J. V. Dawkins, ed., Elsevier Applied Science Publishers, London, 1986
2. A. Davis and D. Sims, *Weathering of Polymers*, Applied Science Publishers, London, 1983.
3. J. M. Margolis, *Engineering Thermoplastics: Properties and Applications*, Marcel Dekker, Inc. NY, 1985
4. D. R. Askeland, *The Science and Engineering of Materials*, PWS-KENT Publishing Co., Boston, p.805, 1989
5. M. Kelly, *Private Communication*, 1995
6. R. P. Brown, *Handbook of Plastics Test Methods*, George Godwin Limited, London, 1981.
7. T. Ricco and T.L. Smith, "Rate of Physical Aging of Polycarbonate at a Constant Tensile Strain," *Journal of Polymer Science: Part B: Polymer Physics*, **28**, 513-520 (1990)
8. A. J. Hill, K. J. Heater, and C. M. Agrawal, "The Effects of Physical Aging in Polycarbonate," *Journal of Polymer Science: Part B: Polymer Physics*, **28**, 387-405 (1990)
9. D. E. Nikles and C. E. Forbes, "Accelerated Aging Studies for Polycarbonate Optical Disk Substrates," *Optical Data Storage*, **1499**, 39-40 (1991)
10. J. D. Ferry, *Viscoelastic Properties of Polymers*, John Wiley and Sons, NY (1980)
11. M. M. Qayyum and J. R. White, "Weathering of injection-moulded glassy polymers: Changes in residual stress and fracture behavior," *Journal of Materials Science*, **20**, 2557-2574 (1985)

12. A. Ram, O. Zilber, and S. Kenig, "Residual Stresses and Toughness of Polyethylene Plastics," *Polymer Engineering and Science*, **25**, 577-581 (1985)
13. M. M. Qayyum and J. R. White, "Effect of Water Absorption and Temperature Gradients on Polycarbonate Injection Moldings," *Journal of Applied Polymer Science*, **43**, 129-144 (1991)

CHAPTER 2

EXPOSURE OF POLYCARBONATE TO ULTRAVIOLET RADIATION

INTRODUCTION

The focus of this paper will be on the changes in mechanical properties of polycarbonate caused by exposure to sunlight. Although only about 5% of sunlight reaching the earth's surface is in the ultraviolet region of the spectrum, ultraviolet light is the most important contributor to the degradation of polymers caused by the natural outdoor environment [1]. The ultraviolet region of the solar spectrum is commonly divided into three ranges which are called UV-A, UV-B, and UV-C [2]. The wavelength limits of the UV-A region are from 315 to 400 nm which causes only minor damage to polymeric materials. The UV-B wavelength range is from about 290 to 315 nm. The most severe polymer degradation is caused by UV-B radiation although the UV-B region is partially absorbed by the ozone layer of the atmosphere. Some studies have been conducted on the effect of the partial depletion of the ozone layer on polymer degradation since more ultraviolet light in the UV-B region will reach the earth's surface [3]. Wavelengths lower than 290 nm fall into the UV-C region. This portion of the spectrum is totally absorbed by the atmosphere at current levels of ozone.

Quantum theory states that the energy in light is transmitted in discrete units which are called photons. The amount of this energy is inversely proportional to the wavelength of light [1]. Chemical bonds in a polymer chain have a threshold wavelength so that light of any wavelength shorter than the threshold wavelength contains the energy to break the bond in the polymer chain. This process is called chain scission and results in degradation of the mechanical properties of the polymer. Table 2.1 [4] shows the threshold wavelength of some common chemical bonds.

More than one mechanism of degradation has been proposed to occur in polycarbonate under ultraviolet exposure. Several investigators have suggested that

photo-Fries rearrangement occurs which is a photochemical rearrangement of the polymer structure as shown in Figure 2.1 [5-10]. Searle [7] suggests that polycarbonate experiences two separate mechanisms of degradation. He found that exposure to ultraviolet light caused scission of the C-O bonds in the carbonate group followed by a photo-Fries rearrangement. The chemical reactions are discussed in more detail in work published by Osawa [6] and Hawkins [11]. The scission of the C-O bonds is caused by longer wavelength ultraviolet rays while the photo-Fries rearrangement is due to the shorter wavelength light. For this reason polycarbonate was found to have two different regions of photodegradative spectral sensitivities which are 280 to 305 nm and 333 to 360 nm [12]. These are the two regions of the spectrum where the most severe damage occurs.

Natural Versus Artificial Weathering

Some terms that will be used throughout this paper are irradiance, spectral irradiance, and spectral energy (power) distribution. The irradiance is defined as the rate at which the energy of the light falls on a unit area of surface. The spectral irradiance is the distribution of the irradiance with respect to the wavelength. The spectral energy distribution is a plot of the irradiance against the wavelength of the light [13].

Many papers have been published that study the weathering characteristics of polycarbonate [7, 14-18]. Other studies have been conducted that look specifically at natural and artificial exposure to ultraviolet radiation [1, 2, 7, 13,19-34]. Natural weathering refers to exposing the material to its natural outdoor service environment. The long amounts of time required to obtain results from natural exposure make it impossible for this to be the only type of exposure trials to be used by present day companies. When a company develops a new material it is unreasonable to wait the entire service life required by natural weathering trials to test the serviceability of the new material. Also, the seasonal and diurnal variations in the amount of sunlight and precipitation would cause

different amounts of degradation in different parts of the world [1, 12, 13]. For example, if a material is exposed in Florida where the climate is hot and wet and then used in Arizona where the climate is hot and dry, then the material would undergo different amounts of degradation in service than in testing.

To obtain faster results a technique known as accelerated natural weathering has been commonly used. In this method the material is exposed to extreme climates to obtain the maximum amount of ultraviolet exposure in the shortest amount of time. Some common places of accelerated exposure are Florida, Arizona, and Saudi Arabia [12, 15]. Exposure to extreme climates could give erroneous results if the ultraviolet spectrum in the area of the world in which the material is being exposed contains wavelengths shorter than the ultraviolet spectrum in the service area. If this is the case then the mechanism of degradation could be different in the testing environment than in the service environment.

Another technique to accelerate the amount of exposure naturally uses mirrors to concentrate the ultraviolet rays. A testing apparatus has also been developed that follows the sun throughout the day to allow the face of the specimens to be exposed directly to the sun for the maximum amount of time. The Emmaqua (Equatorial Mount with Mirrors for Acceleration with Water) test was developed to both concentrate ultraviolet radiation with the use of mirrors and automatically track the sun [19]. One advantage to this method is that a reasonable lifetime prediction can be obtained for a specific geographic location.

Artificial Weathering Chambers

Several artificial weathering machines have been developed to operate in the laboratory. Some commonly used machines include carbon arc lamps, xenon lamps, and the QUV testing apparatus [19-21]. The most widely used artificial methods today are the xenon lamp and the QUV testing machine. Some of the advantages and disadvantages of each type of artificial exposure are listed below.

The carbon arc lamp filters out all of the ultraviolet wavelengths below 275 nm. The advantage to using carbon arc lamps is the low operating cost. One problem involved with this type of test is that the material is not sufficiently exposed to the wavelengths of ultraviolet between 290 and 350 nm which are present in sunlight [19]. Another disadvantage is that the output level of the lamps decreases over time, which makes the testing of the material impossible to reproduce. Additionally, testing temperatures in a carbon arc lamp are much higher than the temperatures reached in normal outdoor exposure. This could cause mechanisms of degradation to occur that would not naturally occur in the service life of the material.

The xenon lamp is one of the more popular types of lamps because it produces the most accurate artificial sunlight when comparing the spectral distributions, but there are also some problems involved with the xenon lamp. The ultraviolet output is inconsistent, which makes it very difficult to reproduce the test conditions. Also, like the carbon arc lamp, the testing temperature is much higher than the material would experience in natural sunlight.

Finally, the advantages and disadvantages of the QUV weathering apparatus will be discussed. The QUV is considered by many researchers to be the best laboratory weathering device [13, 19-20]. It uses eight fluorescent lamps to expose the material to ultraviolet radiation. If the lamps are rotated regularly, according to ASTM standard G53 [35], then the ultraviolet output of the lamps remains relatively constant. Since the output is almost constant, the test conditions can be easily reproduced from one batch of specimens to another. The Q-Panel Company has developed a feedback irradiance control system called the "Solar Eye" [25]. The "Solar Eye" continuously monitors the ultraviolet intensity of the lamps in the QUV and adjusts the power to maintain a near constant output throughout the exposure time. The QUV also offers the most natural condensation which is provided by vaporized water condensing on the test panels and can be programmed to provide alternating cycles of moisture and ultraviolet radiation at specified temperatures.

The Q-Panel Company manufactures four different fluorescent lamps for use in the QUV weathering device which are the UVA-340, UVB-313, FS-40, and UVA-351. The UVA-340 lamps are the closest match to natural sunlight, but the UVB-313 lamps allow for the maximum amount of acceleration. The spectral power distribution (SPD) of the four types of lamps are compared in Figure 2.2 [36] which shows that the range of wavelengths covered by the UVB-313 lamp are shorter than the wavelengths spanned by the UVA-340 lamp. For this reason the UVB-313 lamps produce faster acceleration in the degradation process. Also, when comparing the UVB-313 lamp to the FS-40 lamp it can be seen that the wavelength ranges for both lamps are similar, but the irradiance level of the UVB-313 lamp is significantly higher. The higher irradiance level produces faster acceleration.

Figure 2.3 [36] at the end of this chapter compares the spectral power distribution of the UVB-313 and FS-40 lamps to natural sunlight. It can be seen that the UVB-313 lamps contain all of the shortest wavelengths that are in natural sunlight which assures that the maximum amount of acceleration occurs. The problems with these lamps occur in the region where the wavelengths fall below the wavelength cut-off of natural sunlight. It is possible that these shorter wavelengths could cause mechanisms of degradation to occur that would not occur naturally which would make an attempt to correlate the artificial exposure to natural exposure difficult.

There are many things to consider when comparing natural outdoor exposure to artificial exposure in the laboratory. The cost of testing is a very important variable. The real-time natural exposure and accelerated natural exposure are the most expensive. The cost is very high because the real-time natural exposure takes several years at the test site, and the equipment used in the accelerated natural exposure (Emmaqua) is very expensive. Out of the artificial testing devices the QUV weathering machine is the least expensive [19-20]. The annual cost of operating the QUV continuously has been quoted by the Q-Panel Company to be about \$1000 which is much lower than the xenon lamp devices [20].

Another important comparison can be made on time of testing. As mentioned before, real-time natural exposure takes several years which makes it infeasible to be used as the only type of testing. Accelerated natural weathering techniques decrease the testing time significantly but are still considerably longer than the laboratory devices. Out of the artificial devices the QUV is convenient since it can be programmed to operate 24 hours per day and 7 days per week which reduces the overall testing time.

The last comparison will be made on the ability to accurately predict the service life of a component. Obviously, real-time outdoor exposure gives an accurate account of the lifetime of a material for a specific geographic region. Also, the accelerated natural testing can be correlated to real-time natural weathering which results in a fairly accurate real-time prediction of the service life [19]. Many studies over the past several years have been conducted to attempt to correlate artificial laboratory exposure to real-time natural exposure [27-29]. Very little success has resulted from these studies. The most important thing to consider is whether the same mechanisms of degradation are occurring in the laboratory that occur naturally. According to White and Turnbull [34], the variables that should be considered in the correlation are the rate constants for all of the degradation reactions and the products of reaction, the diffusion constants of all of the reagents, the reagent concentrations with respect to position within the article and time, the level of ultraviolet radiation with respect to the distance from the exposed surface, the diurnal and seasonal variations in the ultraviolet intensities and in temperature, and the effect of residual stresses and applied stresses.

EXPERIMENTAL DETAILS

The material investigated was an aircraft grade polycarbonate obtained from Rohm and Haas in Philadelphia, Pennsylvania. It was exposed in the form of coupons that were

4 by 12 by 1/8 inches from which test specimens were cut after each exposure interval. The artificial weathering device that was used was a QUV weathering machine manufactured by the Q-Panel Company in Cleveland, OH. The details, an overall view and a cross-sectional view of the QUV apparatus are given in Table 2.2 and Figures 2.4 and 2.5 [1]. The lamps used in this study were the fluorescent UVB-313 lamps manufactured by the Q-Panel Company. These lamps were chosen since they allow the maximum amount of acceleration as mentioned above. The spectral power distribution of the UVB-313 lamps is compared to natural sunlight in Figure 2.3 [36].

The material was exposed for twenty-four hours each day and seven days each week for intervals of three, seven, ten, and twenty weeks. At the end of each interval the coupons were machined into tensile, impact, dynamic mechanical, and positron annihilation lifetime spectroscopy (PALS) test specimens. The exposure involved only ultraviolet radiation with no condensation at an exposure temperature of 60° Celsius.

REFERENCES

1. D. M. Grossman, "Know Your Enemy: The Weather and How to Reproduce it in the Laboratory", Bulletin #L-821, The Q-Panel Company, Cleveland, OH
2. G. Grossman, "Correlation of Laboratory to Natural Weathering," *Journal of Coatings Technology*, Vol 49, No 633, Oct. 1977
3. A. L. Andradý and S. H. Hamid, "Ozone Depletion Effect on Weatherability of Plastics", *Handbook of Polymer Degradation*, S. H. Hamid, M. B. Amin, and A. G. Maadhah, eds. Marcel Dekker, Inc. NY (1992)
4. R. W. Logan, "Ultraviolet Light Takes on CPI Role", *Chemical Engineering*, Jan 25. 1982, (95-96)
5. A. Gupta, A. Rembaum, and J. Moacanin, "Solid state photochemistry of polycarbonates", *Macromolecules*, 11, 1285 (1978)
6. Z. Osawa, "Photoinduced Degradation of Polymers", *Handbook of Polymer Degradation*, S. H. Hamid, M. B. Amin, and A. G. Maadhah, eds. Marcel Dekker, Inc. NY (1992)
7. N. D. Searle, "Effect of Light Source Emission on Durability Testing", *Accelerated and Outdoor Durability Testing of Organic Materials*, p. 52, W. D. Ketola and D. Grossman, eds., ASTM, Philadelphia (1994)
8. D. Bellus, P. Hardlovic, Z. Manasek, "Photoinitiated Rearrangements in Poly[2,2-propanebis (4-phenyl carbonate)]," *Journal of Polymer Science Part B: Polymer Letters*, 4, 1-7 (1966)
9. J. S. Humphrey, A. R. Schultz, D. G. B. Jacquiss, "Flash Photochemical Studies of Polycarbonate and Related Model Compounds, Photodegradation vs. Photo-Fries Rearrangement," *Macromolecules*, 6, 305-314 (1973)
10. P. A. Mullen, N. Z. Searle, "The Ultraviolet Activation Spectrum of Polycarbonate," *Journal of Applied Polymer Science*, 14, 765-776 (1970)

11. W. L. Hawkins, *Polymer Degradation and Stabilization*, Springer-Verlag, Berlin, 1984
12. A. Davis and D. Sims, *Weathering of Polymers*, Applied Science Publishers, London, 1983.
13. P. Brennan and C. Fedor, "Sunlight, UV, and Accelerated Weathering", Bulletin # L-822, The Q-Panel Company, Cleveland, OH
14. A. Ram, O. Zilber, and S. Kenig, "Residual Stresses and Toughness of Polycarbonate Exposed to Environmental Conditions," *Polymer Engineering and Science*, **25**, 577-581 (1985)
15. M. M. Qayyum and J. R. White, "Plastic Fracture in Weathered Polymers," *Polymer*, **28**, 469-476 (1987)
16. C. A. Pryde and M. Y. Hellman, "Solid State Hydrolysis of Bisphenol-A Polycarbonate. I. Effect of Phenolic End Groups," *Journal of Applied Polymer Science*, **25**, 2573-2587 (1980)
17. A. Rivaton, D. Sallet, and J. Lemaire, *Journal of Polymer Degradation and Stability*, **14**, 1-22 (1986)
18. M. M. Qayyum and J. R. White, "Weathering of injection-moulded glassy polymers: Changes in residual stress and fracture behaviour," *Journal of Materials Science*, **20**, 2557-2574 (1985)
19. A. Peterson, "Accelerated Weathering: UV resistance of single-ply is being put to test.", RSI Magazine, February 1987
20. "QUV Compared to Xenon Arc", Bulletin # L-8006, The Q-Panel Company, Cleveland, OH
21. R. M. Fischer, "Results of Round Robin Studies of Light and Water Exposure Standard Practices", *Accelerated and Outdoor Durability Testing of Organic Materials*, pp. 112-132, W. D. Ketola and D. Grossman, eds., ASTM, Philadelphia, 1994

22. G. A. Zerlaut, "Solar Ultraviolet Radiation: Aspects of Importance to the Weathering of Materials", *Accelerated and Outdoor Durability Testing of Organic Materials*, pp. 3-26, W. D. Ketola and D. Grossman, eds., ASTM, Philadelphia, 1994
23. J. W. Martin, J. A. Lechner, and R. N. Varner, "Quantitative Characteristics of Photodegradation Effects of Polymeric Materials Exposed in Weathering Environments", *Accelerated and Outdoor Durability Testing of Organic Materials*, pp. 27-51, W. D. Ketola and D. Grossman, eds., ASTM, Philadelphia, 1994
24. D. M. Grossman, "Errors Caused by Using Joules to Time Laboratory and Outdoor Exposure Tests", *Accelerated and Outdoor Durability Testing of Organic Materials*, pp. 68-87, W. D. Ketola and D. Grossman, eds., ASTM, Philadelphia, 1994
25. G. R. Fedor and P. J. Brennan, "Irradiance Control in Fluorescent UV Exposure Testers", *Accelerated and Outdoor Durability Testing of Organic Materials*, pp. 199-215, W. D. Ketola and D. Grossman, eds., ASTM, Philadelphia, 1994
26. J. B. Howard and H. M. Gilroy, "Natural and Artificial Weathering of Polyethylene Plastics," *Polymer Engineering and Science*, **9**, 286-294 (1969)
27. E. S. Sherman, A. Ram, and S. Kenig, "Tensile Failure of Weathered Polycarbonate," *Polymer Engineering and Science*, **22**, 457-465 (1982)
28. M. R. Kamal and B. Huang, "Natural and Artificial Weathering of Polymers", *Handbook of Polymer Degradation*, S. H. Hamid, M. B. Amin, and A. G. Maadhah, eds. Marcel Dekker, Inc. NY (1992)
29. R. P. Brown, *Handbook of Plastics Test Methods*, George Godwin Limited, London, 1981
30. D. R. Askeland, *The Science and Engineering of Materials*, PWS-KENT Publishing Co., Boston, p.805, 1989
31. T. Kelen, *Polymer Degradation*, Van Nostrand Reinhold Company, NY, 1983
32. R. M. Fischer, "Accelerated Weathering Test Development with Fluorescent UV - Condensation Devices", SAE Technical Paper Series # 841022 (1984)

33. M. Raab, L. Kotulak, J. Kolarik, and J. Pospisil, "The effect of Ultraviolet Light on the Mechanical Properties of Polyethylene and Polypropylene Films," *Journal of Applied Polymer Science*, **27**, 2457-2466 (1982)
34. J. R. White and A. Turnbull, "Review, Weathering of polymers: mechanisms of degradation and stabilization, testing strategies and modelling," *Journal of Materials Science*, **29**, 584-613 (1994)
35. ASTM Standard G53-93, "Standard Practice for Operating Light- and Water-Exposure Apparatus (Fluorescent UV-Condensation Type) for Exposure of Nonmetallic Materials", *Annual Book of ASTM Standards*, Vol. 14.02, p.1108
36. "A Choice of Lamps for the QUV", Bulletin U-8160, The Q-Panel Company, Cleveland, OH

TABLE 2.1

Threshold UV Wavelengths For Breaking Various Bonds [From R. W. Logan, "Ultraviolet Light Takes on CPI Role", *Chemical Engineering*, Jan 25, 1982, (95-96)]

Bond	Dissociation Energy (kcal/gmol)	Threshold Wavelength Below Which Bond Will Break (nanometers)
C-N	72.8	392.7
C-Cl	81.0	353.0
C-C	82.6	346.1
S-H	83.0	344.5
N-H	85.0	336.4
C-O	85.5	334.4
C-H	98.7	289.7

TABLE 2.2

QUV Weathering Apparatus

Manufacturer:	The Q-Panel Company 26200 First Street Cleveland, Ohio 44145 USA (216) 835-8700
Volts:	120
Hertz:	60
Watts:	1500
Serial No:	90-6751-40

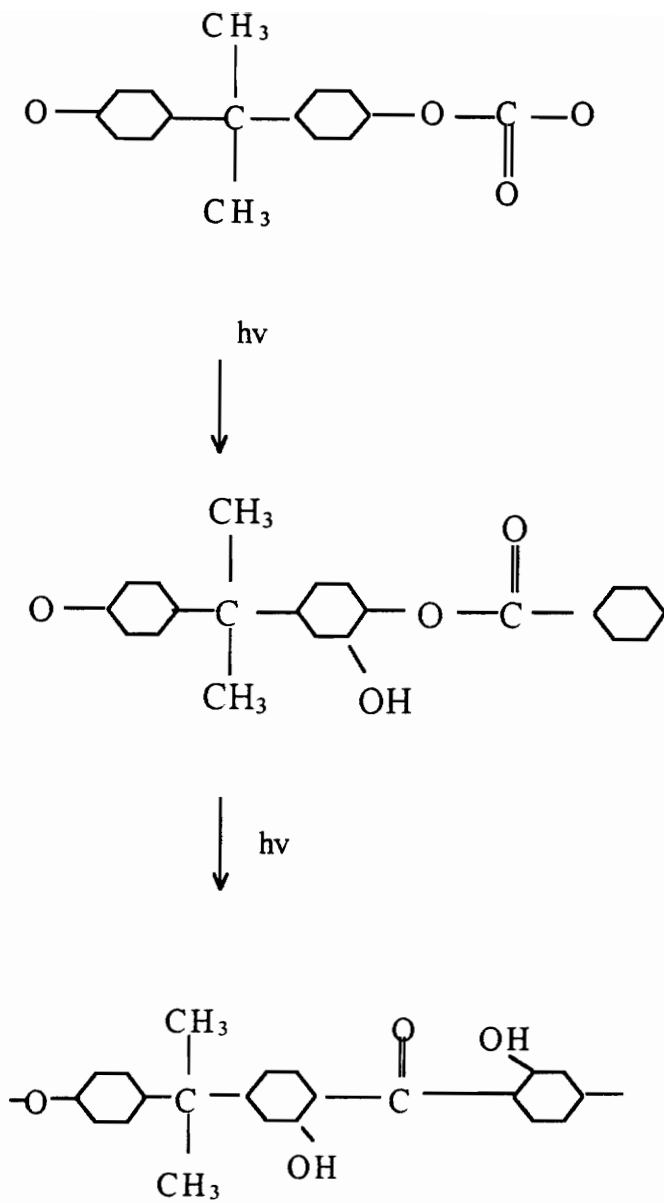


FIGURE 2.1 Photo-Fries rearrangement of polycarbonate

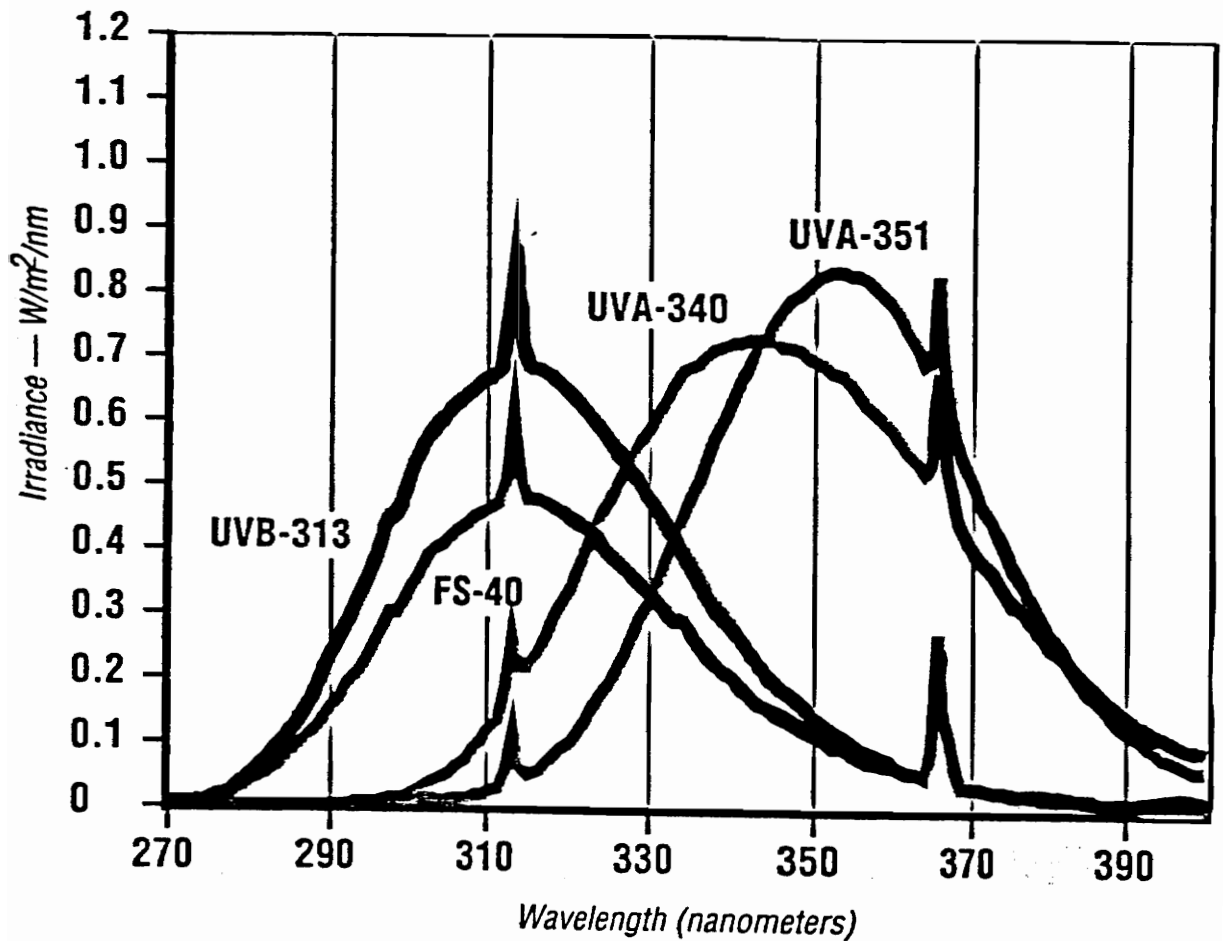


FIGURE 2.2 The Spectral Power Distribution (SPD) of the Four Types of Lamps for use in the QUV Weathering Device [From “A Choice of Lamps for the QUV”, Bulletin U-8160, The Q-Panel Company, Cleveland, OH]

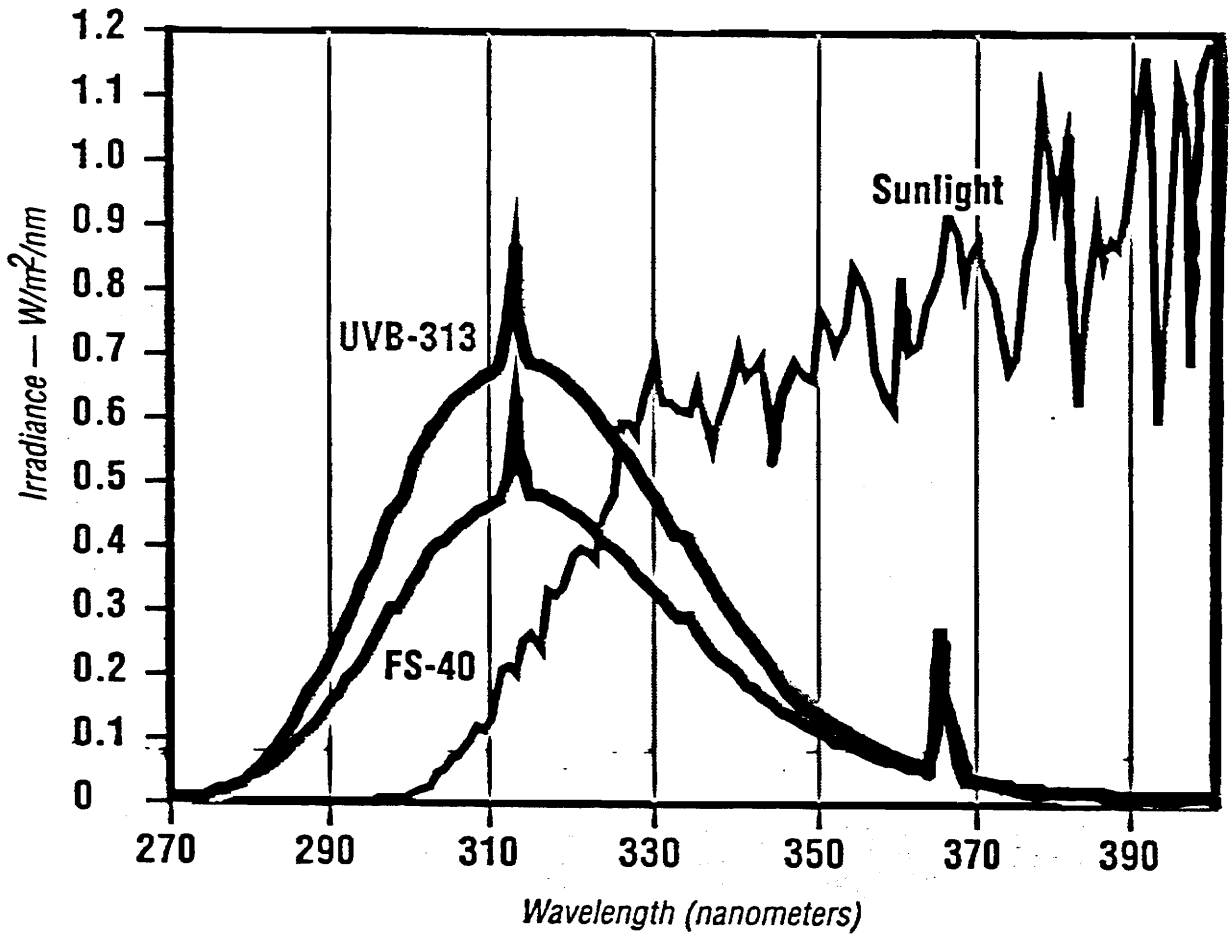


FIGURE 2.3 The Spectral Power Distribution of the UVB-313 and the FS-40 Fluorescent Lamps Compared to Natural Sunlight [From “A Choice of Lamps for the QUV”, Bulletin U-8160, The Q-Panel Company, Cleveland, OH]

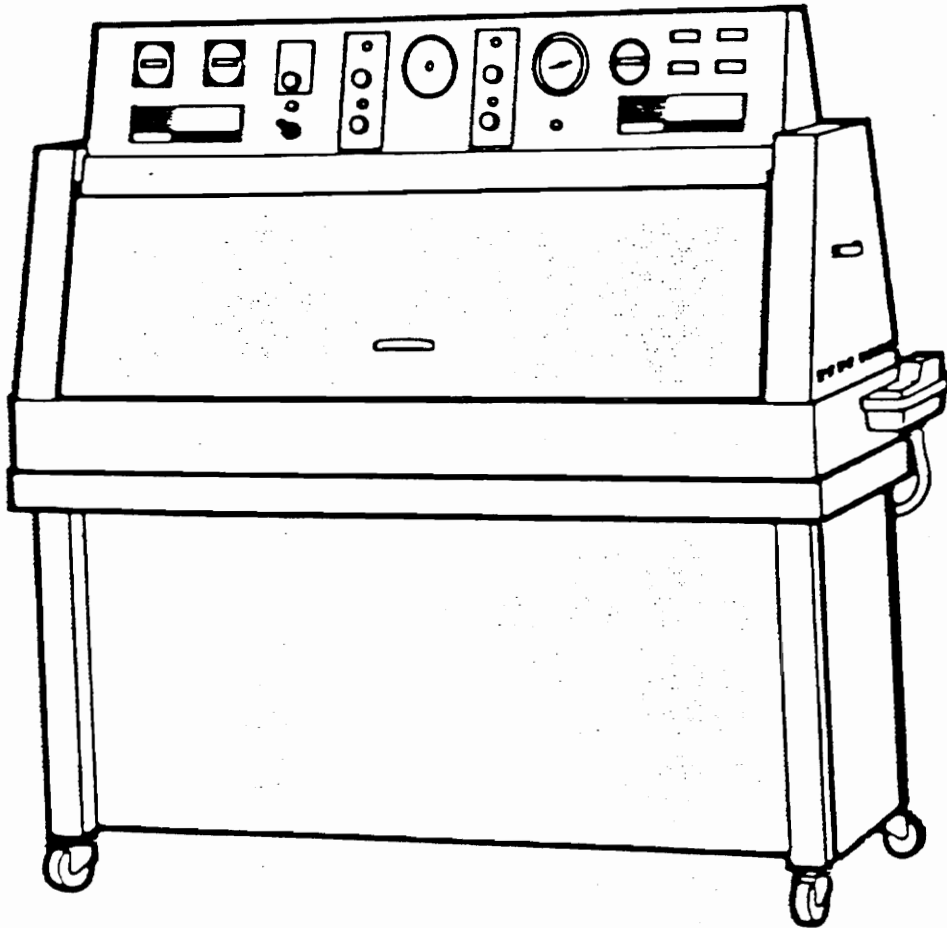


FIGURE 2.4 Overall View of the QUV Weathering Apparatus [From D. M. Grossman, "Know Your Enemy: The Weather and How to Reproduce it in the Laboratory", Bulletin #L-821, The Q-Panel Company, Cleveland, OH]

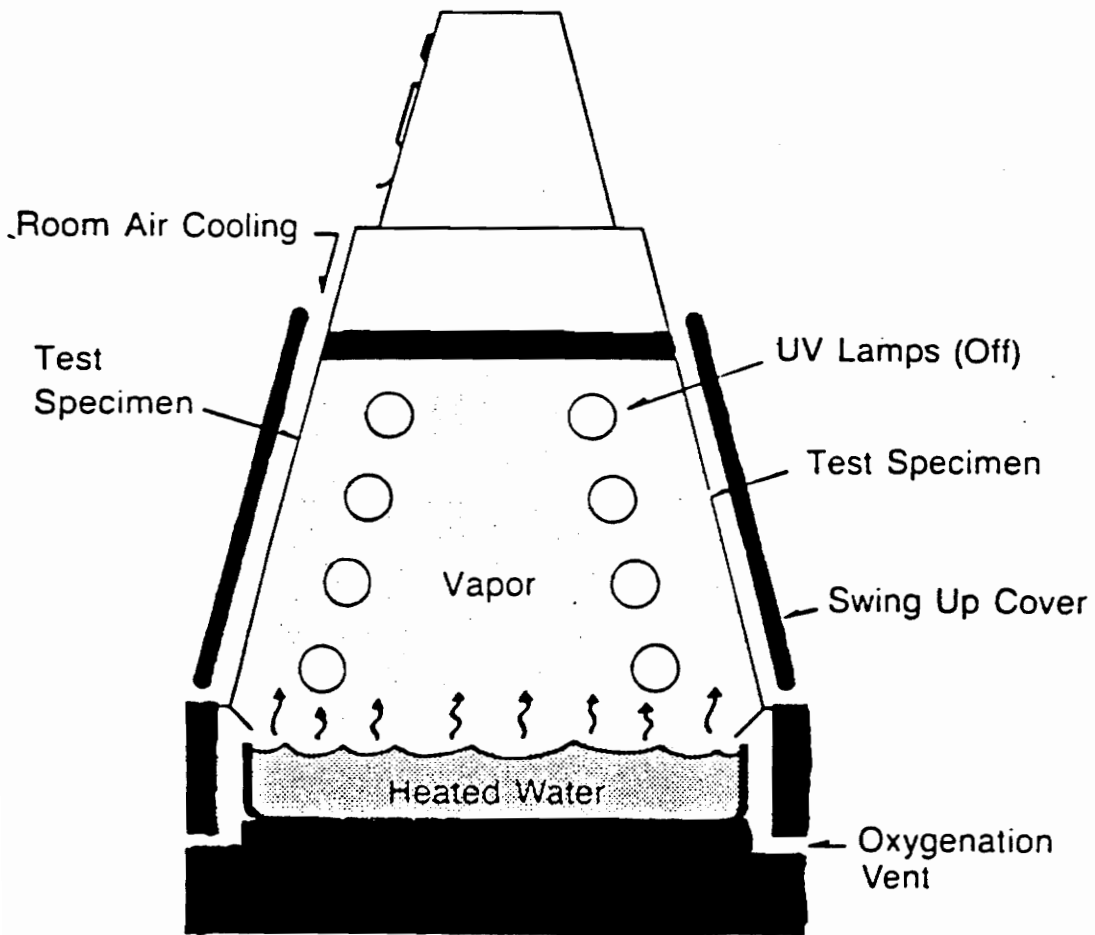


FIGURE 2.5 Cross-Sectional View of the QUV Weathering Apparatus
[From D. M. Grossman, "Know Your Enemy: The Weather and How to Reproduce it in the Laboratory", Bulletin #L-821, The Q-Panel Company, Cleveland, OH]

CHAPTER 3

EFFECT OF ULTRAVIOLET EXPOSURE ON THE VISCOELASTIC MODULI AND THE GLASS TRANSITION TEMPERATURE OF POLYCARBONATE

INTRODUCTION

Viscoelasticity usually refers to behavior that changes with respect to time and temperature. Viscoelastic materials are neither purely viscous nor purely elastic but exhibit a combination of the two [1]. To a certain extent all real materials are viscoelastic in nature, but polymers are a class of materials in which the viscoelastic properties are evident in a relatively short amount of time. Many test methods have been developed to study the viscoelastic properties of materials. Two common types of static tests that are performed are creep and relaxation experiments. In a creep test a constant stress is applied to the material, and the changes in displacement as a function of time are observed. A constant strain is applied to the specimen in a relaxation test and the stress is measured as it changes with time. Another common test method is a dynamic mechanical test in which the material undergoes either a free or forced vibration. Dynamic mechanical testing is discussed in more detail below.

Dynamic Mechanical Analysis

Dynamic mechanical testing refers to testing in which the test specimen undergoes an oscillation, usually sinusoidal, with continuous measurements of important quantities such as stress and strain. Typical dynamic mechanical tests are conducted over a range of frequencies or temperatures and will result in variations in viscoelastic properties of the material such as damping or modulus [2]. Sepe [3] suggests that dynamic mechanical analysis is an excellent method to determine the temperature limits of a polymer, compare

different materials for a particular service, and predict the long term properties of a material. To be denoted as dynamic mechanical thermal analysis (DMTA) the test should be carried out over a range of temperatures at a fixed frequency showing changes in the state of molecular motion as a function of temperature [4].

The behavior of a polymer can be approximately modeled by a combination of Voigt and Maxwell elements which contain springs (perfectly elastic) and dashpots (perfectly viscous). The Voigt and Maxwell models are shown in Figure 3.1 at the end of this chapter. If the dynamic test is run at a fixed frequency and no static strain exists then the polymer can simply be modeled by only the Voigt element [5].

If a stress is sinusoidally applied to the element then the value of the stress at any time is given by

$$\sigma = \sigma_0 \sin(\omega t) \quad (1)$$

where σ_0 is the maximum applied stress, ω is the frequency of the applied stress, and t is the time.

The strain of the Voigt element lags behind the stress because the dashpot cannot respond instantaneously. The value of the strain at any time is given by

$$\varepsilon = \varepsilon_0 \sin(\omega t - \delta) \quad (2)$$

where ε_0 is the maximum strain that is reached and δ is the phase angle between the stress and the strain.

The dynamic relationship between the stress, strain, and phase angle are shown graphically in Figure 3.2 at the end of this chapter [6]. Some viscoelastic properties that may be calculated with the use of stress and strain include the storage modulus (E'), loss modulus (E''), and loss tangent ($\tan \delta$). The definition and calculation for each of these properties is given below [6].

The storage modulus can be calculated by the portion of the stress that is in-phase with the strain. In the Voigt model, the storage component comes from the perfectly elastic behavior of the spring. The value for the storage modulus is given by

$$E' = \sigma_0' / \epsilon_0 \quad (3)$$

where σ_0' is the peak in-phase stress and ϵ_0 is the peak strain.

The loss modulus is obtained from the out-of-phase stress which comes from the damping effect of the purely viscous behavior of the dashpot in the Voigt model. The value for the loss modulus is given by

$$E'' = \sigma_0'' / \epsilon_0 \quad (4)$$

where σ_0'' is the peak out-of-phase stress.

The static and dynamic properties of a material can be related with the following equations [1].

$$E'(\omega) = \omega \int_0^{\infty} \sin(\omega s) E(s) ds \quad (5)$$

$$E''(\omega) = \omega \int_0^{\infty} \cos(\omega s) E(s) ds \quad (6)$$

where ω is the frequency of oscillation, s is the variable of integration and equals $t - u$, and $E(s)$ is the relaxation modulus as a function of time, s . Equations (5) and (6) have been derived from the Boltzman superposition integral in which u is the variable of integration that takes into account the entire stress history, and t is the fixed time of strain observation [1]. Since the above relations represent the Fourier sine and cosine transforms of $E(t)$,

Fourier transform methods can be used to determine the static modulus as a function of the dynamic properties [1].

The loss tangent represents the ratio of the loss modulus and the storage modulus [4] and is given by

$$\tan \delta = E''/E'. \quad (7)$$

where δ is the phase angle between the stress and strain.

Another important quantity is the complex modulus (E^*), which is a combination of the loss modulus and storage modulus as

$$E^* = E' + i E'' \quad (8)$$

where “i” is the square root of negative one.

Some types of dynamic tests that have been developed include the torsional pendulum, the shaker table, the viscoelastometer, many types of mechanical spectrometers and the dynamic mechanical (thermal) analyzer [6, 7]. The torsional pendulum allows free vibration of the polymer specimen, while the other methods use various types of forced vibration modes. This paper will concentrate on the theory and use of the dynamic mechanical analyzer.

Dynamic Mechanical Analyzer

The type of dynamic testing apparatus that will be discussed in this paper is the dynamic mechanical analyzer. The function of the dynamic mechanical analyzer is to hold the ends of a uniform plastic specimen, which is usually rectangular in cross section, between two clamps so that the specimen acts as the elastic and damping components of a mechanical system that is undergoing forced vibration [6]. One end of the specimen is

clamped to a pivot arm which undergoes a forced transverse sinusoidal oscillation as shown in Figure 3.3 [8-9] at the end of this chapter. The test may be operated at either fixed or varying frequency and fixed or varying temperature. Some of the material properties which may be obtained from a dynamic mechanical analyzer experiment are the storage modulus, loss modulus, loss tangent, and the glass transition temperature.

As mentioned above, the storage modulus is the real (elastic) portion of the complex modulus. The value for the storage modulus can be obtained from the natural frequency of the system with following equation [7, 10].

$$E' = \left[\frac{4 \pi^2 f^2 I - H}{2b \left(\frac{L}{2} + D \right)^2} \right] \left[\frac{L}{t} \right]^3 \left[1 + 0.71 \left(\frac{2t}{L} \right)^2 - 0.1 \left(\frac{2t}{L} \right)^3 \right] \quad (9)$$

where f is the frequency of oscillation of the system in Hertz, I is the second moment of area of the sample arm in $\text{kg}\cdot\text{m}^2$, H is the torsional spring constant of flexure pivot in $\text{N}\cdot\text{m}/\text{rad}$, b is the specimen width in meters, L is the length of the specimen between the clamps in meters, D is the clamping distance which is generally 9.50×10^{-3} to 9.85×10^{-3} meters, and t is the specimen thickness in meters. Most of these values are shown in Figure 3.3 [8-9] at the end of this chapter.

The loss tangent is the ratio of the loss and storage parts of the complex modulus and can be calculated from the following equation [7].

$$\tan \delta = J * V / f^2 \quad (10)$$

where J is a constant of the instrument, V is an instrument provided variable, and f is the frequency of oscillation.

The dynamic mechanical analyzer maintains a constant amplitude and frequency of oscillation by electronically supplying energy to the system to make up for the energy lost due to the damping of the polymer sample. The loss modulus is obtained from the amount of energy that the machine has to provide to compensate for damping.

Glass Transition Temperature

The glass transition temperature is one of the most important properties to consider in a polymer. Polymers experience a glass-rubber transition region which usually spans a temperature range of twenty to thirty degrees Celsius. The glass transition temperature is generally taken to be the center of this glass-rubber transition region, below which the material behaves as a glass, and above which the material behaves as a rubber. Unlike the first-order transitions of boiling and melting in crystalline materials, the glass transition in high molecular weight polymers is a second-order transition at very slow heating and cooling rates [5].

Several different thermodynamic and viscoelastic phenomena occur in the glass-rubber transition region [1]. At the glass transition temperature, a change in slope occurs in a plot of volume and enthalpy as a function of temperature. The viscoelastic phenomena that occur include a decrease in the relaxation modulus and an increase in the creep compliance by approximately three orders of magnitude. The relaxation modulus and creep compliance are the proportionality variables between stress and strain in stress relaxation and creep experiments, respectively. In dynamic experiments the storage modulus and compliance behave similarly to the relaxation modulus and creep compliance, but the loss modulus, loss compliance, and loss tangent experience maxima in the region of the glass-rubber transition.

These glass-transition phenomena provide ways to experimentally measure the glass transition temperature. Some common methods for measuring the glass-transition temperature experimentally include dilatometry, thermal, mechanical, dielectric, magnetic,

and melt viscosity [5]. This paper will concentrate on the measurement of the glass transition temperature with the use of the dynamic mechanical analyzer, which is a mechanical method.

As mentioned above, significant changes occur in the storage modulus, loss modulus, and loss tangent in the glass-rubber transition region. The peak of the loss modulus is commonly taken to be the glass transition temperature since it generally occurs near the center of the temperature range where the storage modulus drops significantly. One limitation of the dynamic mechanical analyzer is that there is a lower thickness limit of about 0.2 mm which limits the possibility of depth profiling for polycarbonate that has been exposed to ultraviolet radiation [11].

Hill, et al., studied the dynamic mechanical properties of acrylic clearcoats that had been exposed to ultraviolet light in a QUV weathering apparatus [12]. They found that after 250 hours of exposure to ultraviolet radiation the storage modulus, E' , increased significantly at all temperatures for the unstabilized material. They attributed this increase to an increase in the crosslink density which was caused by ultraviolet exposure. Also, the glass transition temperature which was taken to be the loss tangent peak increased after exposure. They determined that dynamic mechanical analysis was a very effective method to measure changes in the physical properties during weathering.

EXPERIMENTAL DETAILS

The material investigated was an aircraft grade polycarbonate obtained from Rohm and Haas in Philadelphia, Pennsylvania. Tests were conducted on material that was exposed to continuous ultraviolet light in the QUV weathering apparatus described in Chapter 2. The material was exposed for durations of three, seven, ten, and twenty weeks.

The instrument that was used to measure the dynamic mechanical properties of polycarbonate was the DuPont Instruments 983 Dynamic Mechanical Analyzer (DMA) manufactured by E. I. du Pont de Nemours and Co., Inc. The details of the Dynamic Mechanical Analyzer are shown in Table 3.1. The analysis software that was used to determine the storage modulus, loss modulus, and loss tangent was Thermal Analyst 2100 produced by E. I. du Pont de Nemours and Co., Inc.

The DuPont 983 DMA can be operated in four different modes: resonant frequency, fixed frequency, stress relaxation, and creep [13]. For this study the operation mode was chosen to be a fixed frequency of one hertz with an oscillation amplitude of three tenths of a millimeter. The operating temperature range was from thirty to one hundred seventy degrees Celsius with a heating rate of both one degree Celsius per minute and five degrees Celsius per minute.

The unexposed specimens had a uniform rectangular cross section of 0.118 inches by 0.5 inches and a length of 2.5 inches. Only a very thin surface layer of the polycarbonate is believed to be degraded by exposure to ultraviolet radiation as described in the following chapter. For this reason the specimens exposed for ten and twenty weeks were machined down to a thickness of one millimeter in an attempt to determine the viscoelastic properties of the degraded surface layer. Several DMA tests were conducted on exposed material that had not been machined down. Although the bending mode of the DMA is somewhat sensitive to surface changes, the test results showed no noticeable change in the viscoelastic properties after exposure.

A heating rate of both one and five degrees Celsius per minute were used to show the drastic differences occurring at different rates of heating. The relatively slow heating rate of one degree Celsius per minute was chosen to be more accurate since a slower heating rate is closer to thermal equilibrium. Haidar and Smith [14] studied the time dependence of the storage modulus of polycarbonate. They found that polycarbonate is clearly dependent on the time that has elapsed after a rapid change in temperature. It was

found that sometimes it took up to one hundred minutes to reach an equilibrium value for the storage modulus.

RESULTS AND DISCUSSION

Yee and Smith [15] used dynamic mechanical analysis to study the relation of molecular motion of polycarbonate to the relaxation properties. In most of the polycarbonate specimens tested they found three distinct peaks in the dynamic mechanical response. From descending temperature the peaks are denoted as α , γ , and β . The α peak was due to large scale molecular motion associated with the glass transition temperature. They attributed the γ peaks to the motion of phenylene rings. The β peaks were not found in all of the tested specimens and were not found to be caused by one distinct molecular motion or structure.

As mentioned above heating rates of one and five degrees Celsius per minute were compared. Figure 3.4 shows that the T_g for a heating rate of five degrees Celsius per minute is significantly higher than the T_g at one degree Celsius per minute. At the higher heating rate, the molecules are not given as much time to increase mobility which is shown by the higher T_g . The large difference seen here requires that the rate of heating be reported for any dynamic mechanical testing results in order to accurately compare two different tests. All of the viscoelastic properties reported from this point forward are for a heating rate of one degree Celsius per minute.

The storage modulus, loss modulus, and loss tangent for a typical dynamic mechanical test are plotted as a function of temperature in Figure 3.5. A log scale is used for the storage and loss moduli. It can be seen that the loss modulus experiences a peak at approximately the center of the glass transition region where the storage modulus undergoes a rapid decrease.

The log of the storage modulus, $\log E'$, for the unexposed polycarbonate and the ten and twenty week samples are shown as a function of temperature in Figure 3.6. It can be seen that E' increased significantly after exposure to ultraviolet radiation at all temperatures below the glass transition region. This result agrees with previously conducted studies on ultraviolet degradation by Hill and co-workers [12]. Figure 3.7 shows the value for $\log E'$ as a function of weeks of exposure at a temperature of 35 °C. $\log E'$ increased from 9.29 for the unexposed polycarbonate to 9.463 for the twenty week samples and was modeled linearly. The exposed samples were machined down from a thickness of 0.118 inches to 0.040 inches, leaving the surfaces directly exposed to ultraviolet light to be tested. Thus, an increase in the storage modulus indicates an embrittlement or hardening of the exposed surfaces.

The log of the loss modulus, E'' , is plotted as a function of temperature in Figure 3.8. As a general trend E'' appears to increase after exposure to ultraviolet radiation, but these results are not conclusive since the loss modulus curves intersect at several different temperatures.

The glass transition temperature, T_g , was determined from the peak of the loss modulus curves shown in Figure 3.8. The T_g is plotted against weeks of exposure to ultraviolet radiation in Figure 3.9 which shows a slight increase from 156.3 °C for the unexposed polycarbonate to 157.1 °C for the twenty week specimens. The change in T_g is less than 1 °C, and the points for the ten and twenty week samples were each determined from only one DMA experiment. Therefore, no definite conclusions can be drawn from the minor change in T_g .

Dynamic mechanical analysis proved to be a reliable method to characterize the viscoelastic properties of polycarbonate after exposure to ultraviolet radiation although some difficulty developed when attempting to test a thin surface layer. It has been stated that DMA analysis can be conducted on specimens as thin as 0.2 mm, but in this study a minimum thickness of 1 mm was required to provide enough stiffness in the system to obtain readable results.

REFERENCES

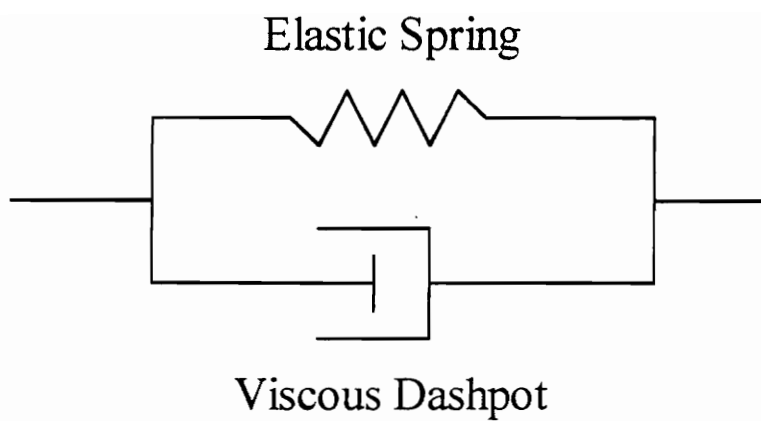
1. J. J. Aklonis and W. J. MacKnight, *Introduction to Polymer Viscoelasticity, 2nd Ed.*, John Wiley and Sons, NY, 1983
2. R. P. Brown, *Handbook of Plastics Test Methods*, George Godwin Limited, London, 1981
3. M. P. Sepe, "Challenges for Plastics/Composites," *Advanced Materials and Processes*, **141**, 31-43, Apr 4 (1992)
4. R. E. Wetton, "Dynamic Mechanical Thermal Analysis of Polymers and Related Systems", *Developments in Polymer Characterisation - 5*, J. V. Dawkins, ed., Elsevier Applied Science Publishers, London, 1986
5. L. H. Sperling, *Introduction to Physical Polymer Science, 2nd Ed.*, p.368, p.309, John Wiley & Sons, Inc. NY, 1992
6. D. A. Dillard, Class Notes in Polymer Viscoelasticity, Virginia Polytechnic Institute and State University, 1995
7. ASTM Standard D4065-93, "Standard Practice for Determining and Reporting Dynamic Mechanical Properties of Plastics", *Annual Book of ASTM Standards*, Vol. 08.02, pp. 524-528.
8. H. J. Lee and R. A. Heller, "Propulsion System Hazards and Structural Service Life Prediction", *Technical Report CR-RD-PR-88-3*, U. S. Army Missile Command, Redstone Arsenal, Alabama, 1988
9. Du Pont Co., "Du Pont 982 Dynamic Mechanical Analyzer Operator's Manual."
10. R. P. Kusy and A. R. Greenberg, "Influence of Molecular Weight on the Dynamic Mechanical Properties of Poly(methyl methacrylate)," *Journal of Thermal Analysis*, **18**, 117-126 (1980)
11. J. R. White and A. Turnbull, "Review Weathering of polymers: mechanisms of degradation and stabilization, testing strategies and modelling," *Journal of Materials Science*, **29**, 584-613 (1994)

12. L. W. Hill, J. S. Grande, and K. Kozlowski, "Dynamic Mechanical Analysis of Weathered (Q-U-V[®]) Acrylic Clearcoats with and without Stabilizers," *Polymeric Materials: Science and Engineering, Proceedings of the ACS Division of Polymeric Materials: Science and Engineering*, **63**, Fall Meeting 1990, Washington D.C., ACS p.654-659 (1990)
13. *Thermal Analyst 2100 Operator's Manual, Version 1.0*, PN 996504.001 Rev C, E. I. du Pont de Nemours and Co. (Inc.), Wilmington, DE (1988)
14. B. Haidar and T. L. Smith, "Time Dependence of the Storage Modulus of Polycarbonate Following Temperature Jumps Within the Glassy State," *Macromolecules*, **23**, 3712-3714 (1990)
15. A. F. Yee and S. A. Smith, "Molecular Structure Effects on the Dynamic Mechanical Spectra of Polycarbonates," *Macromolecules*, **14**, 54-64 (1981)

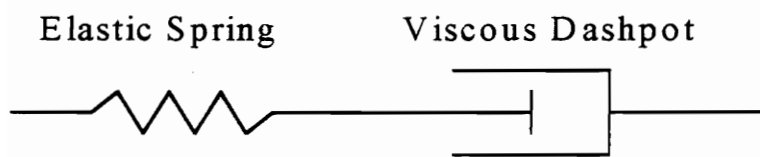
TABLE 3.1

DuPont Instruments 983 Dynamic Mechanical Analyzer (DMA)

<u>Manufacturer:</u>	E. I. du Pont de Nemours and Co, Inc. Wilmington, Delaware 19898
<u>Model #:</u>	982001.002
<u>Serial #:</u>	244
<u>Volts:</u>	115
<u>Hertz:</u>	60



(a)



(b)

FIGURE 3.1 (a) Voigt and (b) Maxwell elements

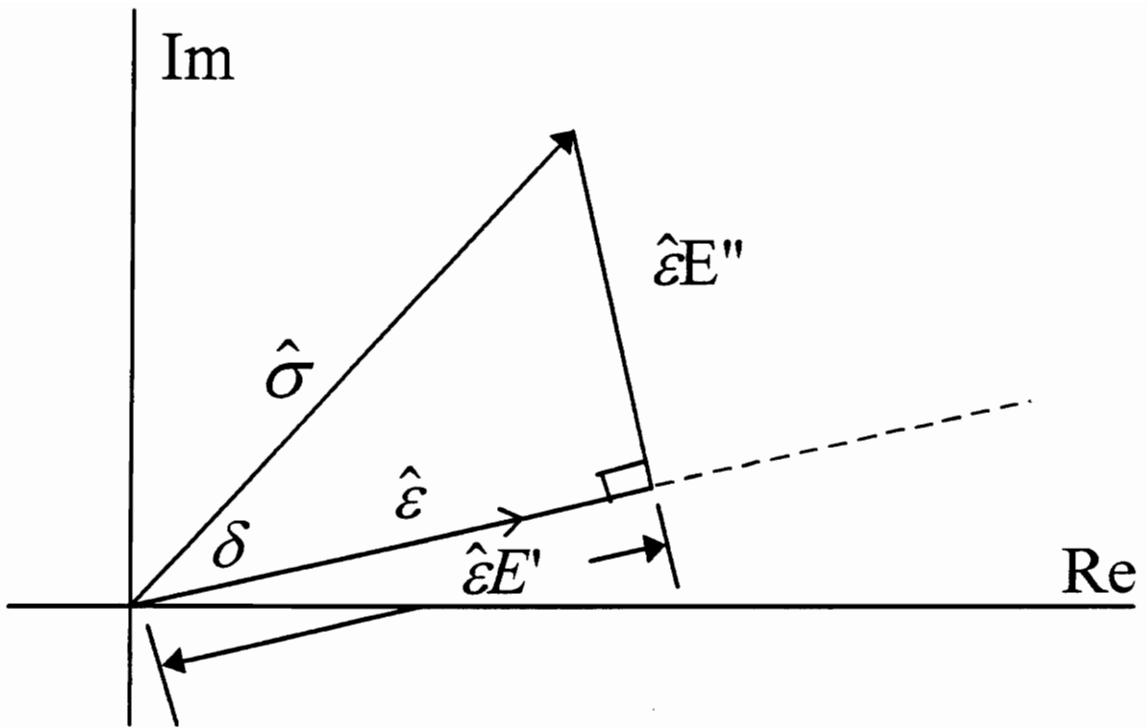


FIGURE 3.2 Simple dynamic relationships between stress and strain, illustrating the role of the phase angle [From D. A. Dillard, Class Notes in Polymer Viscoelasticity, Virginia Polytechnic Institute and State University, 1995]

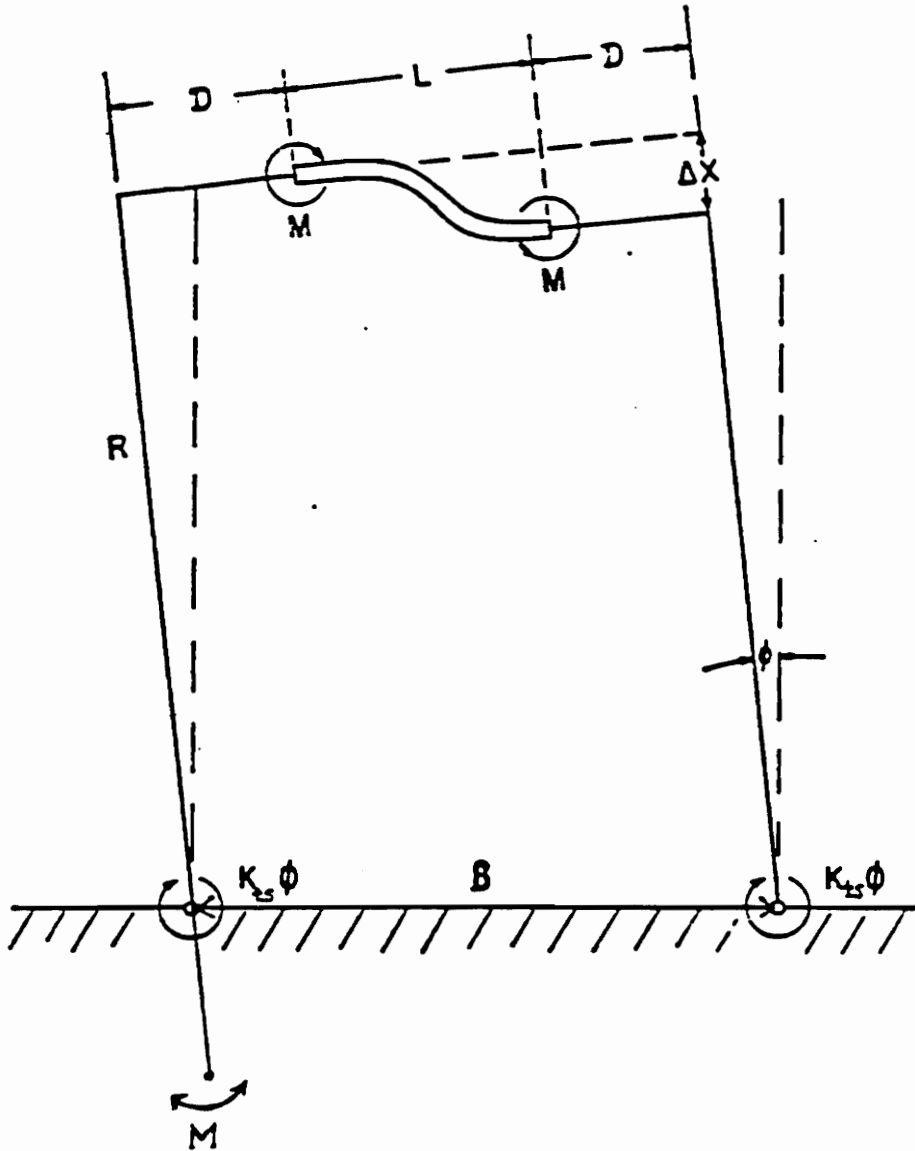


FIGURE 3.3 Dynamic mechanical analyzer mode of vibration [From Du Pont 982 Dynamic Mechanical Analyzer Operator's Manual]

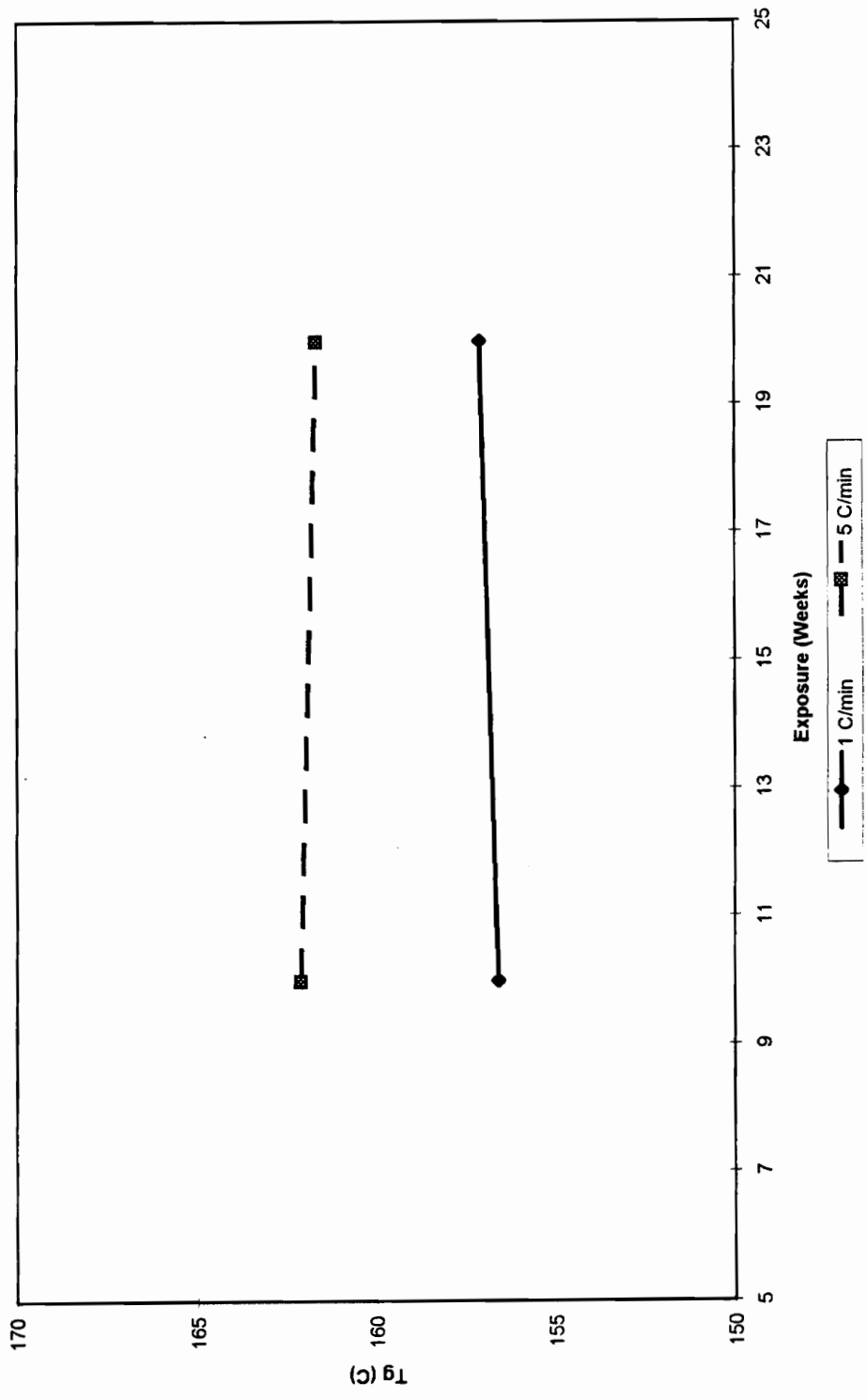


FIGURE 3.4 Glass transition temperature of polycarbonate versus weeks of exposure to ultraviolet radiation obtained from dynamic mechanical analysis at heating rates of 1 °C per minute and 5 °C per minute.

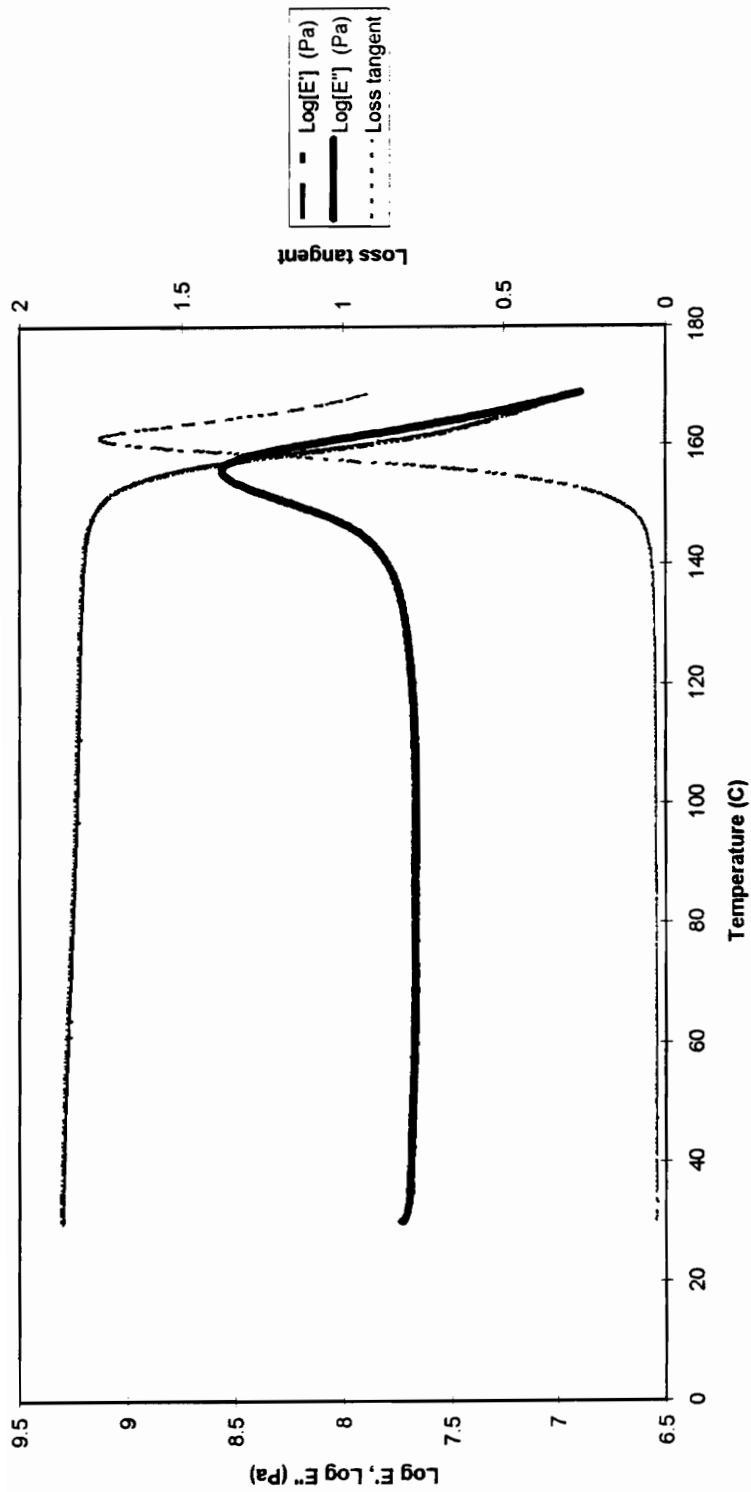


FIGURE 3.5 Storage modulus, loss modulus, and loss tangent (at a frequency of 1 Hz) versus temperature for polycarbonate as recorded by the DuPont DMA 983

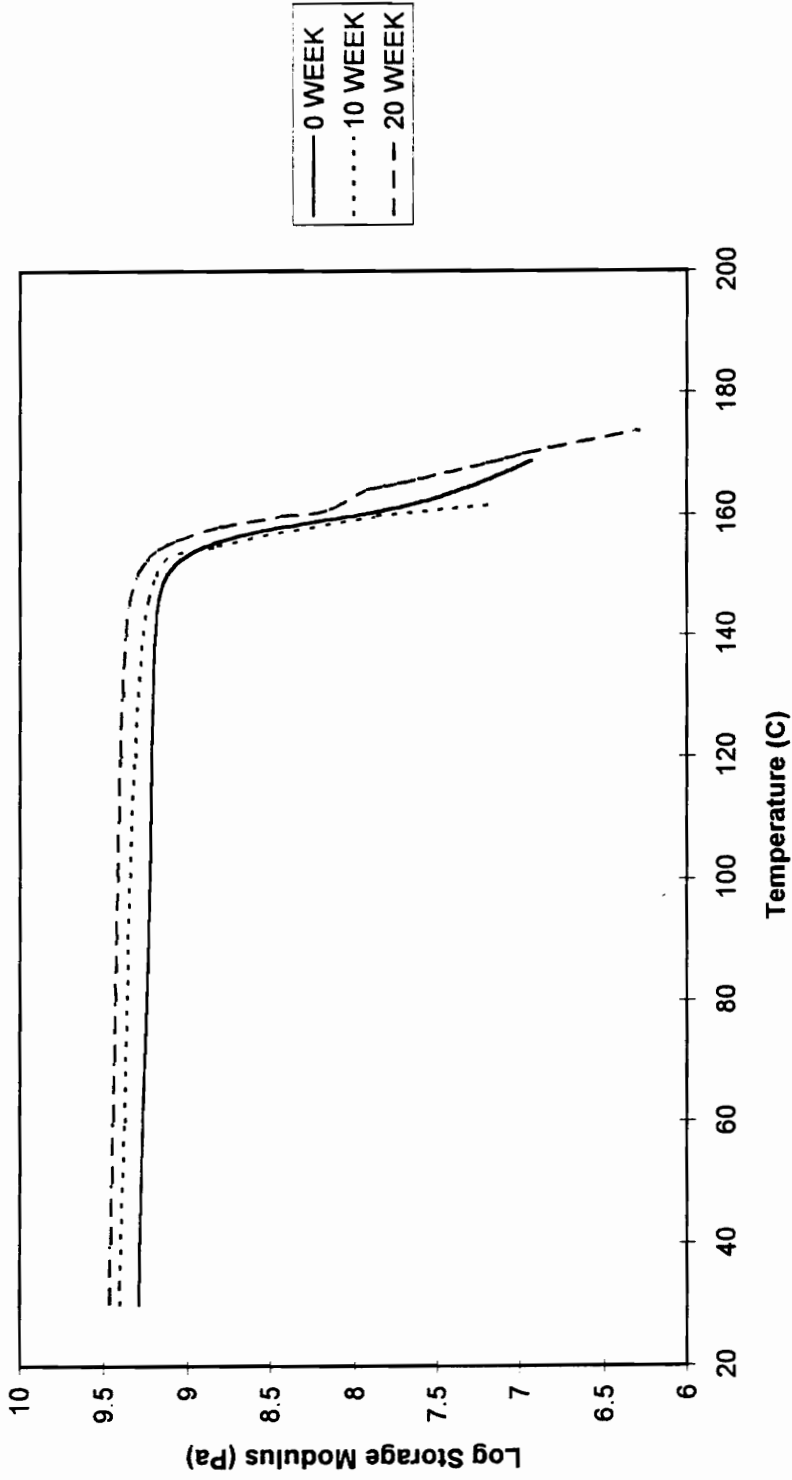


FIGURE 3.6 Log of storage modulus (at a frequency of 1 Hz) versus temperature for unexposed polycarbonate and polycarbonate exposed to ultraviolet radiation for ten and twenty weeks

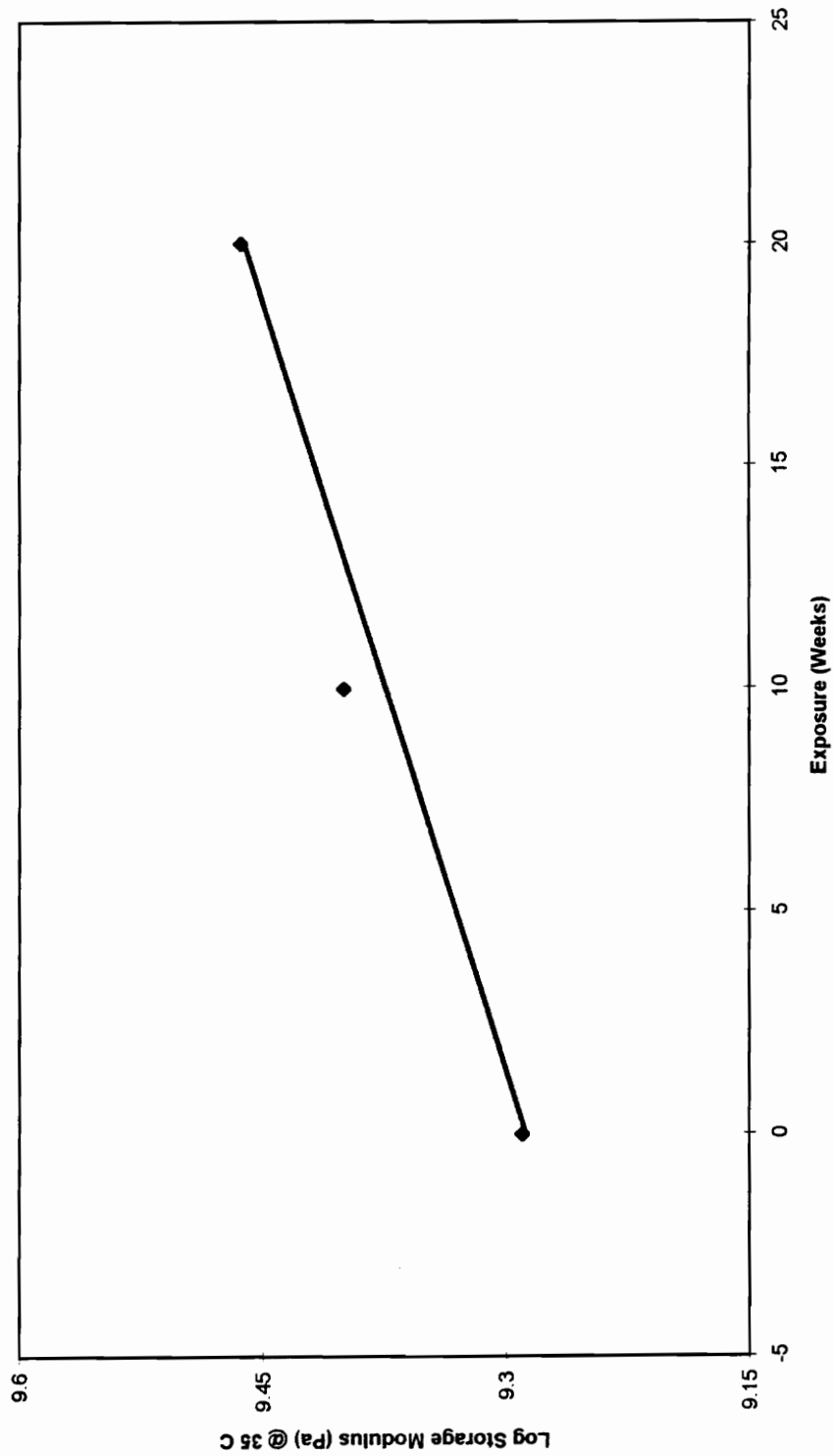


FIGURE 3.7 Log of storage modulus (at a frequency of 1 Hz) of polycarbonate at a temperature of 35 °C versus weeks of exposure to ultraviolet light.

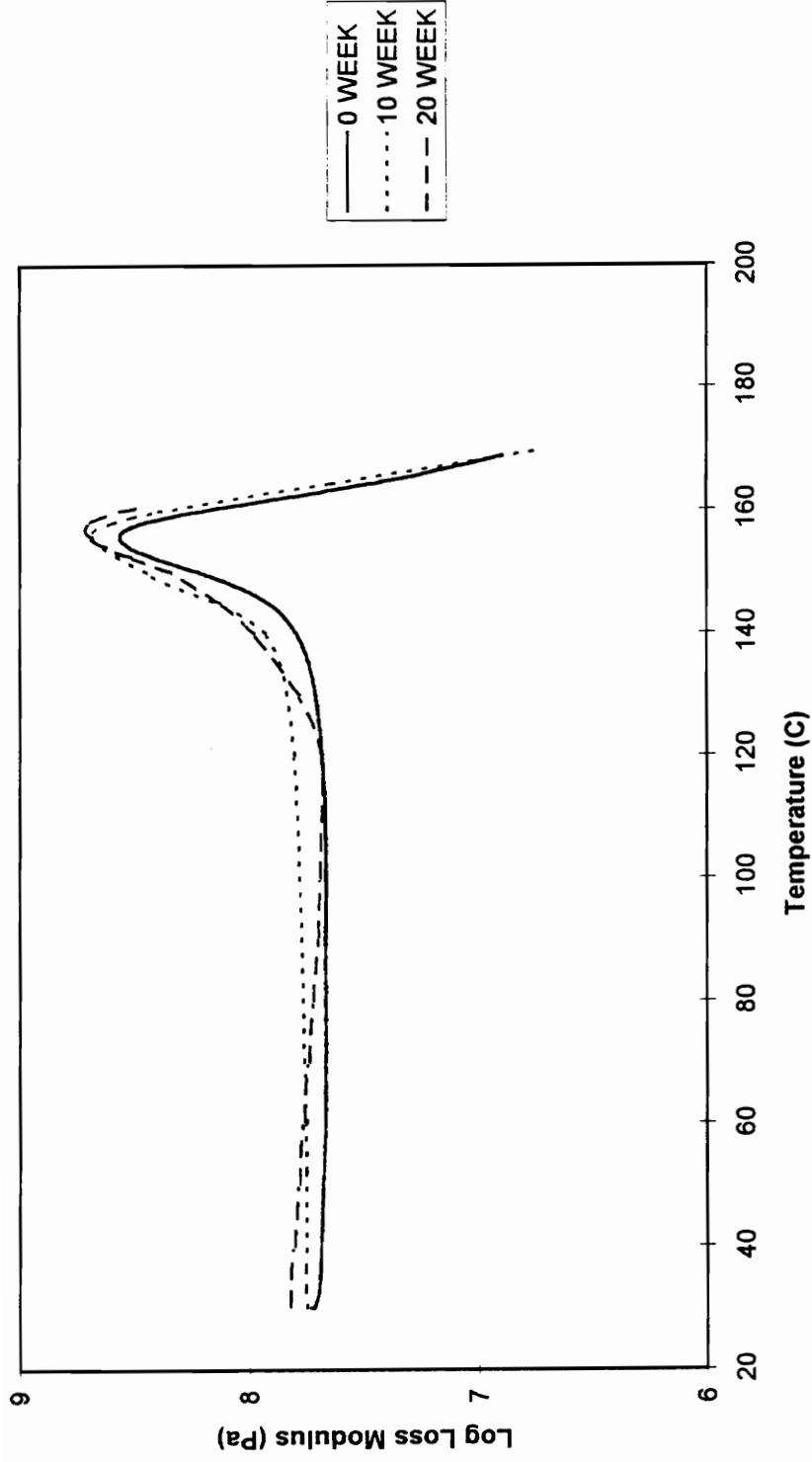


FIGURE 3.8 Log of loss modulus (at a frequency of 1 Hz) versus temperature for unexposed polycarbonate and polycarbonate exposed to ultraviolet radiation for ten and twenty weeks

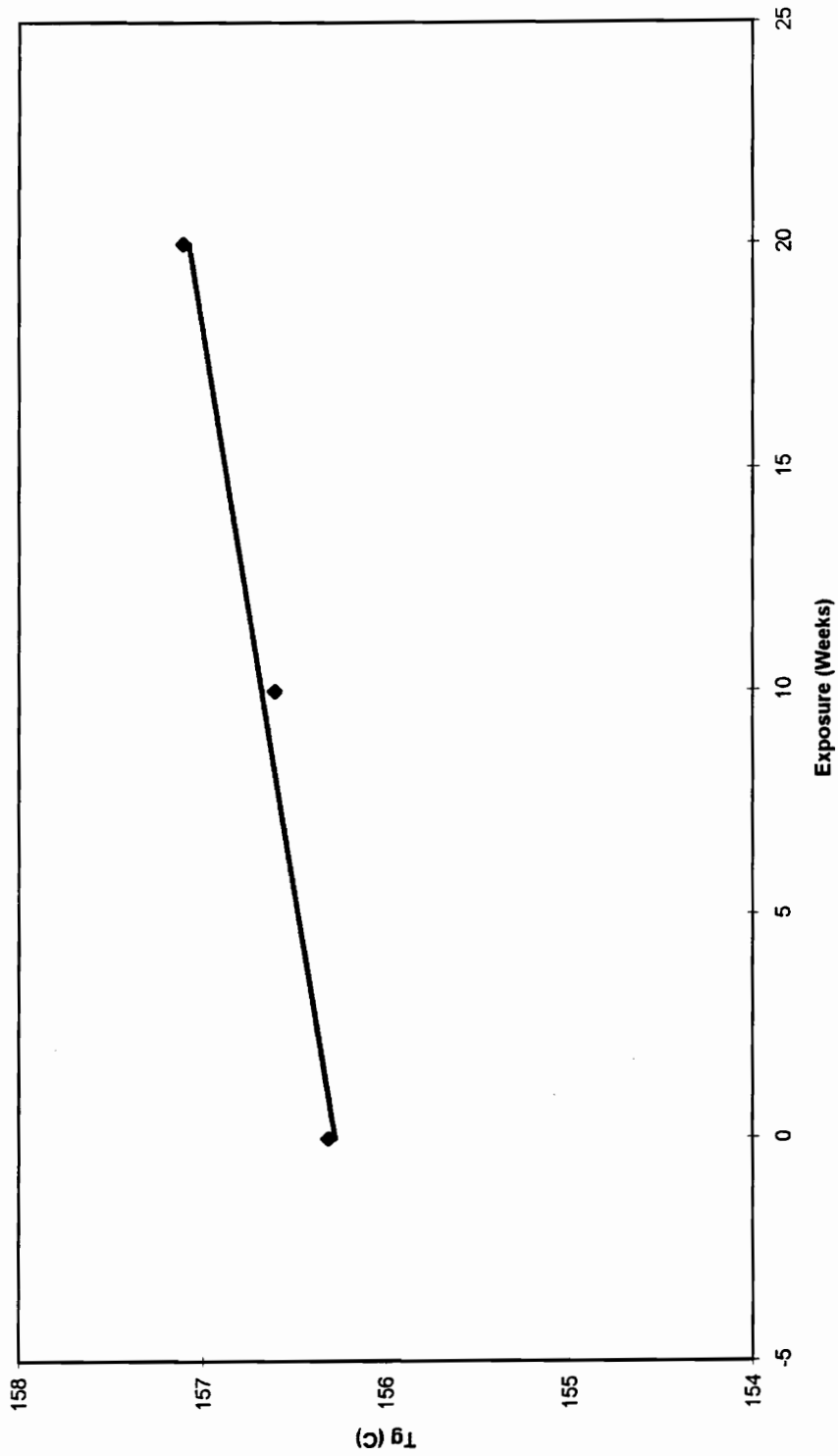


FIGURE 3.9 Glass transition temperature of polycarbonate (at a heating rate of 1 °C/min) versus weeks of ultraviolet exposure.

CHAPTER 4

EFFECT OF ULTRAVIOLET EXPOSURE ON THE STRENGTH AND

DUCTILITY OF POLYCARBONATE

INTRODUCTION

After a material is subjected to exposure to ultraviolet radiation the strength and ductility are usually altered depending on the mechanism of degradation that occurs. Generally, degradation of a polymer by ultraviolet light has been found to cause only a small change in the strength of a material but a significant reduction in the ductility [1].

One of the most common test methods to determine the strength and ductility of a material is the uniaxial tension test. Dumbbell-shaped tensile test specimens are commonly used to avoid having the specimen break where it is being gripped [2]. Conditions that need to be chosen with care include the rate of straining and the method of preparation of the test specimen. Tension test results are very sensitive to these variables, and comparison cannot accurately be made between tests of extremely different conditions [3].

Strength

For comparison the overall strength of a material is commonly taken to be the tensile or ultimate strength which can be obtained from a uniaxial tension test. The engineering tensile strength, σ_u , is defined as

$$\sigma_u = \frac{P_{\max}}{A_o} \quad (1)$$

where P_{\max} is the maximum tensile load that the specimen experiences during the tension test and A_0 is the original cross-sectional area. If the maximum load is obtained at the yield point of the material then the tensile strength is denoted as the tensile strength at yield. If the maximum load is obtained at fracture then the tensile strength is denoted as the tensile strength at break [3].

Since Equation (1) uses the original cross-sectional area of the specimen then it is known as engineering stress. A measure of strength that uses the instantaneous area is the true stress which is given by [4]

$$\sigma_T = \frac{P}{A} \quad (2)$$

where σ_T is the true stress, P is the applied load, and A is the instantaneous cross-sectional area. The true stress is always larger than the engineering stress in a tension test because of Poisson's effect in which the cross-sectional area decreases as the specimen stretches.

Ductility

Another tensile property that may be obtained from a uniaxial tension test is the percent elongation. The percent elongation is an excellent measure of the ductility of the material and is calculated by

$$\%Elongation = \left(\frac{L_f - L_o}{L_o} \right) \times 100 \quad (3)$$

where L_f is the final length of the gage section, and L_o is the original gage length [3].

The ductility is directly proportional to the value obtained for percent elongation.

Another mechanical property that is related to ductility is the percent reduction of area. The percent reduction of area is found by

$$\% \text{ RA} = \frac{A_0 - A}{A_0} \times 100 \% \quad (4)$$

where A_0 is the original cross-sectional area of the gage section and A is the smallest cross-sectional area in the gage section at a given time during the test [3].

Surface Effects

Exposure to ultraviolet radiation degrades only a thin layer of surface material which becomes brittle and affects the ductility of the entire material [5-15]. Visible cracks often form on the surface after fairly long periods of exposure [5]. Several studies show that these cracks are likely to be the reason for brittle failure of the undamaged inner material which would otherwise exhibit ductile behavior [5-11, 13].

Schoolenberg and coworkers [5-7] used a fracture mechanics approach to study the degradation of polypropylene caused by exposure to ultraviolet radiation. They measured the brittle surface layer on exposed polypropylene to be only around 400 to 500 μm . They saw three distinct stages of behavior as described below.

- (I) Short degradation times -- no effect on material degradation,
- (II) Intermediate degradation times -- a decrease in the fracture energy caused by flaws in the degraded surface layer, and
- (III) Long degradation times -- an increase in the fracture energy caused by multiple cracking.

So and Broutman [8-9] applied brittle coatings to acrylonitrile-butadiene-styrene and high impact polystyrene which normally behave in a ductile manner and found a significant reduction in elongation of the coated material. This loss in ductility is due to the surface layer being a site for crack initiation. With the use of fracture mechanics they determined that for the ductile bulk material beneath the brittle coating to experience brittle fracture then the thickness of the brittle coating must be larger than the critical crack size for unstable crack growth in the coating material.

Raab and coworkers [14] compared the behavior of polyethylene and polypropylene films that had been exposed to ultraviolet radiation to unexposed material with an initiated crack of 0.1 mm in length. They found very similar behavior between the exposed material and cracked material which indicates that the cracks in the surface layer of the exposed material cause brittle failure of the unyielded material.

EXPERIMENTAL DETAILS

The material investigated was an aircraft grade polycarbonate obtained from Rohm and Haas in Philadelphia, Pennsylvania. Tests were conducted on material that was exposed to continuous ultraviolet light in the QUV weathering apparatus described in Chapter 2. The material was exposed for durations of three, seven, ten, and twenty weeks.

Uniaxial tension tests were conducted on an Instron Model 2402 universal testing machine. All tests were ran at room temperature and at a constant crosshead speed of 0.2 inches per minute. The specimen geometry used is shown in Figure 4.1. A two inch 50% Instron extensometer was used on all tests conducted on unexposed material, and a two inch 10% Instron extensometer was used on two tests that were exposed for ten and twenty weeks. The crosshead displacement was used for the material that was exposed for three and seven weeks to avoid the possibility of the specimens breaking prematurely

at the point where the extensometer was connected. Four tension tests were run at each exposure duration.

The cross-sectional area of the tension specimens were measured periodically during testing of the ten and twenty week specimens to obtain the true stress values. This measurement was taken with micrometers which were read to the nearest thousandth of an inch.

RESULTS AND DISCUSSION

A limited amount of material was available for this study due to the small exposure area in the QUV weathering apparatus described in Chapter 2. Four tension tests were conducted at each exposure level but some of the specimens failed prematurely due to scratches or other flaws. These tests were discarded and replaced with a successful test as suggested by the ASTM standard [3]. All of the values reported in this study are averages depending on the number of tests that did not fail prematurely. Two successful tests were conducted on the unexposed material and on the material that was exposed for three weeks. For the material that was exposed for seven and twenty weeks, only one test strained through the entire gage length. Three successful tests were completed on the material that was exposed for ten weeks.

Strength and Stiffness

Both the strength and stiffness values for polycarbonate are highly dependent on the temperature of testing and rate of straining of the material. The strength and modulus values reported in this paper are for a strain rate of 0.2 inches per minute and a temperature of 75 degrees Fahrenheit.

The tensile strength was taken to be one of the measures of strength for comparison. The maximum engineering stress was attained at the yield point, so all values reported are assumed to be the tensile strength at yield unless otherwise noted. Although the variation in tensile strength is not as significant as the changes in ductility, noticeable changes occurred after the material was exposed to ultraviolet radiation. The tensile strength increased from 9040 psi for the unexposed polycarbonate to 9234 psi for the material that was exposed for twenty weeks. These values fall into the usual range of strength for polycarbonate material [16]. These changes are modeled linearly in Figure 4.2 at the end of this chapter. This minor increase in strength is somewhat deceptive and inconclusive since the actual cross-sectional area of the samples is not considered.

A more realistic measure of ductility may be found in the true stress at break. These values were found by dividing the final load at fracture by the final cross-sectional area. The true stress at break decreased after exposure to ultraviolet radiation as shown in Figure 4.3 where the changes were modeled as linearly decreasing. The true stress values ranged from 12,420 psi for the unexposed polycarbonate to 10,880 psi for the specimens exposed for twenty weeks. These results show that the material is weaker after exposure to ultraviolet radiation which would indicate chain scission.

The elastic modulus is a measure of the stiffness of a material. The elastic modulus can only be determined accurately if a calibrated extensometer is used which was the case for the unexposed polycarbonate specimens. The linear portion of the engineering stress-strain diagram is shown in Figure 4.4 from which the elastic modulus was found to be 331.9 ksi which falls in the accepted range for polycarbonate [16]. The stress-displacement curves were compared for specimens at each exposure time and are shown in Figure 4.5. No significant changes were seen in the stiffness obtained from the engineering stress-displacement diagrams after exposure to ultraviolet radiation.

Ductility

The percent elongation and percent reduction of area are the two measures of ductility that were used for this study. Significant changes were found in the percent elongation while only minor variation was seen in percent reduction of area. The percent elongation decreased from 88.5 % for the unexposed specimens to 62 % for the material that was exposed to ultraviolet radiation for twenty weeks. These results are shown in Figure 4.6 at the end of this chapter where they are modeled as a linearly decreasing function. It was difficult to measure the elongation since many of the degraded specimens broke before all of the material in the gage section was able to yield. This problem was attributed to cracks that formed in the brittle surface causing early failure. Because of this early failure, only the specimens which extended through the entire gage section were used for comparison of percent elongation.

The percent reduction of area reduced from 37.9 % for the unexposed polycarbonate to 32.8 % for the specimens that were exposed to ultraviolet light for seven weeks and then increased to 34.1 % for the twenty week samples. These changes are statistically significant since the largest standard deviation was found to be 0.7. The results of the percent reduction of area are shown in Figure 4.7 which indicate a partial recovery of polycarbonate after long periods of exposure to ultraviolet radiation which agrees with results from previous studies [7, 11]. This partial recovery is probably a result of the degraded surface layer becoming too weak to transmit force to the undamaged inner core material.

The reduction in ductility is due to the embrittlement of the surface layer of the exposed polycarbonate specimens. This embrittlement was evident by crazes that grew normal to the loading direction and became visible on the directly exposed surface after the yielding of the material. Although crazes resemble cracks, the opening in the material which would be considered a crack is covered by a mesh of microfibrils that are able to carry a load [17].

These crazes can be seen in micrographs of the surface of the broken specimens in Figures 4.8 and 4.9. Cracks initiated in the crazes and began to grow from the edge of the tension specimens during loading as shown in the micrograph of the edge of the ten and twenty week samples in Figure 4.10. Ultimate failure occurred when one of these cracks grew across the width of the specimen.

REFERENCES

1. J. R. White and A. Turnbull, "Review Weathering of polymers: mechanisms of degradation and stabilization, testing strategies and modelling," *Journal of Materials Science*, **29**, 584-613 (1994)
2. N. E. Dowling. *Mechanical Behavior of Materials: Engineering Methods for Deformation, Fracture, and Fatigue*. Ch. 5, Prentice Hall, Englewood Cliffs, NJ (1993)
3. ASTM Standard D638-91, "Standard Test Method for Tensile Properties of Plastics", *Annual Book of ASTM Standards*, pp. 52-64.
4. R. A. Heller and A. A. Pap, *Mechanics and Materials TV Tape Series Vol. IV*, pp. 3-4, McGraw-Hill Book Company, New York
5. G. E. Schoolenberg, "A fracture mechanics approach to the effects of UV-degradation on polypropylene," *Journal of Materials Science*, **23**, 1580-1590 (1988)
6. G. E. Schoolenberg and P. Vink, "Ultraviolet degradation of polypropylene: 1. Degradation profile and thickness of the embrittled surface layer," *Polymer*, **32**, 432-437 (1991)
7. G. E. Schoolenberg and H. D. F. Meijer, "Ultraviolet degradation of polypropylene: 2. Residual strength and failure mode in relation to the degraded surface layer," *Polymer*, **32**, 438-444 (1991)
8. P. So and L. J. Broutman, "The effect of Surface Embrittlement on the Mechanical Behavior of Rubber-Modified Polymers," *Polymer Engineering and Science*, **22**, 888-894 (1982)
9. P. K. So and L. J. Broutman, "The Fracture Behavior of Surface Embrittled Polymers," *Polymer Engineering and Science*, **26**, 1173-1179 (1986)
10. A. K. Kulshreshtha, "Chemical Degradation", Ch.3, pp. 55-94, *Handbook of Polymer Degradation*, S. Halim Hamid, M. B. Amin, and A. G. Maadhah eds. Marcel Dekker, Inc. NY (1992)

11. E. S. Sherman, A. Ram, and S. Kenig, "Tensile Failure of Weathered Polycarbonate," *Polymer Engineering and Science*, **22**, 457-465 (1982)
12. M. R. Kamal and B. Huang, "Natural and Artificial Weathering of Polymers", Ch.5, pp. 127-168, *Handbook of Polymer Degradation*, S. Halim Hamid, M. B. Amin, and A. G. Maadhah eds. Marcel Dekker, Inc. NY (1992)
13. M. M. Qayyum and J. R. White, "Plastic fracture in Weathered Polymers," *Polymer*, **28**, 469-476 (1987)
14. M. Raab, L. Kotulak, J. Kolarik, and J. Pospisil, "The effect of Ultraviolet Light on the Mechanical Properties of Polyethylene and Polypropylene Films," *Journal of Applied Polymer Science*, **27**, 2457-2466 (1982)
15. A. Davis and D. Sims, *Weathering of Polymers*, Applied Science Publishers, London, 1983.
16. D. R. Askeland, *The Science and Engineering of Materials, 2nd Edition*. p.537, PWS-KENT Publishing Company, Boston, 1989
17. J. I. Kroschwitz, Ed. *Concise Encyclopedia of Polymer Science and Engineering*, p. 210-211, Wiley-Interscience, NY, 1990

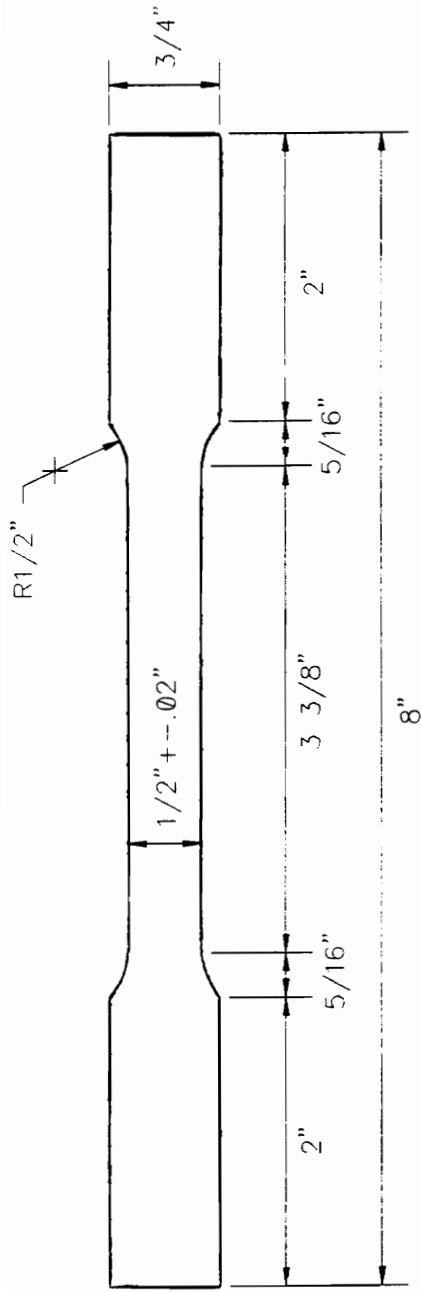


FIGURE 4.1 Tension specimen geometry

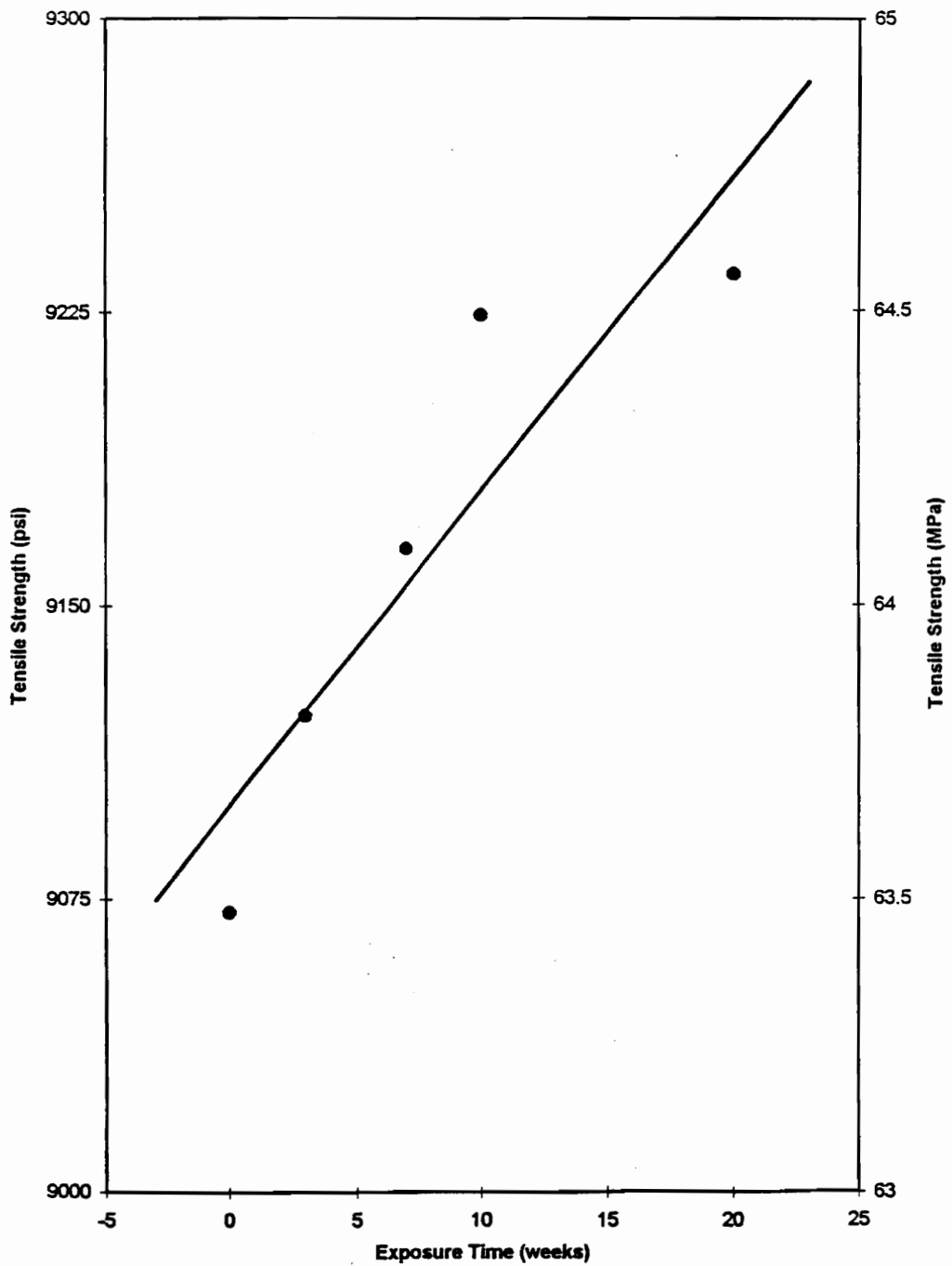


FIGURE 4.2 Engineering tensile strength at yield versus weeks of ultraviolet exposure

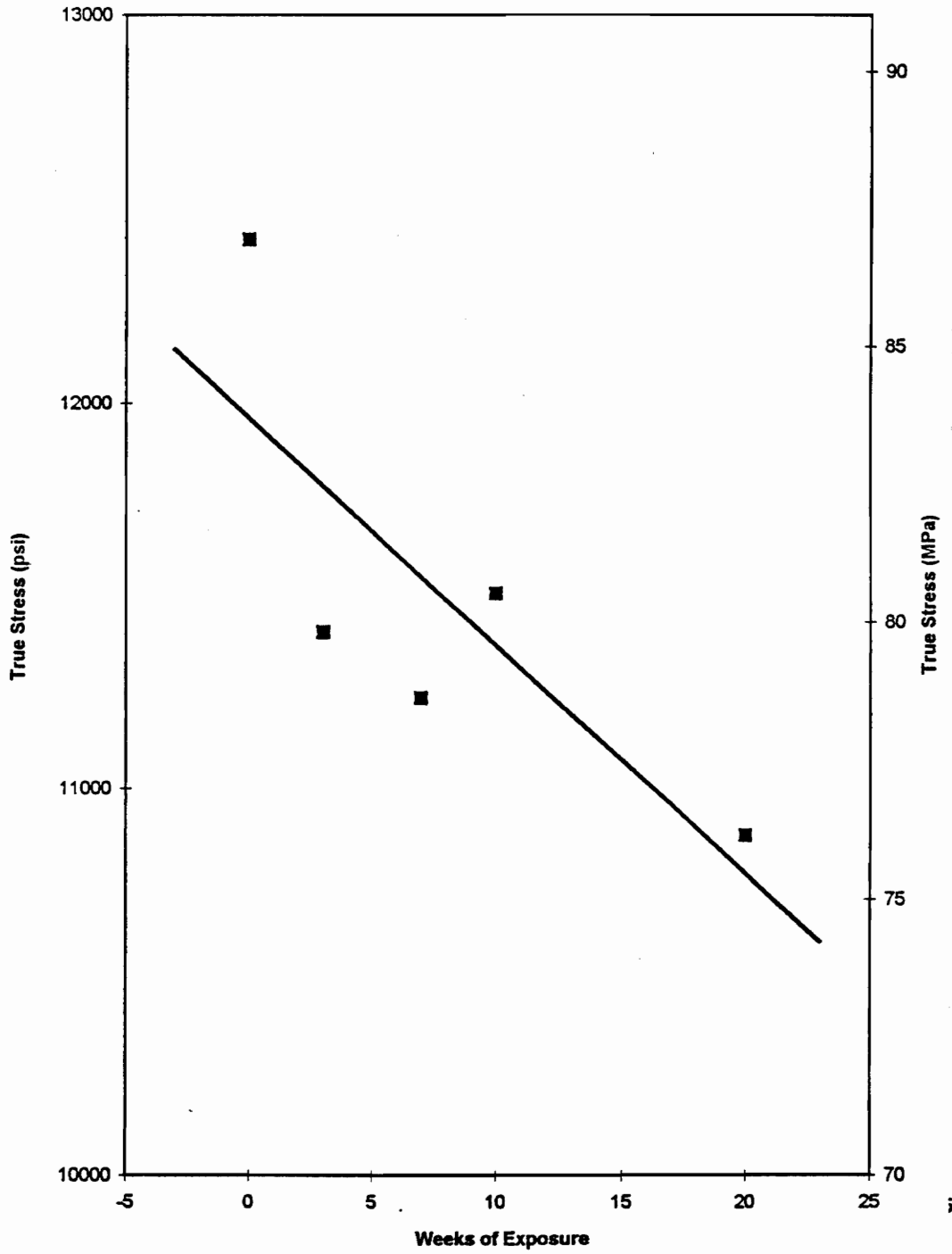


FIGURE 4.3 True stress at fracture of polycarbonate tension specimens

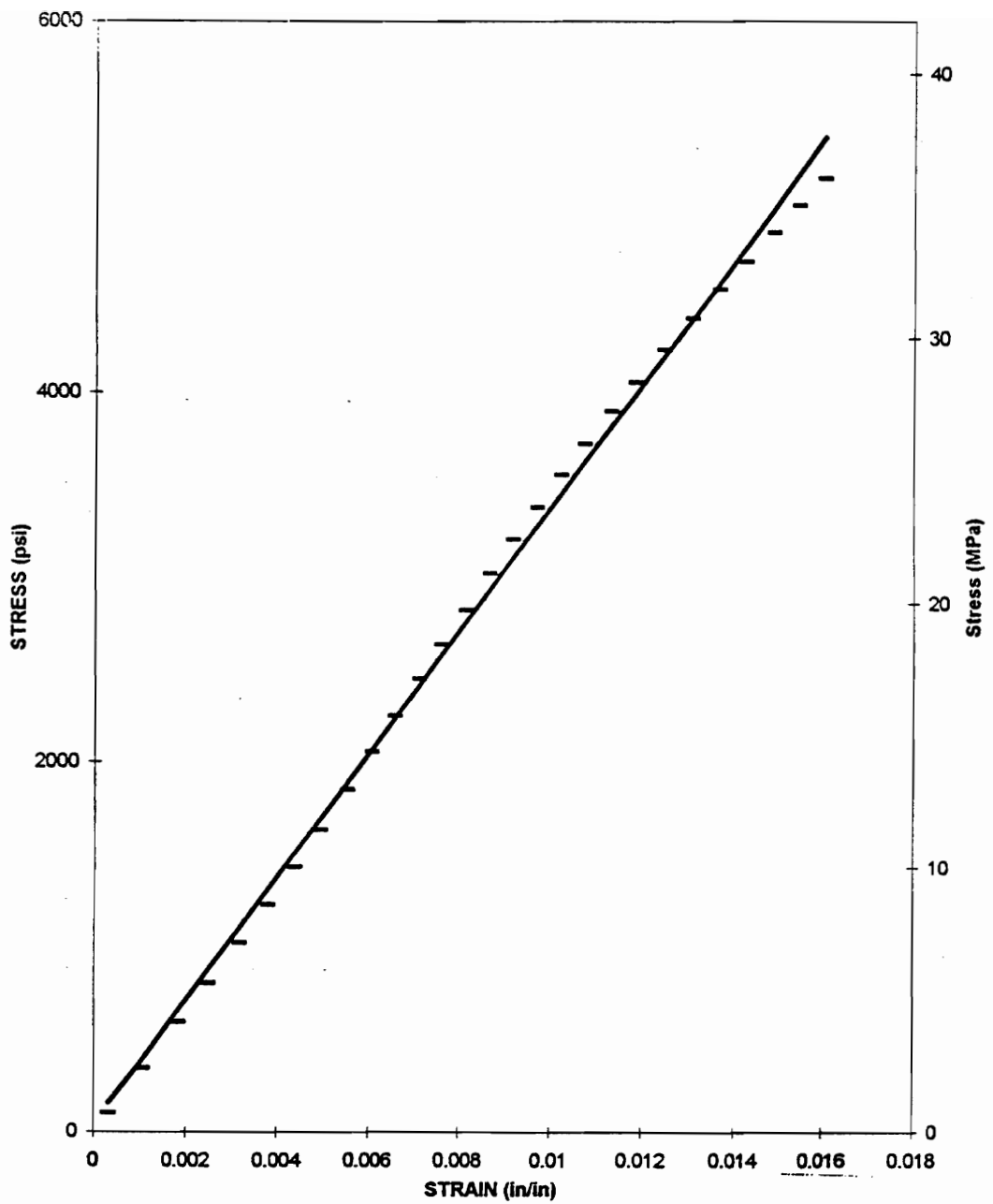


FIGURE 4.4 Linear portion of engineering stress versus extensometer strain of unexposed polycarbonate for determination of Young's modulus

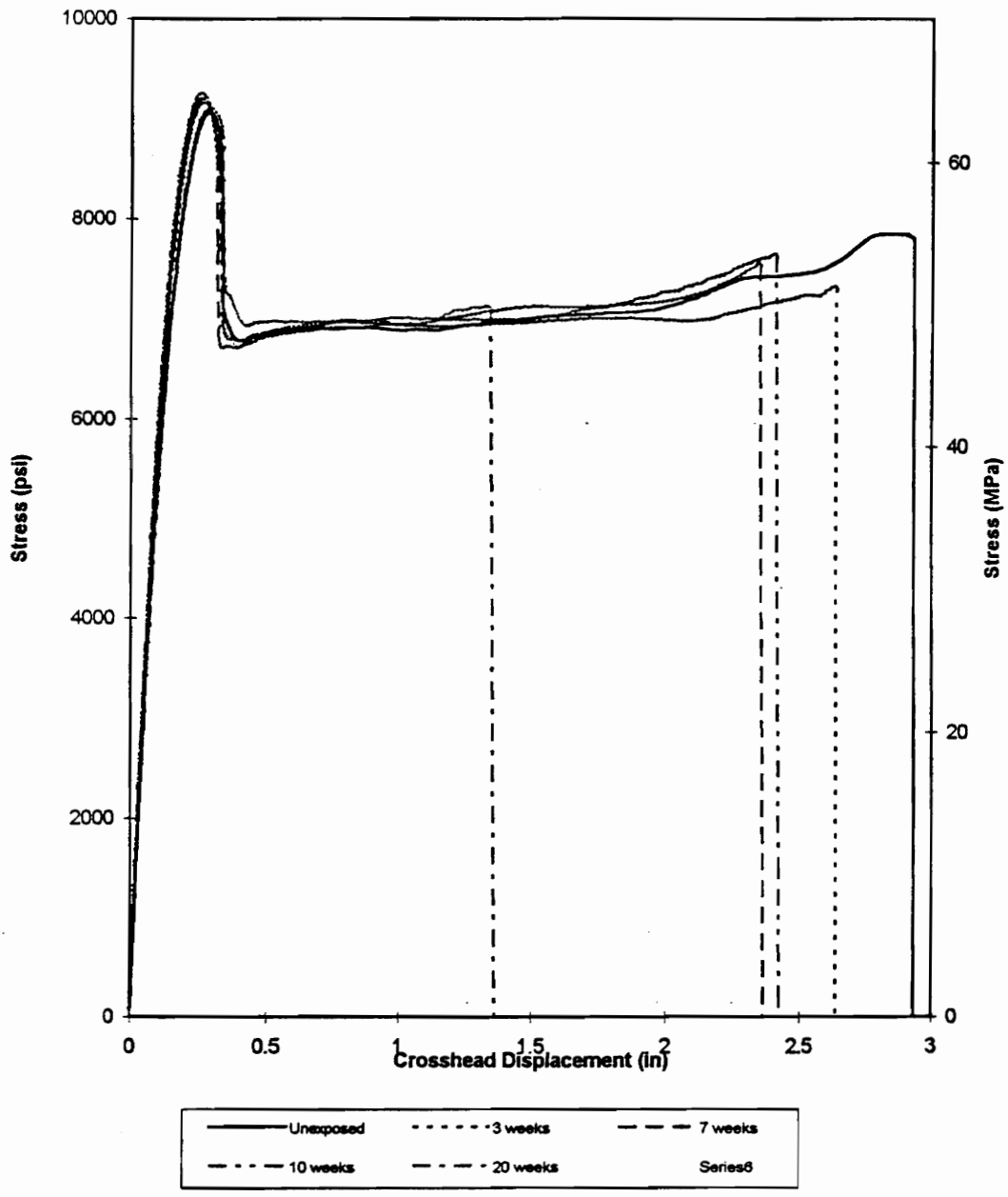


FIGURE 4.5 Engineering stress-displacement diagrams for polycarbonate material exposed to ultraviolet radiation for 0, 3, 7, 10, and 20 weeks.

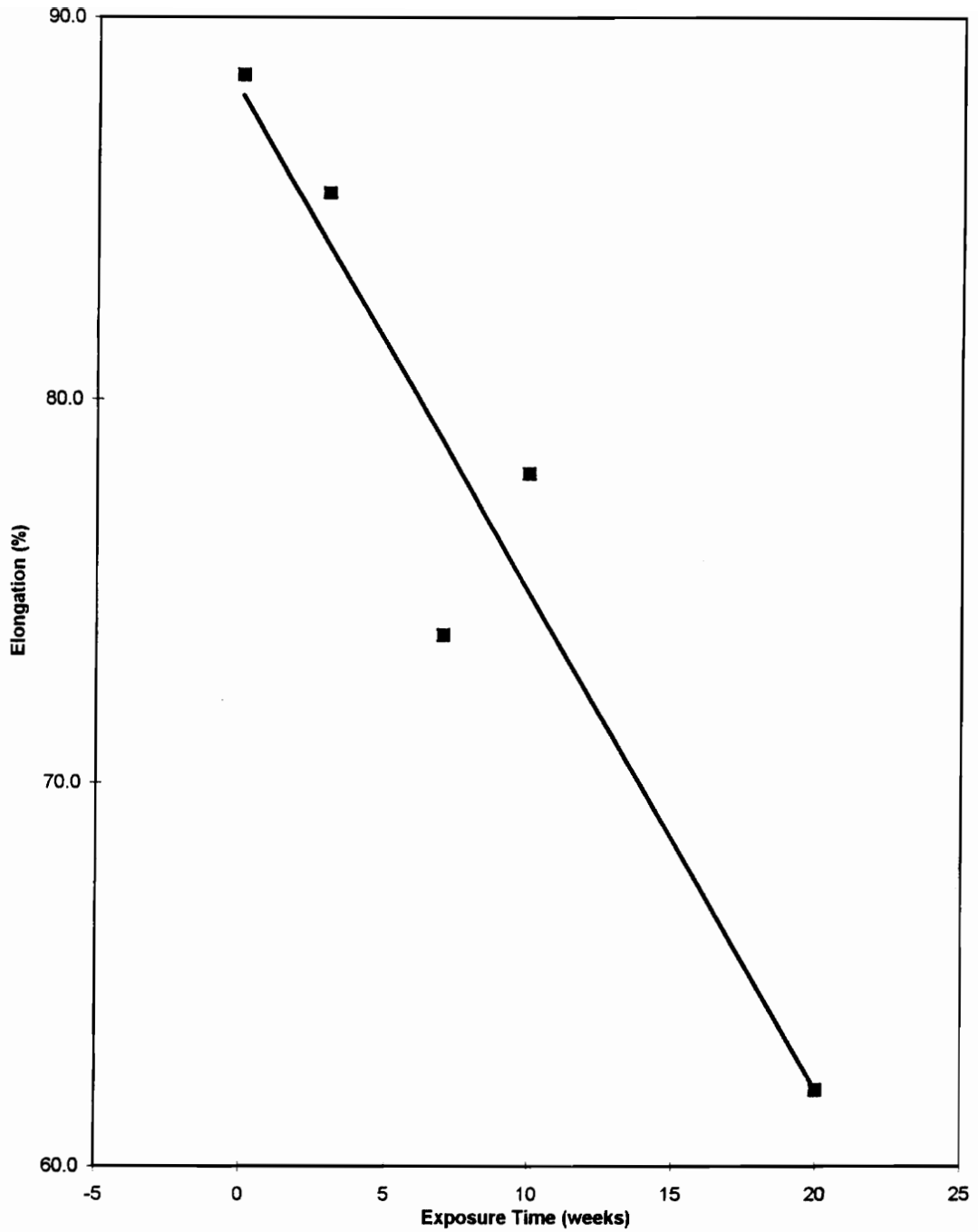


FIGURE 4.6 Percent elongation of polycarbonate tension specimens versus weeks of ultraviolet exposure.

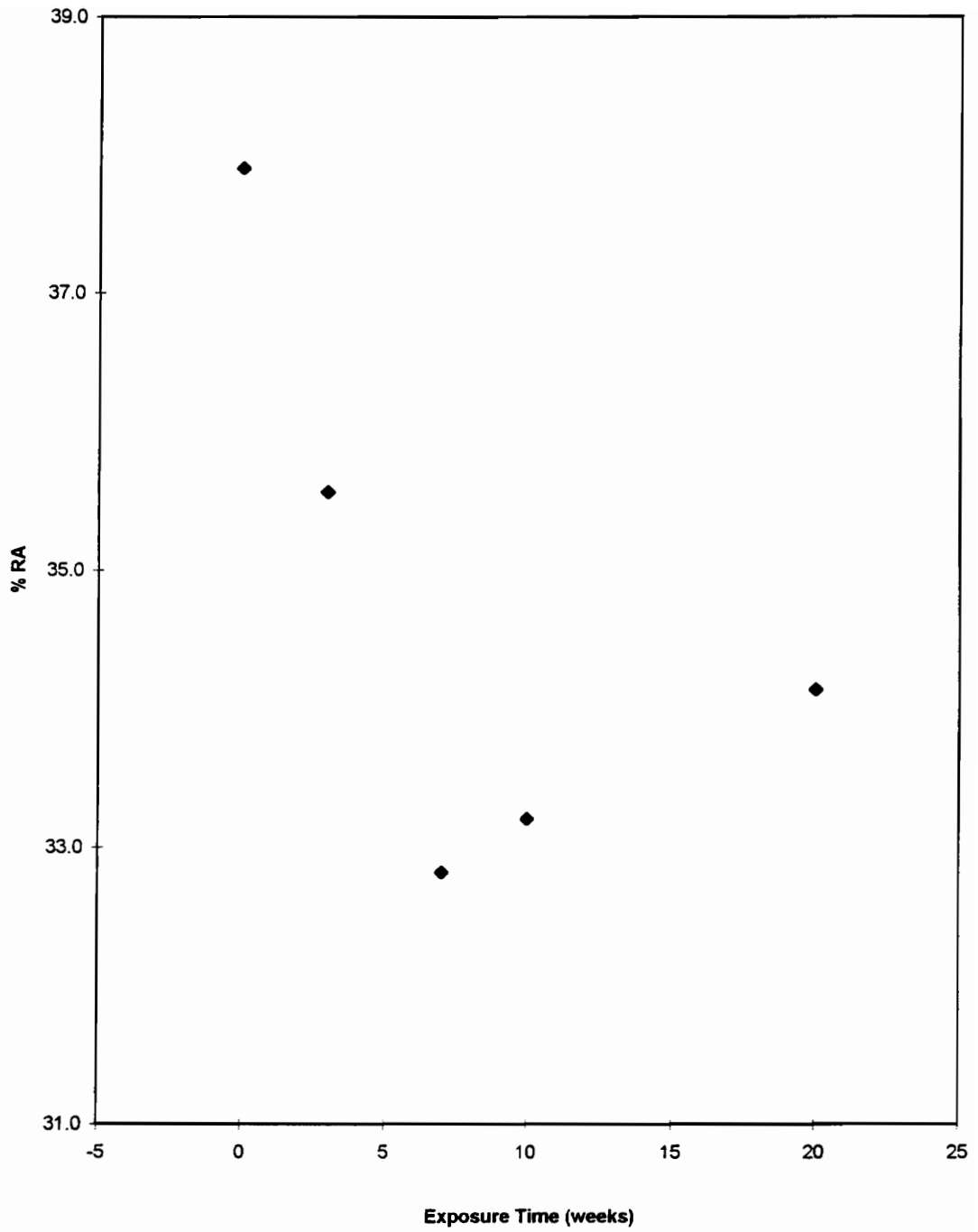


FIGURE 4.7 Percent reduction of area of polycarbonate tension specimens versus weeks of ultraviolet exposure

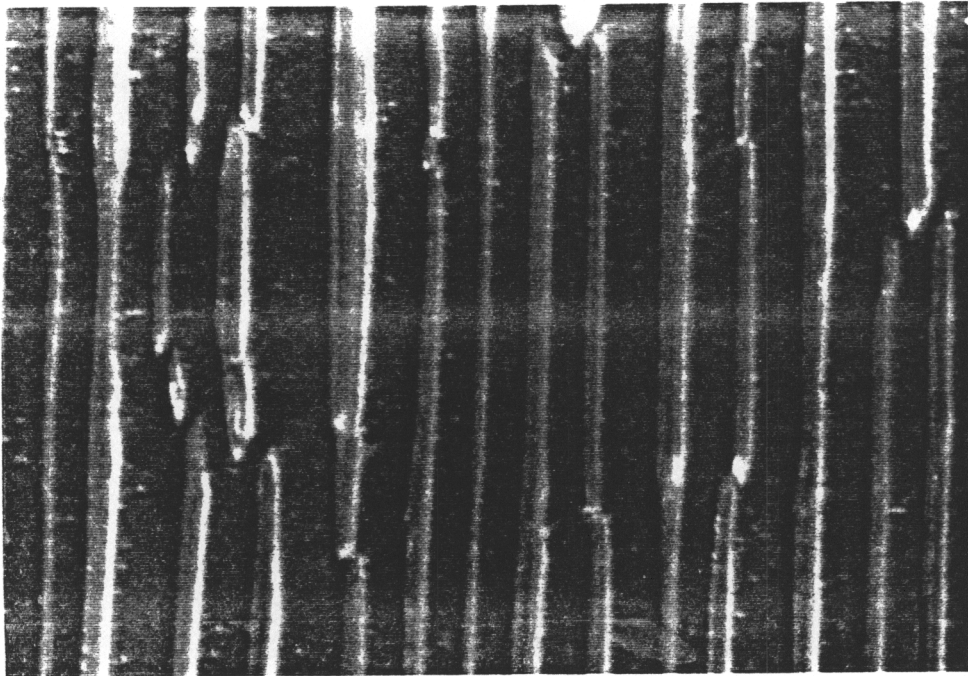
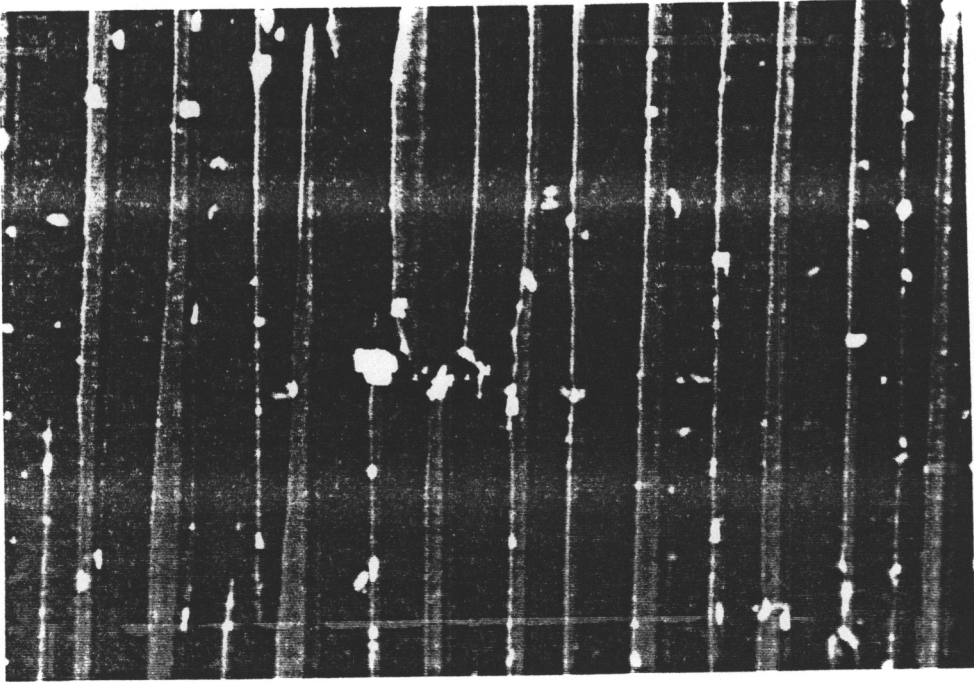


FIGURE 4.8 Micrograph of surface of polycarbonate tension specimens after exposure periods of (top) 3 weeks and (bottom) 7 weeks

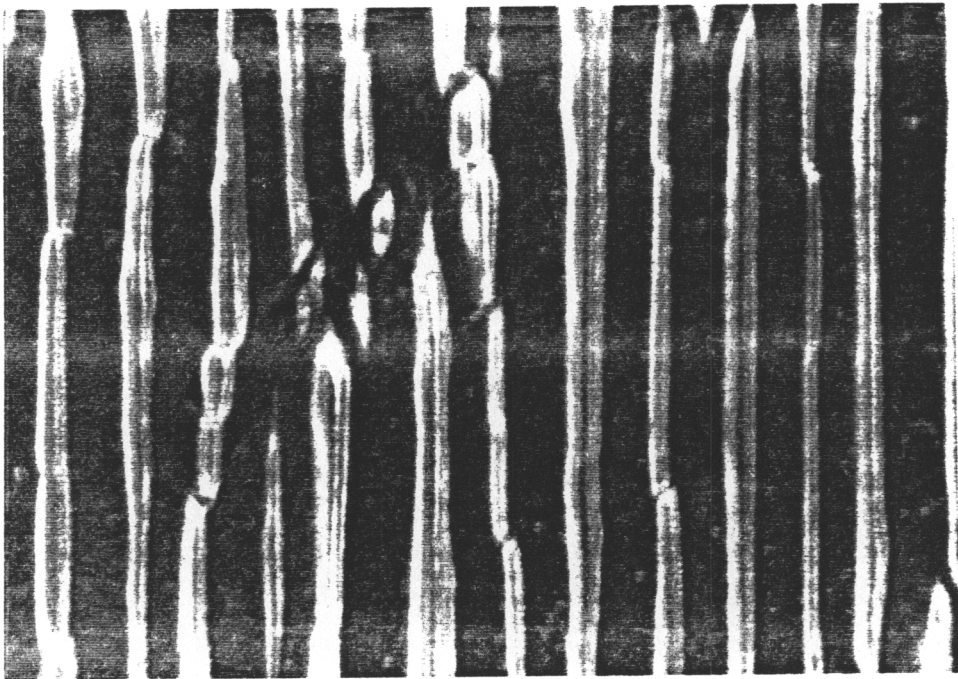
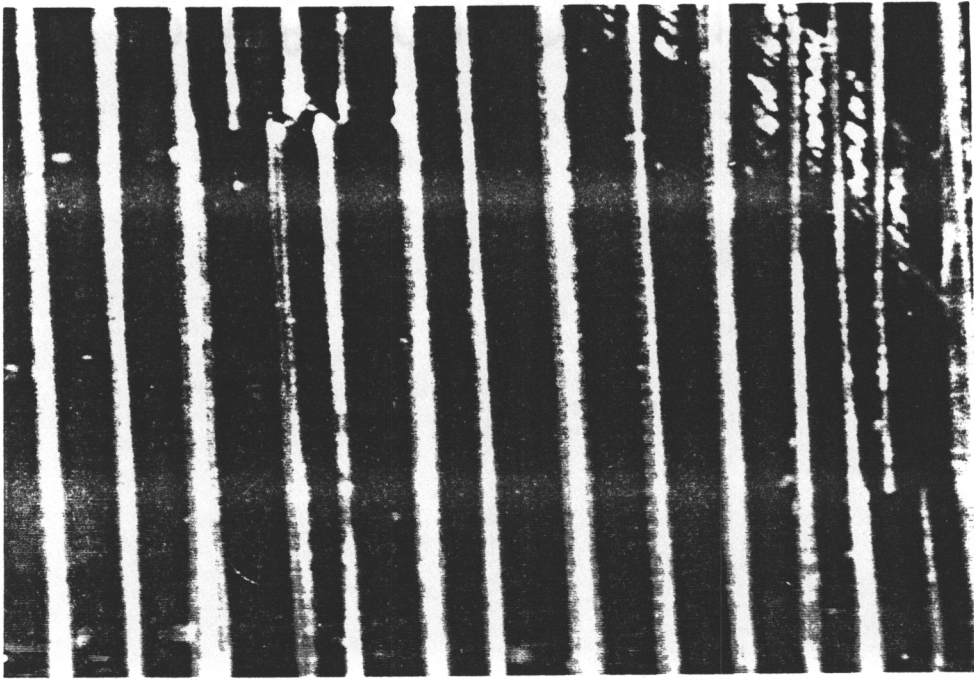


FIGURE 4.9 Micrograph of surface of polycarbonate tension specimens after exposure durations of (top) 10 weeks and (bottom) 20 weeks

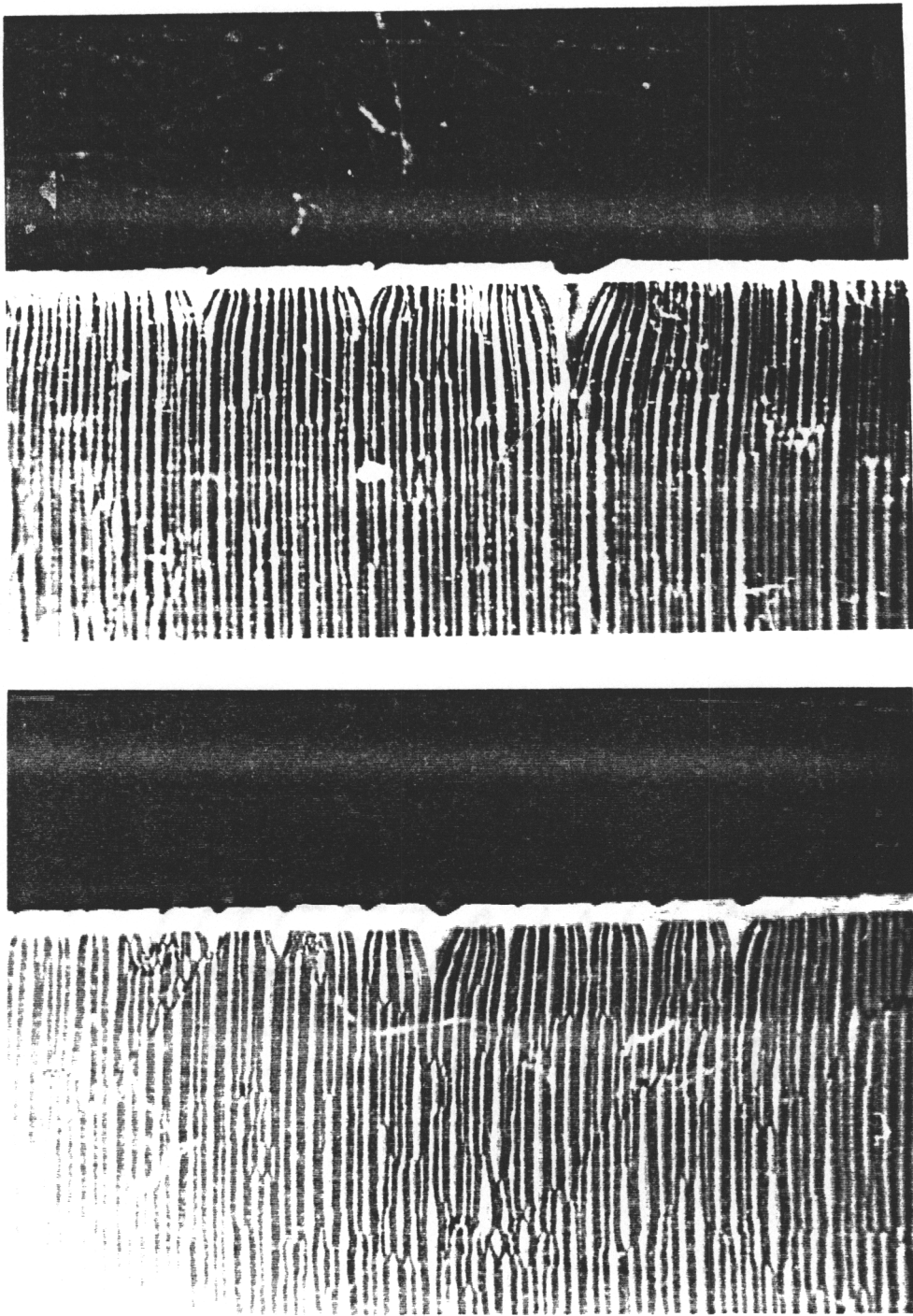


FIGURE 4.10 Micrograph of edge of polycarbonate tension specimens after exposure durations of (top) 10 and (bottom) 20 weeks

CHAPTER 5
EFFECT OF ULTRAVIOLET EXPOSURE ON THE MOLECULAR WEIGHT OF
POLYCARBONATE

INTRODUCTION

The molecular weight of a polymer is a very important characteristic to examine since it is directly related to the material's bulk mechanical properties [1]. Unlike crystalline structures such as metals, a single value for the molecular weight of polymers cannot be defined. Polymeric materials are polydisperse [2] which means that all of the molecules in the material do not have the same weight. Due to polydispersity polymers possess a distribution of molecular weights. Two molecular weight distributions that have been defined are the number average molecular weight, M_n , and the weight average molecular weight, M_w . These averages may be calculated using the following equations [1].

$$M_n = \frac{\sum_i N_i M_i}{\sum_i N_i} \quad (1)$$

$$M_w = \frac{\sum_i N_i M_i^2}{\sum_i N_i M_i} \quad (2)$$

In the above equations N_i is the number of molecules that have the molecular weight M_i . The number average molecular weight is unbiased and gives the distribution of the number of molecules of a polymer. The number average molecular weight is important in determining any changes in physical properties that are related to the free volume since it gives an indication of the number of chain ends in a polymer. The weight average

molecular weight is biased toward the heavier molecules which skews the entire distribution to the right [2]. Unless a material is monodisperse with the weight of each molecule being equal, the weight average molecular weight will always be larger than the number average molecular weight. For a monodisperse material the two values will be equal.

Many material properties of a polymer depend on M_n with the following relation [2]:

$$X = X_\infty - \frac{K}{\langle M_n \rangle} \quad (3)$$

where X is the property of the real material, X_∞ is the material property of an infinitely long polymer chain, K is a constant, and $\langle M_n \rangle$ is the number average molecular weight. Some examples of properties that follow the above relation are the glass transition temperature, tensile strength, density, and heat capacity [2]. Changes in these properties occur with changes in molecular weight since the molecular weight is directly related to the amount of free volume contained in the material [2].

Various methods exist to determine the molecular weight averages of polymeric materials. The most popular method of determining M_n is by osmometry [3] while M_w is usually determined by light scattering techniques [4]. Another method of molecular weight determination is by means of the size exclusion principle. The size exclusion technique that will be discussed in this paper is called gel permeation chromatography (GPC).

Gel Permeation Chromatography

Gel permeation chromatography is a method in which the polymer is dissolved in a solvent passing through columns with a material of various pore sizes [1]. The theory and some common errors that arise with GPC are given in references [5] and [6]. As the mixture passes through the columns the smaller molecules disperse into the small pores while the larger molecules continue flowing. The principle of GPC relies on the fact that the larger molecules pass through the columns more quickly than the smaller ones. A detector is located at the end of the columns that continuously measures the concentration of the solution. The retention time, which is the length of time that a particle remains in the columns, gives a relative distribution of molecular weight, \hat{M}_r [1]. The value for \hat{M}_r is near the average of M_n and M_w . The number average and weight average molecular weight distributions can be derived from the molecular weight distribution obtained by GPC.

The columns in a GPC apparatus are very important components to maintain to obtain accurate results. Rabel [7] describes how to properly care and use the columns. They are calibrated with the use of a polymer with a known molecular weight. Polystyrene, PS, is commonly used as the standard [1]. The recorded molecular weight distributions are frequently those of the equivalent PS radius of gyration which can be considerably different from the absolute molecular weight [1]. Despite the possibility of error the GPC technique has become one of the most popular procedures of determining the molecular weights of polymers. One of the reasons for the popularity of GPC is the fact that the entire distribution of molecular weights can be obtained in a matter of minutes compared to other techniques which may be more complicated and time consuming and only yield the averages [8].

EXPERIMENTAL DETAIL

An aircraft grade polycarbonate was investigated that was obtained from Rohm and Haas in Philadelphia, Pennsylvania. GPC tests were performed on material that was exposed to ultraviolet light in the QUV weathering apparatus for periods of three, seven, ten, and twenty weeks.

The determination of molecular weight was performed on a gel permeation chromatography apparatus produced by Waters Associates. Since photodegradation is primarily a surface phenomenon, molecular weight measurements were made on thin surface layers of both the directly exposed and indirectly exposed sides of the specimens for the unexposed, three week, and seven week samples. The layers were removed with a knife blade and dissolved in chloroform. The solution was then injected into the GPC apparatus to obtain the relative molecular weight distribution. The GPC columns were calibrated with a polystyrene standard. As mentioned above the results obtained with a polystyrene standard are not necessarily equal to the absolute molecular weight of polycarbonate, but the molecular weight distributions found for this study are relative distributions that provide an excellent method for comparing the unexposed polycarbonate to the material that was exposed to ultraviolet radiation.

RESULTS AND DISCUSSION

Exposure to ultraviolet radiation typically causes a weight loss in polymeric materials. Qayyum and White [9] found that after outdoor exposure in the hot and dry climate of Saudi Arabia for three years, the weight average molecular weight changed from 43,400 to 24,400, and the number average molecular weight was reduced from 24,000 to 13,700. This significant reduction in molecular weight suggests that chain

scission occurs in outdoor exposure during which a major contributor to material degradation is ultraviolet radiation from sunlight.

As mentioned in Chapter 4 of this paper, ultraviolet radiation effects only a thin layer on the surface of the material which changes the overall behavior during testing [10-19]. So and Broutman [10] found that the molecular weight of the surface of a polymer is directly related to the ductility of the entire material. After applying a low molecular weight coating to polymers, they found that the amount of elongation in a tension test is significantly reduced. This type of experiment is one method of modeling weathering effects in polymers.

Kusy and Greenberg [20] studied how the molecular weight effects the dynamic mechanical properties of poly/methyl methacrylate. They found that the larger number of chain ends in the lower molecular weight material caused the glass-rubber transition region to shift to lower temperatures.

The relative molecular weight averages of polycarbonate determined by GPC are shown in Figure 5.1. The two curves that are shown represent the molecular weight averages of the directly and indirectly exposed surfaces. It can be seen that the average molecular weight of the directly exposed surface decreased from a value of 55,417 for the unexposed material to 38,500 for the seven week sample. The indirectly exposed surfaces saw only a minor reduction of about seven percent to a value of 51,458. These results indicate that the surface directly exposed to ultraviolet radiation is affected much more than the indirectly exposed surface which agrees with the conclusions drawn in the remainder of the chapters in this report. This decrease in average molecular weight indicates that polycarbonate undergoes chain scission during exposure to ultraviolet radiation which is in agreement with the conclusions drawn from the reduction in strength in Chapter 4.

An entanglement occurs when the chains in a polymer interact with one another decreasing the molecular mobility. The mechanical properties of a polymer are directly related to the molecular weight since more entanglements occur at larger molecular

weights. Polymers possess a critical molecular weight below which the polymer chains are not able to twist together. The critical molecular weight for polycarbonate is only 3000 g/mol [21]. After seven weeks of exposure the material in this study still had a molecular weight of 38,500 g/mol, indicating that a large number of entanglements should still be present.

The samples for both the directly and indirectly exposed surfaces were obtained by identical techniques. The small change in the molecular weight of the indirectly exposed surfaces indicate that chain scission is not occurring on a large scale during removal of the sample.

REFERENCES

1. L. H. Sperling, *Introduction to Physical Polymer Science, 2nd Ed.*, Chapter 3, John Wiley & Sons, Inc. NY, 1992
2. Class notes, *Polymer Engineering*, R. Kander, Virginia Polytechnic Institute and State University (1995)
3. A. R. Cooper, "Determination of number average molecular weight by end-group analysis, vapor pressure measurements, and cryoscopy", Ch. 2, pp.7-14, *Determination of Molecular Weight*, A. R. Cooper ed., John Wiley & Sons, NY (1989)
4. B. Chu, "Laser light scattering", Ch. 5, pp. 53-86, *Determination of Molecular Weight*, A. R. Cooper ed., John Wiley & Sons, NY (1989)
5. A. A. Gorbunov and A. M. Skvortsov, "Separating power of gel permeation chromatography," *Polymer Science USSR*, **32**, 567-574 (1990)
6. D. W. Shortt, "Differential molecular weight distributions in high performance size exclusion chromatography," *Journal of Liquid Chromatography*, **16**, 3371-3391 (1993)
7. F. M. Rabel, "Use and Maintenance of Microparticle High Performance Liquid Chromatography Columns," *Journal of Chromatographic Science*, **18**, 394-408 (1980)
8. J. R. White and A. Turnbull, "Review Weathering of polymers: mechanisms of degradation and stabilization, testing strategies and modelling," *Journal of Materials Science*, **29**, 584-613 (1994)
9. M. M. Qayyum and J. R. White, "Plastic fracture in Weathered Polymers," *Polymer*, **28**, 469-476 (1987)
10. P. So and L. J. Broutman, "The effect of Surface Embrittlement on the Mechanical Behavior of Rubber-Modified Polymers," *Polymer Engineering and Science*, **22**, 888-894 (1982)
11. G. E. Schoolenberg, "A fracture mechanics approach to the effects of UV-degradation on polypropylene," *Journal of Materials Science*, **23**, 1580-1590 (1988)

12. G. E. Schoolenberg and P. Vink, "Ultraviolet degradation of polypropylene: 1. Degradation profile and thickness of the embrittled surface layer," *Polymer*, **32**, 432-437 (1991)
13. G. E. Schoolenberg and H. D. F. Meijer, "Ultraviolet degradation of polypropylene: 2. Residual strength and failure mode in relation to the degraded surface layer," *Polymer*, **32**, 438-444 (1991)
14. P. K. So and L. J. Broutman, "The Fracture Behavior of Surface Embrittled Polymers," *Polymer Engineering and Science*, **26**, 1173-1179 (1986)
15. A. K. Kulshreshtha, "Chemical Degradation", Ch.3, pp. 55-94, *Handbook of Polymer Degradation*, S. Halim Hamid, M. B. Amin, and A. G. Maadhah eds. Marcel Dekker, Inc. NY (1992)
16. E. S. Sherman, A. Ram, and S. Kenig, "Tensile Failure of Weathered Polycarbonate," *Polymer Engineering and Science*, **22**, 457-465 (1982)
17. M. R. Kamal and B. Huang, "Natural and Artificial Weathering of Polymers", Ch.5, pp. 127-168, *Handbook of Polymer Degradation*, S. Halim Hamid, M. B. Amin, and A. G. Maadhah eds. Marcel Dekker, Inc. NY (1992)
18. M. Raab, L. Kotulak, J. Kolarik, and J. Pospisil, "The effect of Ultraviolet Light on the Mechanical Properties of Polyethylene and Polypropylene Films," *Journal of Applied Polymer Science*, **27**, 2457-2466 (1982)
19. A. Davis and D. Sims, *Weathering of Polymers*, Applied Science Publishers, London, 1983.
20. R. P. Kusy and A. R. Greenberg, "Influence of Molecular Weight on the Dynamic Mechanical Properties of Poly(methyl methacrylate)," *Journal of Thermal Analysis*, **18**, 117-126 (1980)
21. D. W. Van Krevelen, *Properties of Polymers*, p. 339, Elsevier Scientific Publishing Company, Amsterdam, 1976

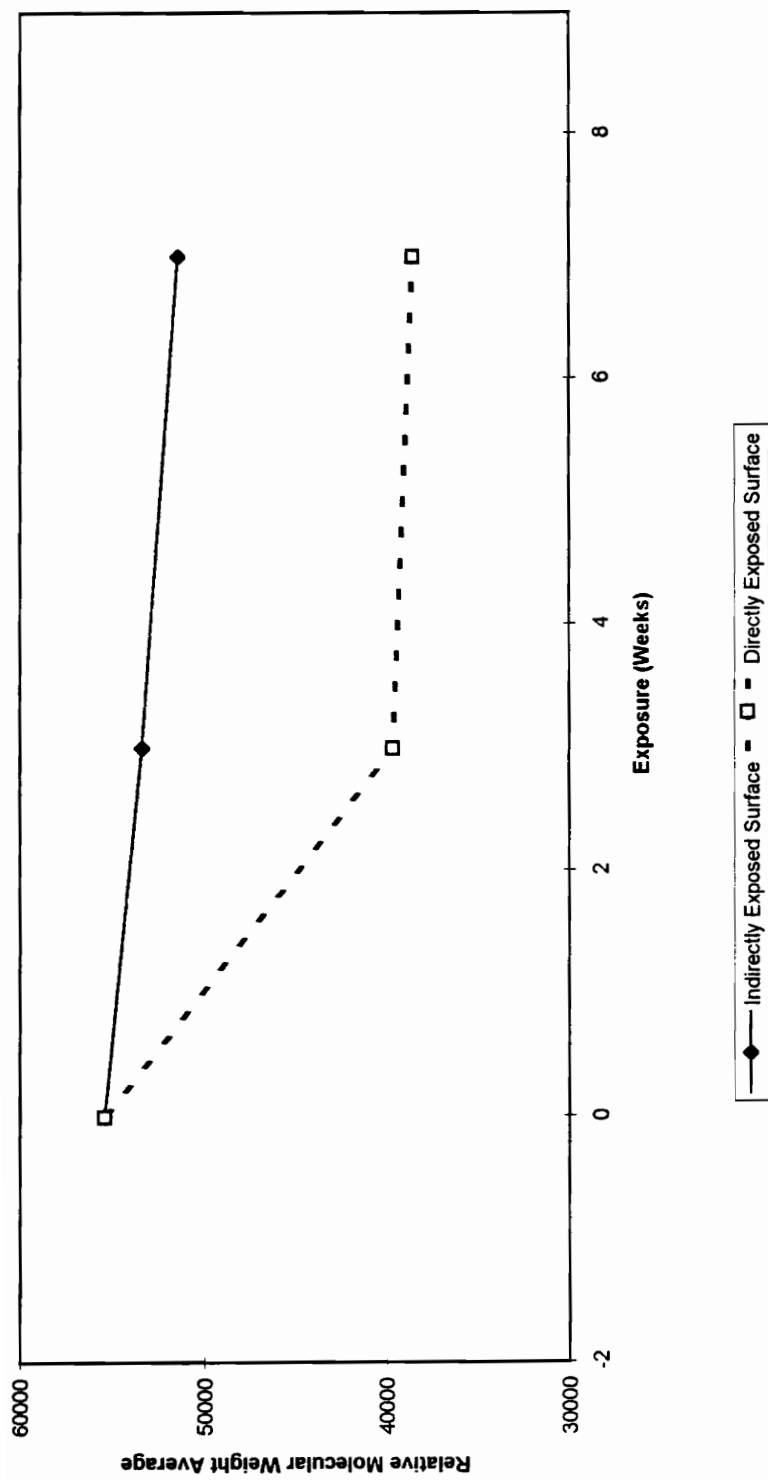


FIGURE 5.1 Relative molecular weight averages of polycarbonate as determined by gel permeation chromatography for surfaces indirectly and directly exposed to ultraviolet radiation for durations of 0, 3, and 7 weeks.

CHAPTER 6
EFFECT OF ULTRAVIOLET EXPOSURE ON THE HARDNESS OF
POLYCARBONATE

INTRODUCTION

Hardness is a mechanical property defined as a material's resistance to penetration. Hardness measurements provide a method of comparison for different materials, like the materials in this study that have been exposed to various doses of ultraviolet radiation. The determination of the microhardness has also been shown to be a way to determine the glass transition temperature, and to track the thermal expansion, density and amount of crystallization of a material [1-2]. Balta-Calleja and co-workers have found that the microhardness of polymers correlates well with the microstructure [3-7].

The hardness of metals and other crystalline structures is determined by a different mechanism than the hardness of polymeric semi-crystalline and amorphous materials [3]. The hardness value of metallic materials depends on dislocation movements along slip systems during indentation. Microindentation in polymeric materials is more of a local deformation in which the hardness value depends upon the arrangement of the crystals if the polymer is semi-crystalline [3]. If the polymer is amorphous then the microhardness depends upon the local restraints in the segments of the chain since a microindentation causes bundles of chains to displace [1].

Hardness Testing

Hardness testing is usually conducted by applying a penetrator to the hardness specimen to create an indentation in the material. The hardness value for the tested material is calculated from the size of the indentation which is a measure of the material's resistance to penetration. Two types of hardness testing are the macro-indentation and

micro-indentation tests. The most commonly used macro-indentation techniques are the Brinell and Rockwell hardness tests. These test methods are generally used on hard materials such as metals since a relatively large load, up to 3000 kg, is used to penetrate the material creating an indentation large enough to be seen without a microscope [8].

The most common micro-indentation methods are the Vickers and Knoop microhardness tests. The indentation made in a microhardness test requires the use of a microscope to measure the size [8]. The Vickers technique uses a pyramidal-shaped diamond penetrator. Both diagonals of the indentation, which should be of equal length, must be measured to obtain a hardness value. The Knoop method also uses a diamond pyramid indenter. The difference in the Knoop indentation is that the shape of the indentation is a parallelogram with the length of one diagonal approximately seven times longer than the other diagonal as shown in Figure 6.1 [9]. Only the length of the longer diagonal is required to obtain the hardness measurement.

One problem associated with obtaining an accurate hardness value is elastic recovery of the material. Several investigators have noted that after the load is removed from the material that a certain amount of elastic recovery occurs depending upon the material's elastic modulus [9-11]. Some amount of recovery will take place for all materials, but polycarbonate is a viscoelastic material for which the recovery could continue for a long period of time. Due to this recovery the area of the indentation after removal of the load is smaller than the area during loading [10] which makes it difficult to get a true hardness reading. To minimize the error due to recovery the hardness measurement should be taken soon after the load is removed. Also, the Knoop indenter produces the smallest error since considerable elastic recovery has been seen in the shorter diagonal but only minor changes occur in the longer diagonal after the load is removed [9]. Thus, a reasonably accurate value for hardness can be obtained by the Knoop technique since the hardness reading is found only from the length of the longer diagonal.

It has been stated throughout this paper that the degradation due to ultraviolet radiation is limited to a thin layer on the surface of the material [12-13]. To obtain an

accurate measurement of the hardness of a thin surface layer the indentation made by the hardness tester should penetrate the surface as little as possible. The Knoop microhardness test is the best choice for this study since it produces the shallowest indentation compared to the other common techniques. In fact, the indentation in a Vickers microhardness test is about twice as deep as the indentation in a Knoop microhardness test for the same applied load as shown in Figure 6.2 [9,14].

EXPERIMENTAL DETAILS

The investigated material was an aircraft grade polycarbonate obtained from Rohm and Haas in Philadelphia, Pennsylvania. Knoop microhardness tests were performed on material that was exposed to ultraviolet light in the QUV weathering chamber for intervals of three, seven, ten, and twenty weeks.

A Tukon Microhardness Tester with attached microscope was used to measure the hardness of the polycarbonate before and after exposure to ultraviolet radiation. The microhardness tester is described in Table 6.1 and shown in Figure 6.3 [14] at the end of this chapter. The Knoop indenter was used with a load of 25 grams which was suggested by the Tukon Microhardness Tester manual [14] to produce a shallow diamond-shaped indentation as shown in Figure 6.1. The length of the longer diagonal of the indentation was measured with a 10x filar unit. The Tukon Microhardness Tester automatically calculated the Knoop hardness number, H_K , from the length of the longer diagonal given a calibration factor of 1.0072 microns. The Knoop hardness number is defined as a ratio of the applied force to the projected area of the indentation which gives units of pressure or stress [9]. The simplified equation for the Knoop hardness value, H_K , is given by

$$H_K = \frac{P(\text{kg} \cdot f)}{A_p} = \frac{P(\text{kg} \cdot f)}{d \times c} = \frac{P(\text{kg} \cdot f)}{0.07028 \times d} = \frac{14.229 \times P(\text{kg} \cdot f)}{d} = \frac{14,229 \times P(\text{g} \cdot f)}{d} \quad (1)$$

where P is the testing load in kilogram-force or gram-force as indicated, A_p is the projected area of the indentation in square millimeters, d is the length of the longer diagonal in millimeters, and c is an indenter constant that relates the indentation projected area to the square of the length of the longer diagonal [14].

Five microhardness measurements were taken on both specimen surfaces in each period of exposure to ultraviolet light. The specimens were not ground and polished since grinding the exposed surfaces would destroy the thin degraded layer, but they were handled carefully to avoid excessive scratches and abrasions. To minimize the effect of elastic recovery, the longer diagonal of each microindentation was measured within thirty seconds after removal of the load. The spacing between each indentation was at least three diameters as suggested by the TUKON microhardness tester manual [14] to avoid interference. No hardness measurements were taken near the edge of the sample to avoid the strain being absorbed by the specimen surface [11] resulting in erroneous hardness values.

RESULTS AND DISCUSSION

The results of the microhardness tests on degraded polycarbonate are shown graphically in Figure 6.4 for which each data point is an average of five hardness readings. No microhardness measurements were taken on the unexposed polycarbonate due to the difficulty in focusing the microscope on the transparent, colorless material.

The specimen surfaces that were not directly exposed to ultraviolet radiation revealed no appreciable change and can be modeled by a straight horizontal line. The mean and standard deviation of the Knoop hardness value for each exposure level are given in Table 6.2. The hardness readings, H_K , ranged from 13.8 for the seven week specimens to 15.0 for the three week samples while the ten and twenty week tests fell

between these values. This behavior indicates that the indirectly exposed surfaces are not degraded from exposure to ultraviolet light. This conclusion is in agreement with several other studies claiming photodegradation to cause only surface changes [12-13].

Conversely, the surfaces exposed directly to ultraviolet radiation showed significant changes. The mean and standard deviation of the Knoop hardness number for the exposed surfaces are shown in Table 6.2. The hardness values, H_K , increased from 16.2 for the three week test to 20.6 for the twenty week test. This result shows a hardening on the exposed sides indicating surface embrittlement which also agrees with previously published reports [12-13].

All of the polycarbonate samples became yellow after exposure to ultraviolet radiation. Although the samples yellowed, the three, seven, and ten week specimens remained transparent causing no difficulty in obtaining a Knoop hardness measurement. The twenty week sample became opaque making it difficult to accurately measure the longer diagonal of the indentation resulting in possible experimental error. However, the mean hardness value for the exposed surface of the twenty week specimen was significantly larger than the hardness measurements for the other samples with a relatively small standard deviation indicating a definite increase in hardness.

The results of this study indicate that microhardness testing with a Knoop diamond-pyramidal indenter provides a good measure of the degradation that occurs in polycarbonate after exposure to ultraviolet radiation. The testing load of 25 grams was sufficient to obtain consistent hardness values with relatively small standard deviations. Preliminary testing was also conducted with larger loads, up to 200 grams, resulting in deeper indentations which is undesirable when testing a thin degraded surface layer.

REFERENCES

1. F. Ania, J. Martinez-Salazar, and F. J. Balta Calleja, "Physical aging and glass transition in amorphous polymers as revealed by microhardness", *Journal of Materials Science*, **24**, 2934-2938 (1989)
2. F. J. Balta Calleja, D. R. Rueda, J. Garcia Pena, F. P. Wolf, and V. H. Karl, "Influence of pressure and crystallization rate on the surface microhardness of high-density polyethylene", *Journal of Materials Science*, **21**, 1139-1144 (1986)
3. F. J. Balta-Calleja, "Dependence of micro-indentation hardness on the superstructure of polyethylene", *Colloid and Polymer Science*, **254**, 258-266 (1976)
4. J. Martinez Salazar and F. J. Balta Calleja, "Correlation of hardness and microstructure in unoriented lamellar polyethylene", *Journal of Materials Science*, **18**, 1077-1082 (1983)
5. F. J. Balta Calleja, C. Santa Cruz, C. Sawatari, and T. Asano, "New Aspects of the Microstructure of PE/iPP Gel Blends As Revealed by Microhardness: Influence of Composition", *Macromolecules*, **23**, 5352-5355 (1990)
6. C. Santa Cruz, F. J. Balta Calleja, H. G. Zachmann, N. Stribeck, and T. Asano, "Relating Microhardness of Poly(ethylene Terephthalate) to Microstructure", *Journal of Polymer Science: Part B: Polymer Physics*, **29**, 819-824 (1991)
7. F. J. Balta Calleja, C. Santa Cruz, R. K. Bayer, and H. G. Kilian, "Microhardness and surface free energy in linear polyethylene: The role of entanglements", *Colloid and Polymer Science*, **268**, 440-446 (1990)
8. D. R. Askeland, *The Science and Engineering of Materials, 2nd Edition*, Ch.6, PWS-KENT Publishing Company, Boston, 1989.
9. D. Tabor, *The Hardness of Metals*, p. 100, Oxford University Press, Amen House, London, 1951
10. B. L. Evans, "The microhardness of injection moulded polystyrene and polyethylene", *Journal of Materials Science*, **24**, 173-182 (1989)

11. J. Bowman and M. Bevis, "The evaluation of the structure and hardness of processed plastics by the Vicker's microhardness test", *Colloid and Polymer Science*, **255**, 954-966 (1977)
12. G. E. Schoolenberg, "A fracture mechanics approach to the effects of UV-degradation on polypropylene," *Journal of Materials Science*, **23**, 1580-1590 (1988)
13. G. E. Schoolenberg and P. Vink, "Ultraviolet degradation of polypropylene: 1. Degradation profile and thickness of the embrittled surface layer," *Polymer*, **32**, 432-437 (1991)
14. *TUKON Microhardness Tester Instruction Manual, Model 300*, Wilson Instruments, a division of SPM Inc., NY

TABLE 6.1

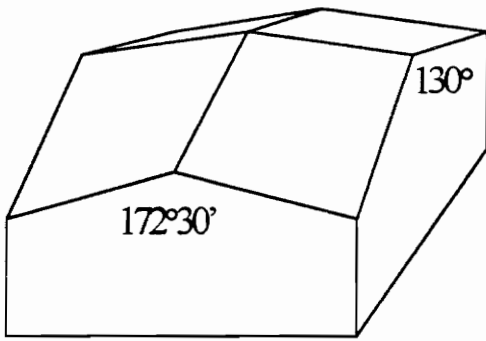
Tukon microhardness tester

<u>Manufacturer:</u>	WILSON INSTRUMENTS a division of Special Products Mfg. 6 Emma Street Binghamton, New York 13905-2508
<u>Model #:</u>	300 FM/DF
<u>Serial #:</u>	89715

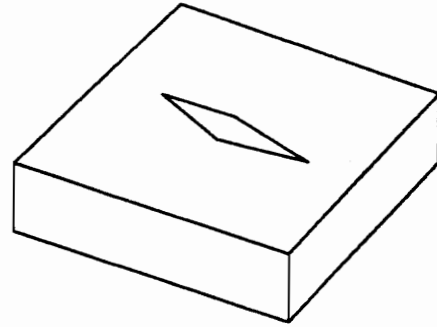
TABLE 6.2

Knoop hardness values

Exposure Time (Weeks)	Mean	Standard Deviation
Indirectly Exposed Surface		
3	15.0	0.1720
7	13.8	0.1356
10	14.5	0.3187
20	14.0	0.2332
Directly Exposed Surface		
3	16.2	0.1720
7	16.3	0.1939
10	17.1	0.3311
20	20.6	0.6248



(a)



(b)

FIGURE 6.1 (a) The Knoop microhardness diamond pyramidal indenter and (b) the Knoop micro-indentation [From D. Tabor, *The Hardness of Metals*, p. 100, Oxford University Press, Amen House, London, 1951]

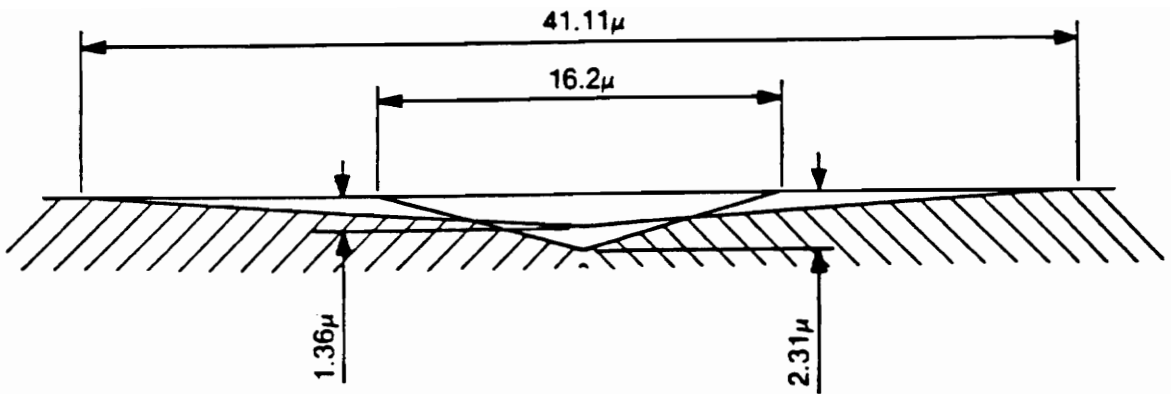


FIGURE 6.2 Comparison of Knoop and Vickers indentations using 100 gram load on hard steel (approximately C60); the Knoop is the shallow indentation. [From *TUKON Microhardness Tester Instruction Manual, Model 300*, Wilson Instruments, a division of SPM Inc., NY]

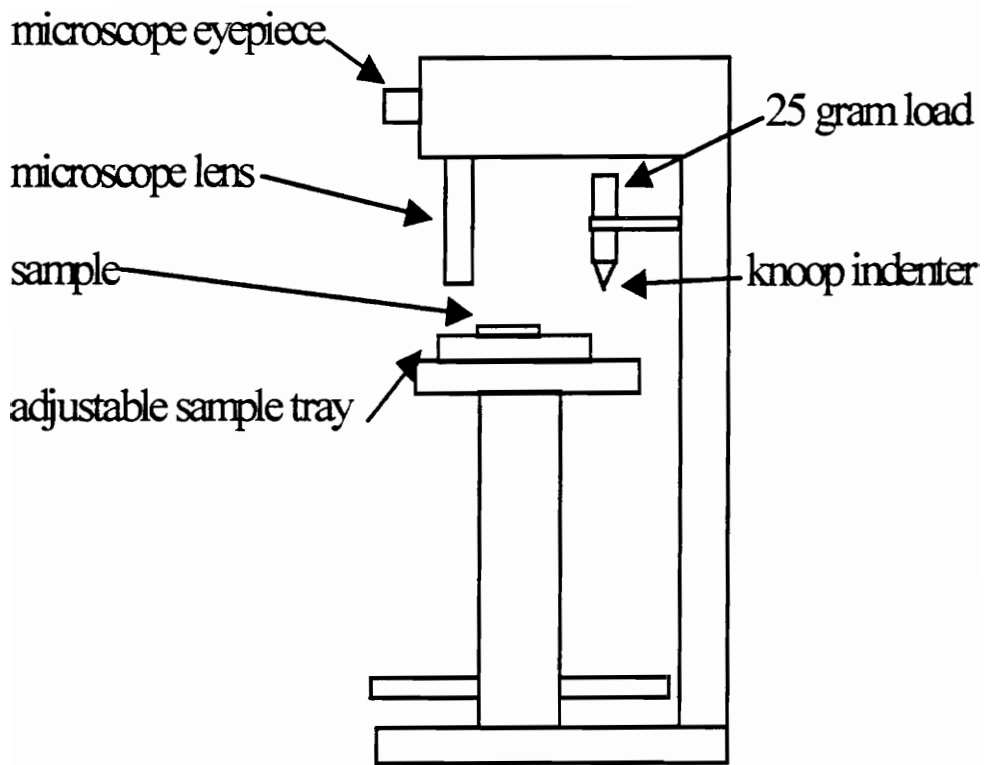


Figure 6.3 TUKON microhardness tester set-up.

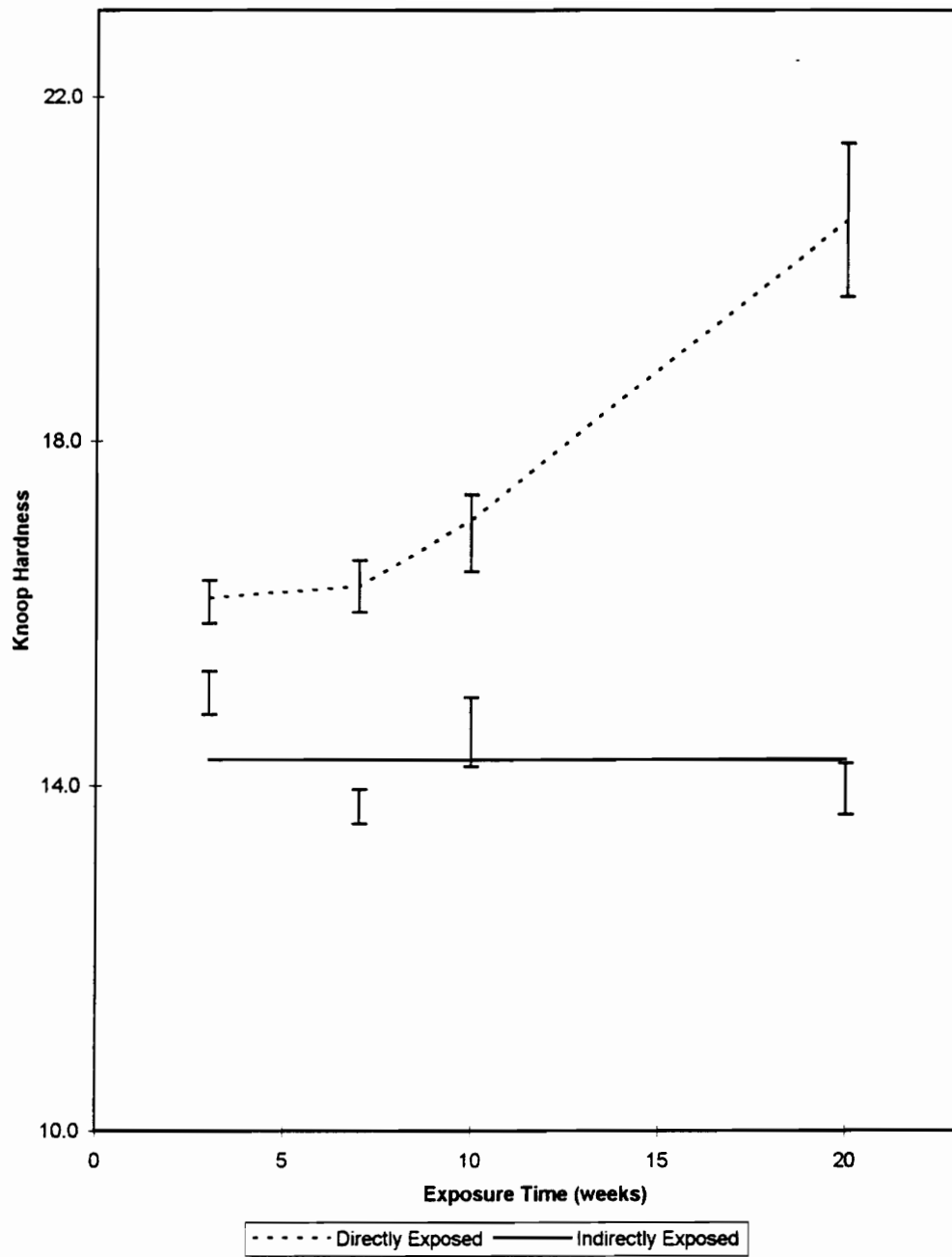


FIGURE 6.4 Knoop hardness value (H_K) versus exposure time of the indirectly and directly exposed surfaces

CHAPTER 7

EFFECT OF ULTRAVIOLET EXPOSURE ON THE IMPACT TOUGHNESS OF POLYCARBONATE

INTRODUCTION

Impact toughness is an important property to consider in this study since common problems associated with military aircraft include birdstrike and impact with debris and pollution. Also, a high-speed aircraft passing through a rain cloud impacts water droplets and hail that can cause some erosion of the polymer [1]. Polycarbonate has been chosen for aircraft transparencies because of its unusually high toughness characteristics at temperatures well below its glass transition temperature of 145 °C. One possible reason for this excellent quality is the presence of the OCO₂ group in the polymer chain which increases the bonding since it is harder to twist [2].

Impact toughness is a material property defined as the ability of a material to withstand impact loading [2]. Impact energy is related to the tensile strength and elongation at break for a given material. Theoretically, the toughness is the area under the load-deformation curve obtained in a tensile test and is proportional to the impact resistance [3]. The difference between impact loading and tensile loading is the rate at which the load is applied. In a tensile test the rate of straining is quite low so that the material is slowly stretched to failure. Valuable information on the impact properties of a material can be obtained from a high-speed tensile test [3]. In an impact test the specimen is loaded at a very fast rate. Although polycarbonate is a viscoelastic material, at the high speed obtained in impact loading it acts as an elastic material since the polymer chains are not given time to react.

In an impact test a stationary specimen, called the target, is commonly struck by a fast-moving projectile, called the striker. If the striker does not remain in the specimen, then the duration of contact between the material and striker can be on the order of

microseconds to milliseconds. Materials that experience ductile behavior in a tensile test may perform in a brittle manner during an impact test [2,5]. This brittle behavior is a result of the high rate of deformation that does not allow sufficient time for the polymer chains to move [2].

The behavior of impacted polymeric materials has been divided into three regions: (i) elastic, (ii) plastic, and (iii) hydrodynamic [6]. The material behaves elastically when the applied stresses remain below the yield point of the target material. Many mathematical models have been developed to describe elastic impact behavior, but most of these models are for semi-infinite bodies [7]. Plastic behavior results from impact loading with an applied stress above the yield point of the target material. Signs of plastic response include large deformations, heating, and sometimes failure of the material [6]. If the load is increased even further then the material behaves hydrodynamically. The pressures that are generated are several orders of magnitude larger than the strength of the material so that the behavior of the material can be treated as a fluid during the initial stages of impact [8]. The previous representation of impact behavior is for a general material. Since polycarbonate is a viscoelastic material, its impact behavior includes rate dependent and time dependent components.

One of the most important parameters in an impact test is the striking velocity. The minimum velocity that is required for the striker to perforate, or completely pierce, the target is called the ballistic limit. The velocity at impact has been divided into four regimes [8]: (i) low, (ii) medium, (iii) high, and (iv) ultra-high. The low-velocity region has been defined to fall below 250 m/s during which the local behavior of the target material is strongly connected to the total dimensions of the structure. The medium-velocity zone falls in the range of 500 to 2000 m/s when a small region in the vicinity of the impacted area behaves somewhat independently of the overall deformation of the structure. The high-velocity region is from 2000 to 3000 m/s in which the material experiences hydrodynamic behavior as described above [8]. The ultra-high regime covers

speeds greater than 12,000 m/s. At these speeds the energy is so large that an explosive vaporization of the material occurs [8].

A thorough analysis of the impact behavior of solids would include the geometry of the colliding bodies, wave propagation, finite deformations, hydrodynamic flow, work hardening, thermal and frictional effects, and induction and propagation of fracture in the impacting solids [8]. The complexity of impact behavior is the reason that the majority of the research conducted has been experimental in nature. This paper will concentrate on experimental results but will give an overview of wave propagation theory.

Wave Propagation

The two types of stress waves that will be discussed are dilatational (longitudinal) and distortional (transverse). A longitudinal wave is one in which the motion of the particles in the impacted material is normal to the wave front. The wave speed, c_L , of a longitudinal wave is given by the following equations [6]:

$$c_L^2 = \frac{E(1-\nu)}{\rho(1+\nu)(1-2\nu)} \text{ for extended media, and} \quad (1)$$

$$c_L^2 = \frac{E}{\rho} \text{ for bounded media,} \quad (2)$$

where E is Young's modulus, ν is Poisson's ratio, and ρ is the density of the impacted material. These equations should be used cautiously for viscoelastic materials such as polycarbonate since Young's modulus is strongly dependent on the temperature of testing, especially when the laboratory temperatures are near the glass transition region.

A shear wave is one in which the particles of the impacted material move parallel to the wave front. The wave speed, c_s , of a shear wave is given by [6]:

$$c_s^2 = \frac{E}{2\rho(1+\nu)} = \frac{G}{\rho} \quad (3)$$

where G is the shear modulus of the impacted material.

During the impact of two solids, initially a compression wave is generated immediately followed by a release wave. When the compression wave reaches a free boundary of the impacted material then another release wave is formed. Failure of the impacted material will begin if the combined effect of the tensile load intensity and duration goes beyond a certain critical value for the material [8].

Impact Failure

The target material can fail during impact loading through a variety of mechanisms. The definition of failure provided by ASTM is the presence of any crack or split created by the impact of the falling tup that can be seen by the naked eye under normal laboratory lighting conditions [9]. The modes of failure that will be discussed in this paper are spalling, fracture by initial stress wave, plugging, and petaling.

Spalling occurs when the initial compressive wave is reflected from the rear surface of a finite-thickness plate causing tensile failure. This mode of failure is common for intense loading conditions, especially in materials that are stronger in compression than in tension [8].

Fracture can also occur when the stress in the initial compressive stress wave surpasses the ultimate strength of the material. This mode of failure usually occurs in weak, low density materials [8].

Plugging failure is common when a blunt or hemispherical-nosed striker is used at a speed near the ballistic limit of the target material. During this mode of failure, an approximately cylindrical slug about the same diameter of the striker is formed [8].

Petaling is a mode of fracture resulting from high radial and circumferential tensile stresses following the initial stress wave. Petaling is common at low velocities when the target material is a thin plate and the striker is an ogival or conical bullet, or at speeds close to the ballistic limit with a blunt striker [8].

Impact Testing

Two of the most common types of impact tests are the swinging pendulum and drop-tower. Charpy and Izod are two types of swinging pendulum tests in which the striker is connected to a pendulum released from a position of high potential energy. The striker impacts a notched target specimen that is either supported on both ends or held in a cantilever style depending on the type of test [5, 10]. The breaking of the sample consumes a portion of the energy of the swinging pendulum. The distance that the pendulum swings beyond the sample location is a measure of the impact resistance of the target material.

The drop-tower impact test involves a striker, called a tup, that undergoes a free vertical drop along guide rods. The tup may be dropped from various heights with a constant weight or with varying weight from a constant height [9]. The goal of the drop-tower impact test is to determine the mean failure energy, which is defined as the energy required to cause 50% of the specimens to fail [9, 11].

EXPERIMENTAL DETAIL

Aircraft grade polycarbonate was investigated that was obtained from Rohm and Haas in Philadelphia, Pennsylvania. Drop-weight impact tests were conducted on material exposed to ultraviolet radiation in the QUV weathering device for periods of three, seven, ten, and twenty weeks.

The impact specimens were flat square plates that measured 4" × 4" × 0.118". They were held in place by a two-piece specimen clamp that with a three inch diameter hole as shown in Figure 7.1. The specimens were sandwiched between the lower stationary mount and the upper movable plate which was bolted to the lower mount with eight 1/4" - 28 hex head bolts. This configuration allowed for no noticeable slippage so that the specimens were fixed around the entire circumference of the three inch opening in the specimen clamp.

It has been noted in this paper that exposure to ultraviolet radiation degrades only a thin layer on the surface of the material (see chapter 4) [12-13]. To obtain consistent results, the sides of the specimens that were exposed directly to ultraviolet radiation were placed in the specimen clamp so that they were the upper surface during testing. The effect of placing the exposed surfaces on the bottom was not considered in this study.

The instrument that was used to measure the impact resistance of polycarbonate was the Dynatup 730 drop-tower impact tester. The striker, called a tup, was dropped from a constant height of 31 inches with a varying weight to change the amount of energy supplied to the system. This procedure was used instead of the constant weight/varying height method since changing the drop height significantly affects the velocity at impact while changing the weight does not [9]. Since the behavior of polycarbonate is extremely rate dependent then the constant height method eliminated the variable of strain rate.

The Bruceton Staircase Method was used to determine the mean failure energy which is defined as the energy required to cause 50% of the impact specimens to perforate [9]. The starting point was calculated from the area under the tensile stress-strain curve multiplied by the impact volume which was approximated to be 0.122 in³.

The Dynatup 730 is equipped with a light/timing device through which a metal strip, called a velocity flag, passes. As the flag passes through the light/timing device it blocks a beam of light for an amount of time dependent on the tup velocity. The velocity of the striker can be calculated with simple equations of motion if the width of the flag and the amount of time of light blockage is known. Since the motion of the striker is a

vertical, linear free-fall then the corresponding equation for the velocity, v , at any time, t , is given by

$$v = v_0 + g(t - t_0), \quad (4)$$

where v_0 is the velocity at an initial time chosen arbitrarily, g is the acceleration due to gravity, and t_0 is the arbitrary initial time [12]. If position 1 is where the beam of light is first blocked, and position 2 is where the beam of light first reappears, then Equation (4) can be written for these two velocities and v_0 can be eliminated to obtain

$$v_2 = v_1 + g(t_2 - t_1). \quad (5)$$

Since the known variables are the width of the flag, $x_2 - x_1$, and the time that the beam of light is blocked, $t_2 - t_1$, Equation (5) should be framed in terms of these quantities [12]. This can be accomplished by using the general equation of motion given by

$$x = x_0 + v_0(t - t_0) + \left(\frac{g}{2}\right)(t - t_0)^2. \quad (6)$$

If x_1 , t_1 , x_2 , and t_2 are substituted into Equation (6) for x and t and equated then the simplified result is

$$v_0 = \left\{ x_2 - x_1 + (g/2) \left[(t_1 - t_0)^2 - (t_2 - t_0)^2 \right] \right\} / (t_2 - t_1). \quad (7)$$

If the initial time, t_0 , is chosen to be at point 1 where the light beam is first blocked, then v_1 can be found from Equation (7) to be

$$v_1 = \frac{x_2 - x_1}{t_2 - t_1} + \frac{1}{2}g(t_2 - t_1). \quad (8)$$

If Equation (8) is substituted into Equation (5) then the velocity at the time that the light first reappears is given by

$$v_2 = \frac{x_2 - x_1}{t_2 - t_1} + \frac{1}{2}g(t_2 - t_1) = \frac{w_{flag}}{t_{block}} + \frac{g \times t_{block}}{2}, \quad (9)$$

where w_{flag} is the width of the velocity flag, t_{block} is the amount of time the beam of light is blocked by the velocity flag, and g is the acceleration due to gravity [12]. From the relation in Equation (5) the impact velocity can be calculated to be

$$v_{imp} = v_2 + g(t_{imp} - t_2), \quad (10)$$

where v_{imp} is the impact velocity and t_{imp} is the time of impact [12].

The absorbed energy at any time during impact can also be determined with the use of the impact velocity and the mass of the tup/weight system. Since the specimen is deformed during impact, the energy lost by the falling weight is transferred to the specimen to create a permanent deformation. The principle of conservation of total energy of the system requires that

$$E(t) = T(t) + V(t) + E_{abs}(t) = \text{constant}, \quad (11)$$

where $E(t)$ is the total energy of the system, $T(t)$ is the kinetic energy at time t , $V(t)$ is the potential energy at time t , and $E_{abs}(t)$ is the absorbed energy of the hammer- specimen

system at time t [12]. If the initial time is chosen to be the time at impact and the initial position to be the position of impact then the potential energy and absorbed energy are both zero and the absorbed energy at any time is given by

$$E_{\text{abs}}(t) = T(0) - T(t) - V(t) = \frac{1}{2} m (v_{\text{imp}}^2 - v(t)^2) + mgx(t), \quad (12)$$

where $E_{\text{abs}}(t)$ is the absorbed energy at time t , m is the mass of the hammer/tup system, v_{imp} is the impact velocity, $v(t)$ is the velocity at time t , g is the acceleration due to gravity, and $x(t)$ is the position at time t [12].

A drop-tower apparatus was used instead of the common swinging pendulum type since the exposed material contains a thin degraded layer on the surface of the specimens. The specimen for the swinging pendulum impact test is commonly notched which would result in a characterization of the core material instead of the brittle surface material [13].

RESULTS AND DISCUSSION

Kulshreshtha [14] claims that degradation causes the polymer chain to break down into smaller fragments which causes the material to become brittle since the smaller fragments do not contribute to the mechanical properties of the material. Although ultraviolet radiation degrades only a thin surface layer [14] the toughness of the entire material is affected [15]. So and Broutman [15] found that after applying a thin brittle coating to normally ductile material, the impact strength dropped. Polymers that have experienced degradation tend to lose some of the toughness because of the break-down of the polymer chain and embrittlement of the surface layer. This tendency has been observed by several researchers after weathering trials of polymers [16-19].

The impact load and impact energy are both measured during the entire duration of the impact test by the Dynatup 730 drop-weight impact tester. Figure 7.2 shows a typical output of the Dynatup 730 data analysis program.

All of the perforated specimens failed by plugging. An approximately cylindrical plug about the same diameter as the tup detached from the specimens. The mean failure energy for all of the impact specimens are plotted against the duration of exposure in Figure 7.3 at the end of this chapter. A range of values are shown since the incremental weight increase or decrease was approximately 2.25 lb. The mean failure energy decreased from approximately 860 in-lb for the unexposed specimens to about 500 in-lb for the samples that were exposed for ten weeks. The mean failure energy then increased to about 580 in-lb for the twenty week tests.

This increase in impact strength after the longest exposure trial is in agreement with previously reported data which showed improved mechanical properties after very long exposure periods [19, 21]. Sherman and co-workers [19] found that after long periods of exposure that the surface of polycarbonate samples flaked off causing a partial recovery of the mechanical properties. Similarly Schoolenberg and coworkers [21] observed that the fracture energy initially decreased but after long degradation times experienced an increase in the fracture strength which they attributed to multiple cracking.

The polycarbonate samples in this study showed no visible signs of surface flaking or multiple cracking. The only difference in appearance of the twenty week samples compared to the other samples was a loss of transparency. The most logical explanation for the increase in fracture energy after twenty weeks of exposure is that the chain segments in the degraded surface layer became too weak to transmit forces to the inner undegraded material resulting in partial recovery of the impact strength.

The load on the tup was measured by the Dynatup 730 during the duration of impact. Figure 7.4 shows the maximum load attained during contact of the striker with the target as determined by the Dynatup data analysis program versus exposure time for an impact energy of 822 in-lb. All of the specimens at this energy were perforated except

for the unexposed polycarbonate. The maximum load decreased from 1640 lb for the unexposed surface to 1420 lb for the seven week sample. The curve then increased to a value of 1530 lb for the specimen that was exposed for twenty weeks showing a partial recovery of the material that began after seven weeks of exposure.

The deflection of the specimens during impact was also recorded by the Dynatup 730. Figure 7.5 shows a plot of maximum deflection versus exposure time for an impact energy of 822 in-lb. The maximum deflection decreased from 0.994 inches for the unexposed material to 0.800 inches for the seven week samples. The curve then increased to a final value of 0.976 inches for the twenty week specimen. The same partial recovery as mentioned above is seen in the deflection data beginning after seven weeks of exposure to ultraviolet radiation.

The impact load is plotted against deflection in Figure 7.6 for an impact energy of 822 in-lb. It can be seen that the unexposed specimen did not perforate but did experience plastic deformation. Figure 7.6 also records the partial recovery mentioned above showing that the impact behavior of the twenty week sample is very similar to the behavior of the three week sample.

The starting point for impact energy at each exposure level was determined from the area under the stress-strain diagram obtained from tension testing. The stress-strain curves for the five levels of exposure are shown in Figure 7.7 through Figure 7.11. The areas under the curves, or toughness per unit volume, was calculated by multiplying the number of rectangles by the area of the rectangle which was

$$A_{rect} = (1000lb / in^2) \times (0.05in / in). \quad (13)$$

The estimated impact energy was then calculated by multiplying the area under the curve by the approximate impact volume which was found by

$$V_{imp} = \frac{\pi}{4} \times (1.15in)^2 \times (0.118in) = 0.122in^3 \quad (14)$$

where the diameter of impact was approximated to be 1.15 inches and the thickness of the specimens was 0.118 inches. The calculated impact energy and mean failure energy are plotted against exposure time in Figure 7.12. It is shown that the calculated impact energy correlates well with the experimental data for the unexposed, three week, and seven week specimens but does not relate well with the ten and twenty week samples.

The conclusions from the impact data are that a partial recovery occurs after long period of exposure. In general, the samples exposed for twenty weeks behave very similarly under impact loading to the specimens exposed for three weeks. This is probably a result of such a large number of bonds being broken on the surface of the specimens that were exposed for twenty weeks that the degraded surface layer did not possess enough strength to transmit stress to the unaffected core material.

Drop-tower impact testing proved to be an excellent method of characterizing the impact behavior of polycarbonate that had been exposed to ultraviolet radiation. Another possible technique of measuring the impact behavior is the air gun impact test. The air gun provides a much higher rate of impact which would better model impact of windshield-canopy structures on high-speed military aircraft.

One method of modifying the impact behavior of polycarbonate that several researchers have investigated is polymer blending [20-24]. Several properties need to exist in the polymer blend to be feasible for use in military aircraft transparencies. The blending agent and polymer would need to possess both chemical and strain compatibility in all of the operating conditions. The blend would also need to be transparent as to not impair the vision of the pilot. The effects of ultraviolet radiation on the polymer blend would also need to be considered since the amount of degradation would be different for the blend.

REFERENCES

1. J. A. Zukas in "Limitations of Elementary Wave Theory", Chapter 2 of *Impact Dynamics*, J. A. Zukas, T. Nicholas, H. F. Swift, L. B. Greszczuk, and D. R. Curran, John Wiley & Sons, NY, 1982
2. D. R. Askeland, *The Science and Engineering of Materials, 2nd Edition*, Ch.6, PWS-KENT Publishing Company, Boston, 1989.
3. A. Davis and D. Sims, *Weathering of Polymers*, p. 88, Applied Science Publishers, London, 1983.
4. J. M. Margolis, *Engineering Thermoplastics: Properties and Applications*, Ch. 3, Marcel Dekker, Inc., NY, 1985
5. N. E. Dowling, *Mechanical Behavior of Materials*, p.5, Prentice Hall, Englewood Cliffs, NJ, 1993
6. J. A. Zukas in "Stress Waves in Solids", Chapter 1 of *Impact Dynamics*, J. A. Zukas, T. Nicholas, H. F. Swift, L. B. Greszczuk, and D. R. Curran, John Wiley & Sons, NY, 1982
7. S. Timoshenko and J. N. Goodier, *Theory of Elasticity, 2nd Edition*, p. 85, McGraw-Hill Book Company, NY, 1951
8. J. A. Zukas in "Penetration and Perforation of Solids", Chapter 5 of *Impact Dynamics*, J. A. Zukas, T. Nicholas, H. F. Swift, L. B. Greszczuk, and D. R. Curran, John Wiley & Sons, NY, 1982
9. ASTM Standard D3029-93, "Standard Test Methods for Impact Resistance of Flat, Rigid Plastic Specimens by Means of a Tup (Falling Weight)", *Annual Book of ASTM Standards*, Vol. 08.01, p.235.
10. L. H. Sperling, *Introduction to Physical Polymer Science, 2nd Edition*, pp. 517-519, John Wiley & Sons, Inc., NY, 1992
11. R. P. Brown, *Handbook of Plastics Test Methods, 2nd Edition*, Ch. 8, George Godwin Limited, London, 1981

12. G. E. Schoolenberg, "A fracture mechanics approach to the effects of UV-degradation on polypropylene," *Journal of Materials Science*, **23**, 1580-1590 (1988)
13. G. E. Schoolenberg and P. Vink, "Ultraviolet degradation of polypropylene: 1. Degradation profile and thickness of the embrittled surface layer," *Polymer*, **32**, 432-437 (1991)
14. *Dynatup 730 Instruction Manual*, Appendix 4, pp. 90-93
15. J. R. White and A. Turnbull, "Review Weathering of polymers: mechanisms of degradation and stabilization, testing strategies and modelling," *Journal of Materials Science*, **29**, 584-613 (1994)
16. A. K. Kulshreshtha, "Chemical Degradation", *Handbook of Polymer Degradation*, p. 55, S. H. Hamid, M. B. Amin, and A. G. Maadhah, eds. Marcel Dekker, Inc. NY (1992)
17. P. So and L. J. Broutman, "The effect of Surface Embrittlement on the Mechanical Behavior of Rubber-Modified Polymers," *Polymer Engineering and Science*, **22**, 888-894 (1982)
18. M. M. Qayyum and J. R. White, "Weathering of injection-moulded glassy polymers: Changes in residual stress and fracture behaviour," *Journal of Materials Science*, **20**, 2557-2574 (1985)
19. E. S. Sherman, A. Ram, and S. Kenig, "Tensile Failure of Weathered Polycarbonate," *Polymer Engineering and Science*, **22**, 457-465 (1982)
20. A. J. Hill, K. J. Heater, and C. M. Agrawal, "The Effects of Physical Aging in Polycarbonate," *Journal of Polymer Science: Part B: Polymer Physics*, **28**, 387-405 (1990)
21. G. E. Schoolenberg and H. D. F. Meijer, "Ultraviolet degradation of polypropylene: 2. Residual strength and failure mode in relation to the degraded surface layer," *Polymer*, **32**, 438-444 (1991)
22. C. Cheng, A. Hiltner, E. Baer, P. R. Soskey, and S. G. Mylonakis, "Deformation of Rubber-Toughened Polycarbonate: Macroscale Analysis of the Damage Zone", *Journal of Applied Polymer Science*, **52**, 177-193 (1994)

23. C. Cheng, N. Peduto, A. Hiltner, E. Baer, P. R. Soskey, and S. G. Mylonakis, "Comparison of Some Butadiene-Based Impact Modifiers for Polycarbonate", *Journal of Applied Polymer Science*, **53**, 513-525 (1994)
24. H. Kanai, V. Sullivan, and A. Auerbach, "Impact Modification of Engineering Thermoplastics", *Journal of Applied Polymer Science*, **53**, 527-541 (1994)
25. Z.-L. Liao and F.-C. Chang, "Mechanical Properties of the Rubber-Toughened Polymer Blends of Polycarbonate (PC) and Poly (Ethylene Terephthalate) (PET)", *Journal of Applied Polymer Science*, **52**, 1115-1127 (1994)
26. T. W. Cheng, H. Keskkula, and D. R. Paul, "Thermal Aging of Impact-Modified Polycarbonate", *Journal of Applied Polymer Science*, **45**, 531-551 (1992)

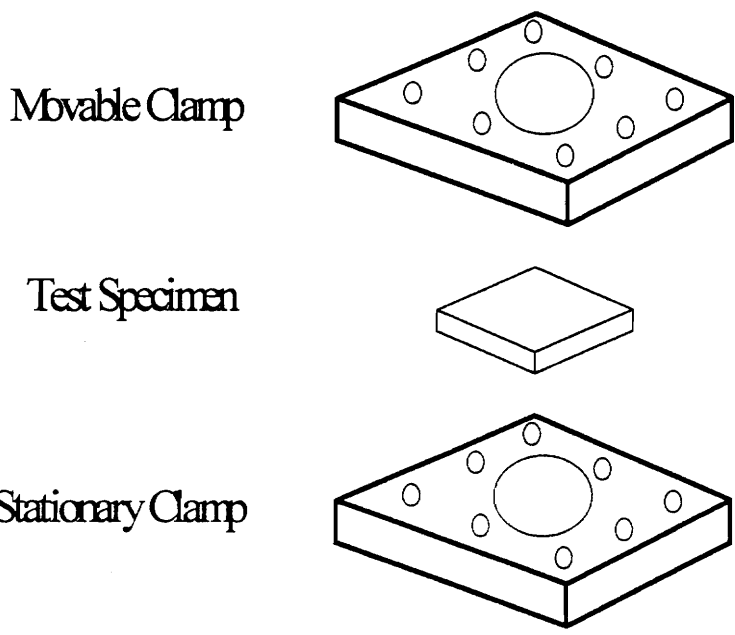


FIGURE 7.1 Drop dart impact test two-piece specimen clamp and test specimen.

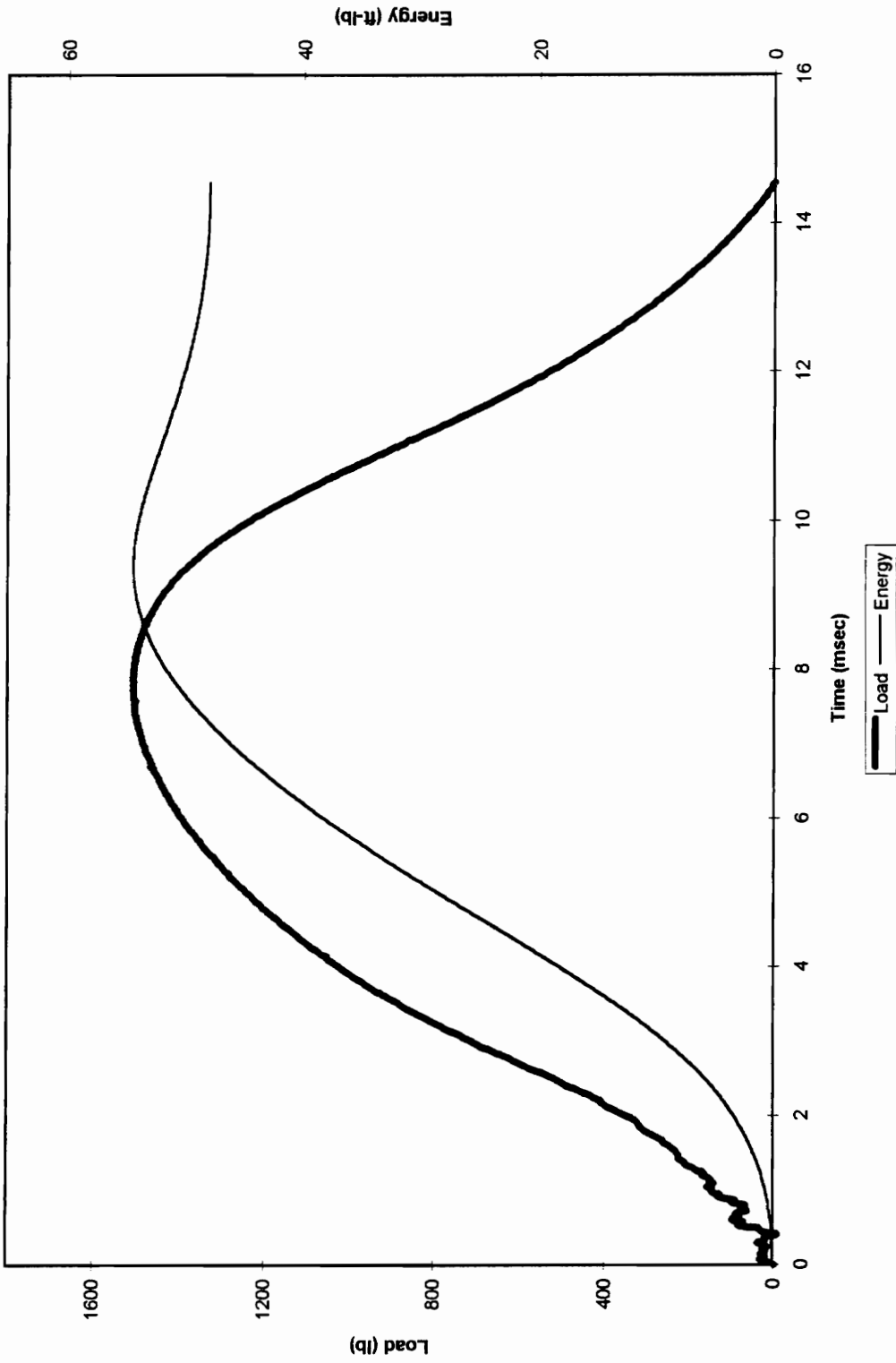


FIGURE 7.2 Load and energy of polycarbonate during drop-weight impact testing versus time as recorded by the Dynatup 730 drop-weight impact tester

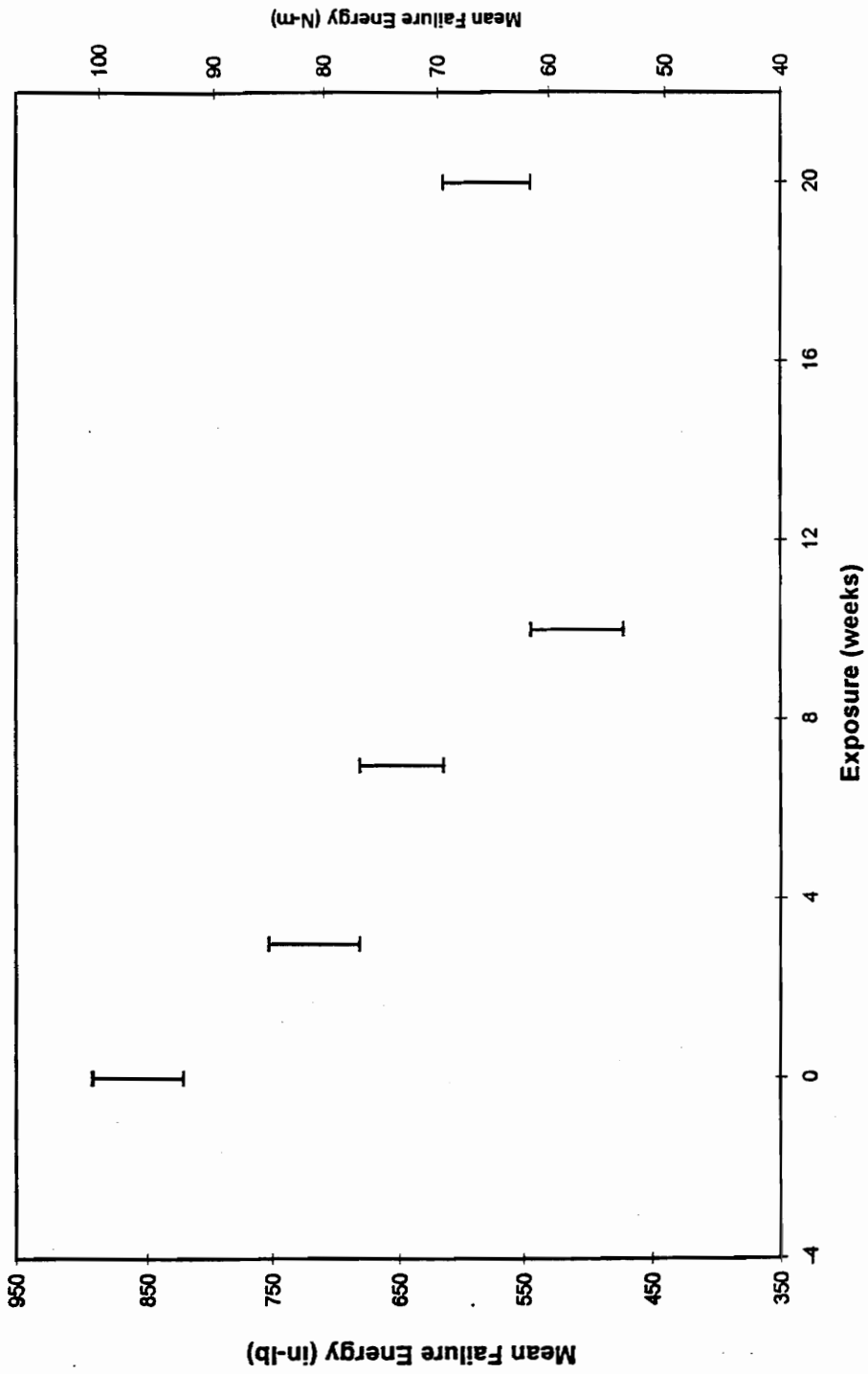


FIGURE 7.3 Mean failure energy versus exposure time

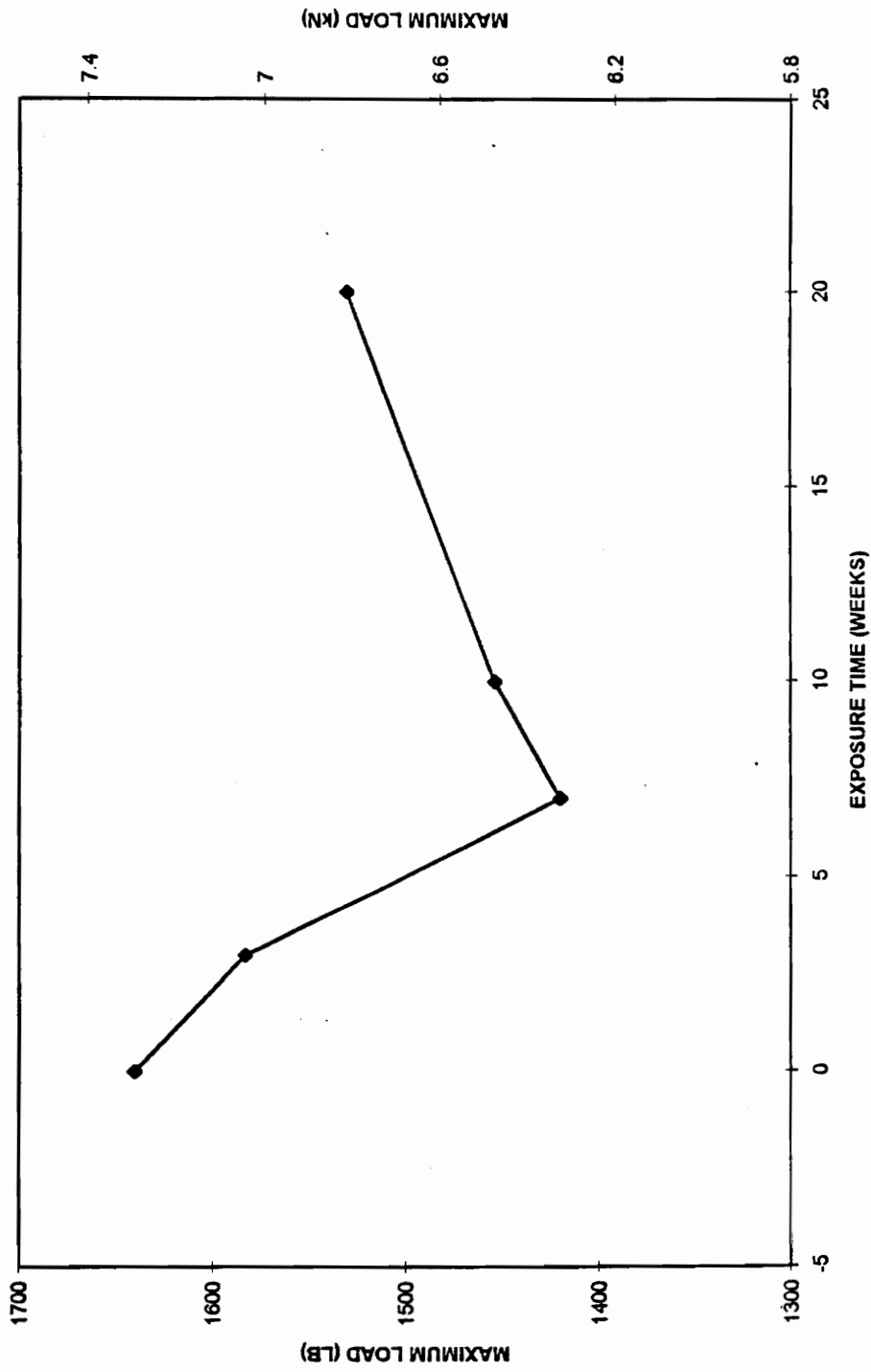


FIGURE 7.4 Maximum load of polycarbonate during impact contact versus weeks of exposure to ultraviolet radiation

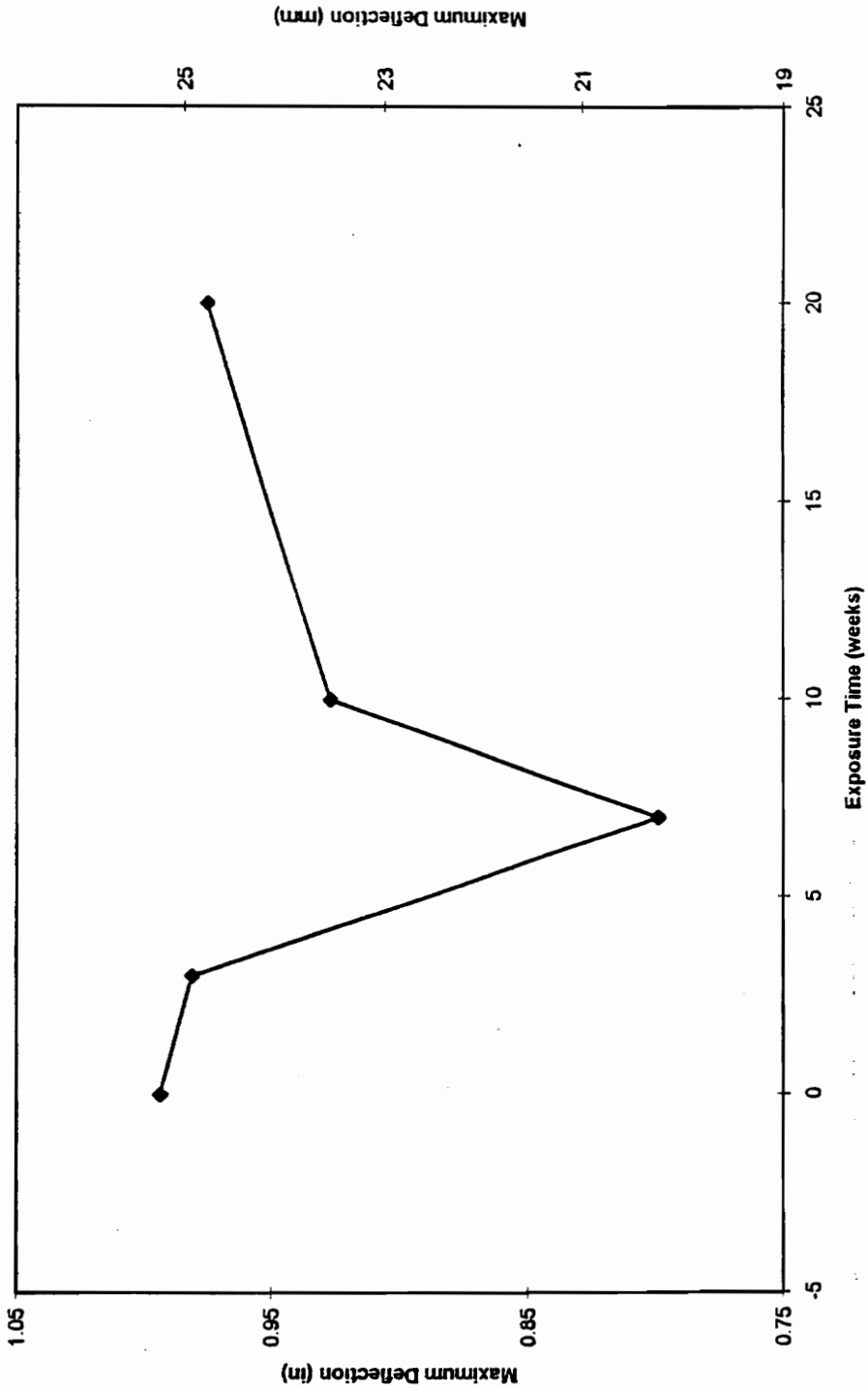


FIGURE 7.5 Maximum deflection of polycarbonate during impact contact versus weeks of exposure to ultraviolet radiation

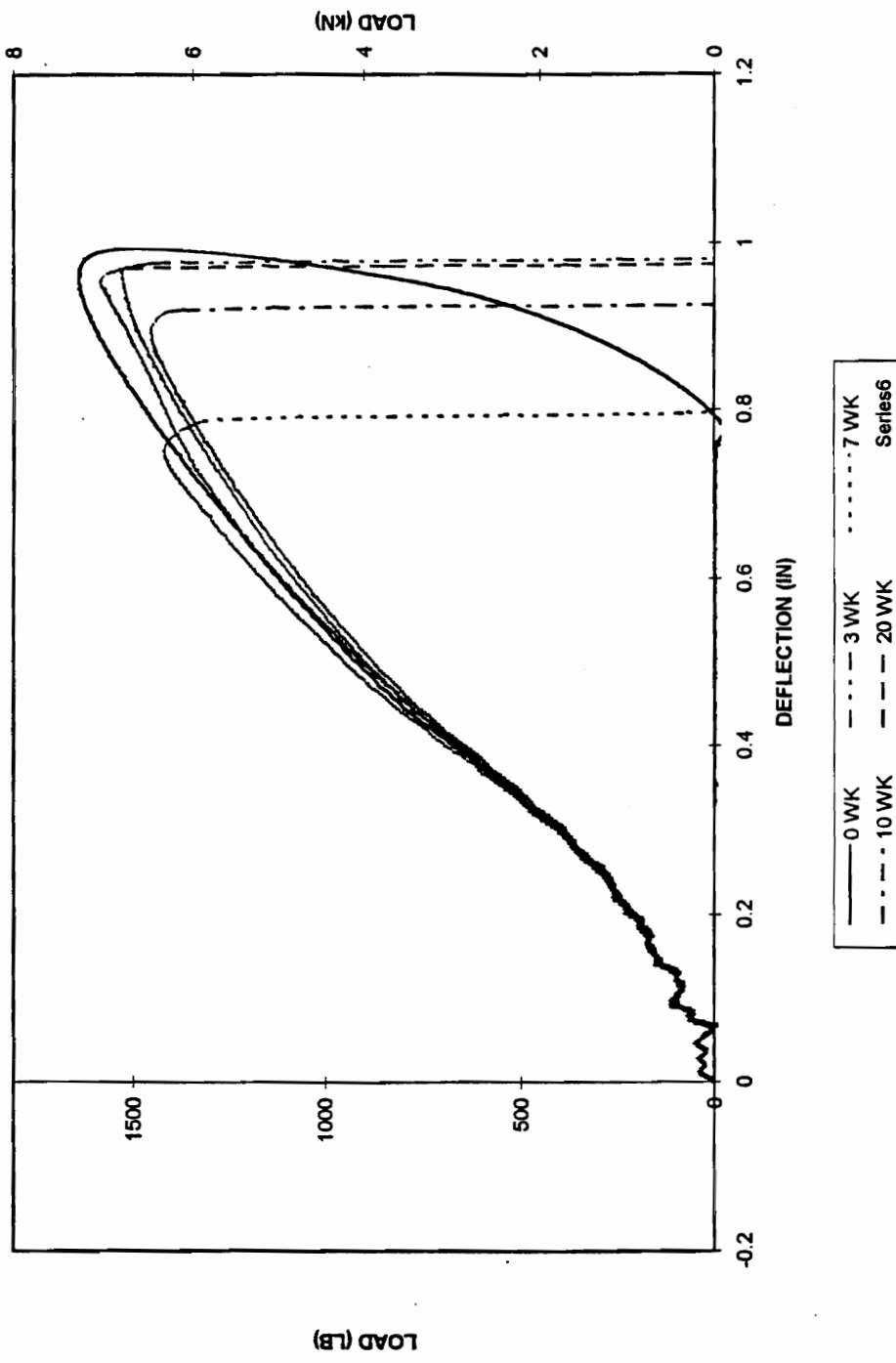


FIGURE 7.6 Contact load of polycarbonate with striker versus deflection during impact contact

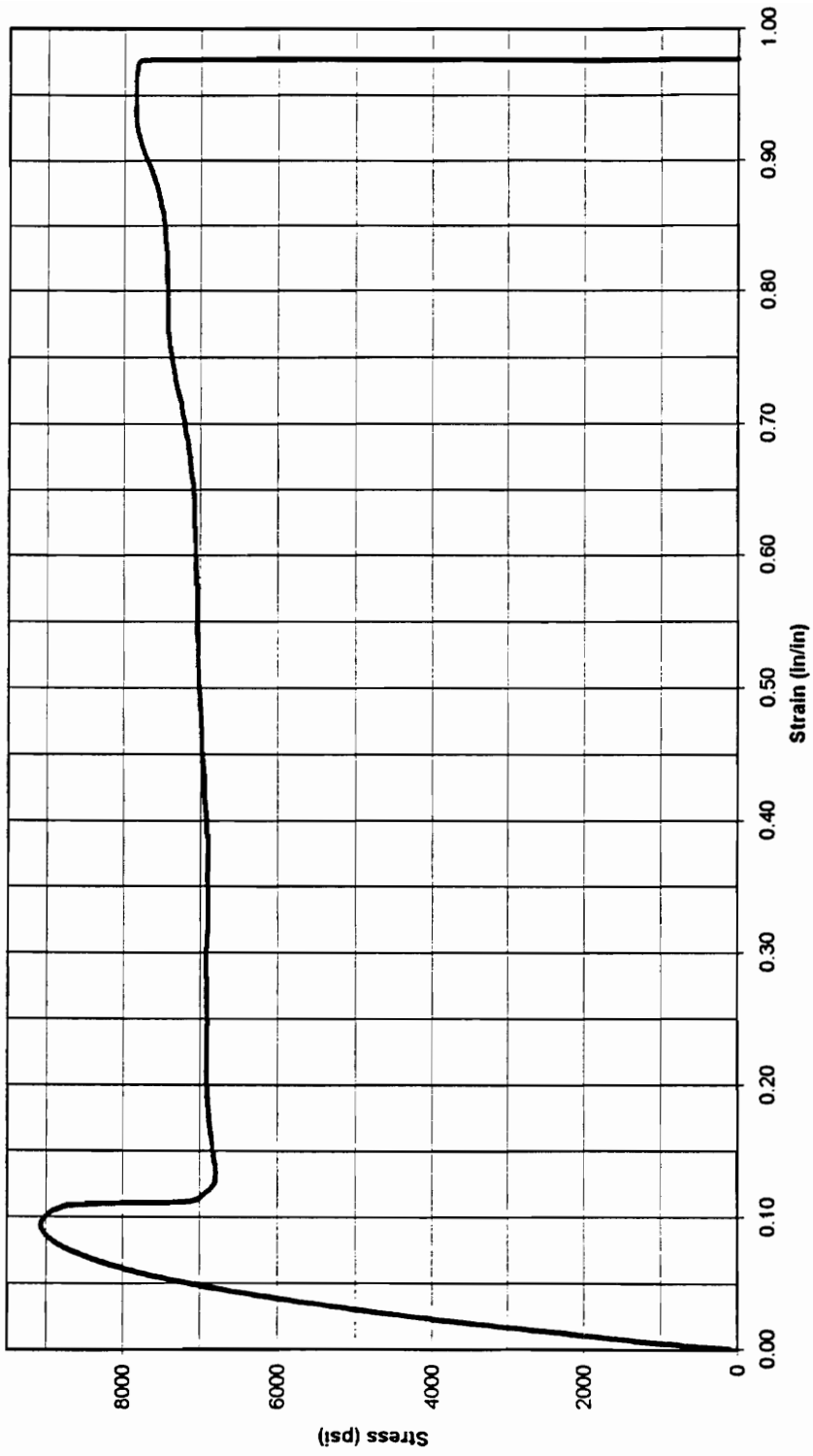


FIGURE 7.7 Stress-strain diagram of unexposed polycarbonate

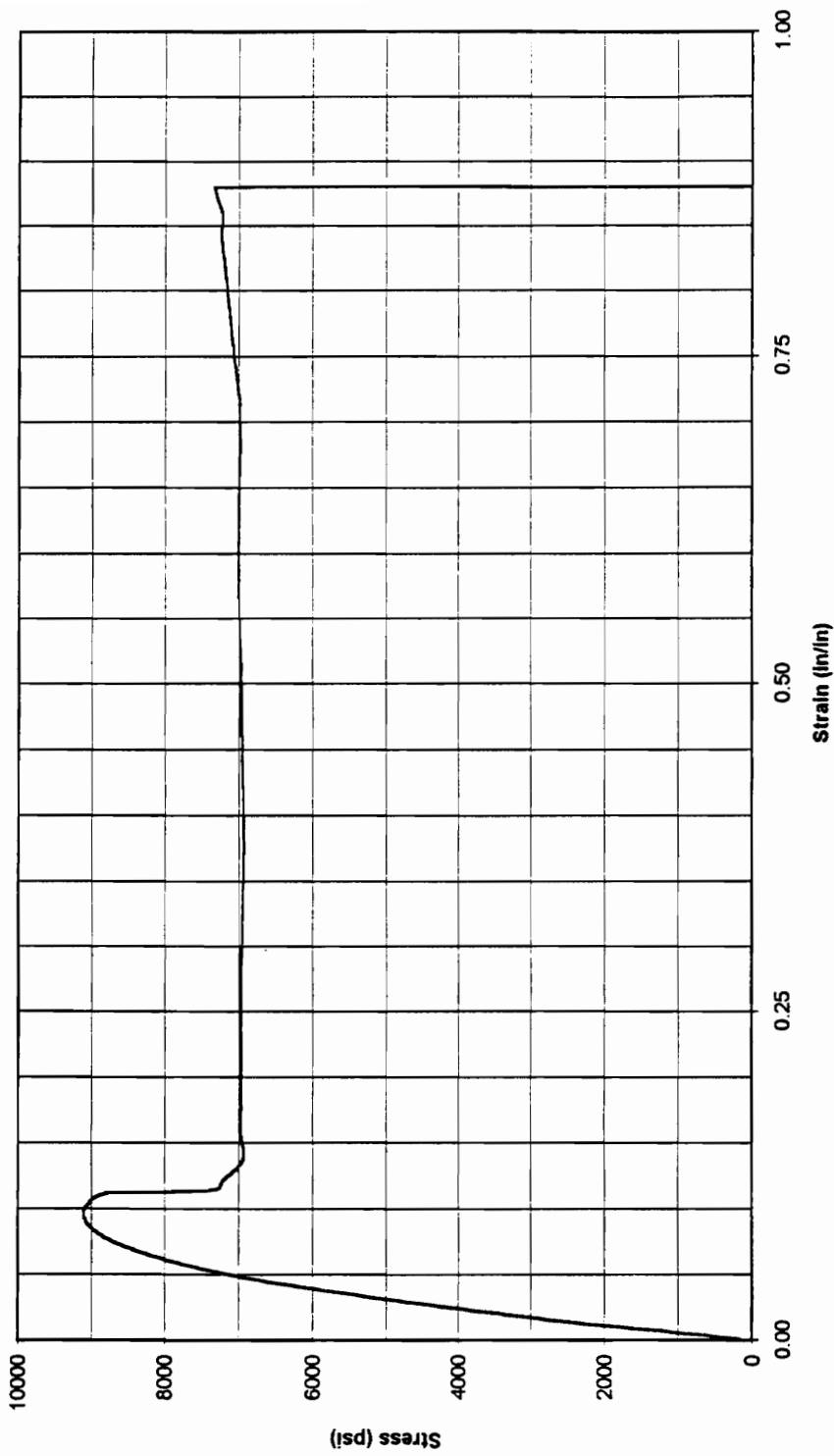


FIGURE 7.8 Stress-strain diagram of polycarbonate exposed to ultraviolet radiation for three weeks

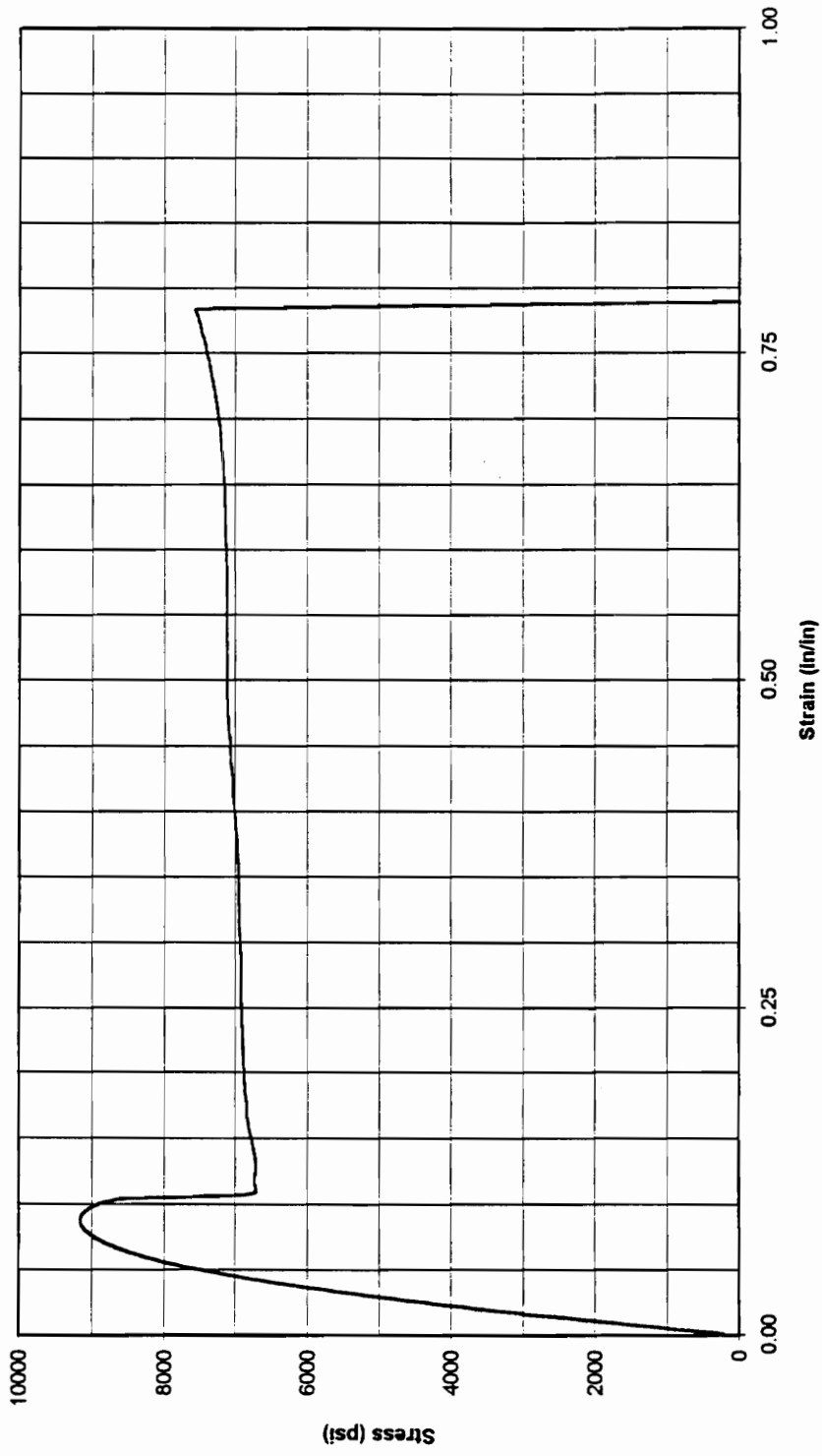


FIGURE 7.9 Stress-strain diagram of polycarbonate exposed to ultraviolet radiation for seven weeks

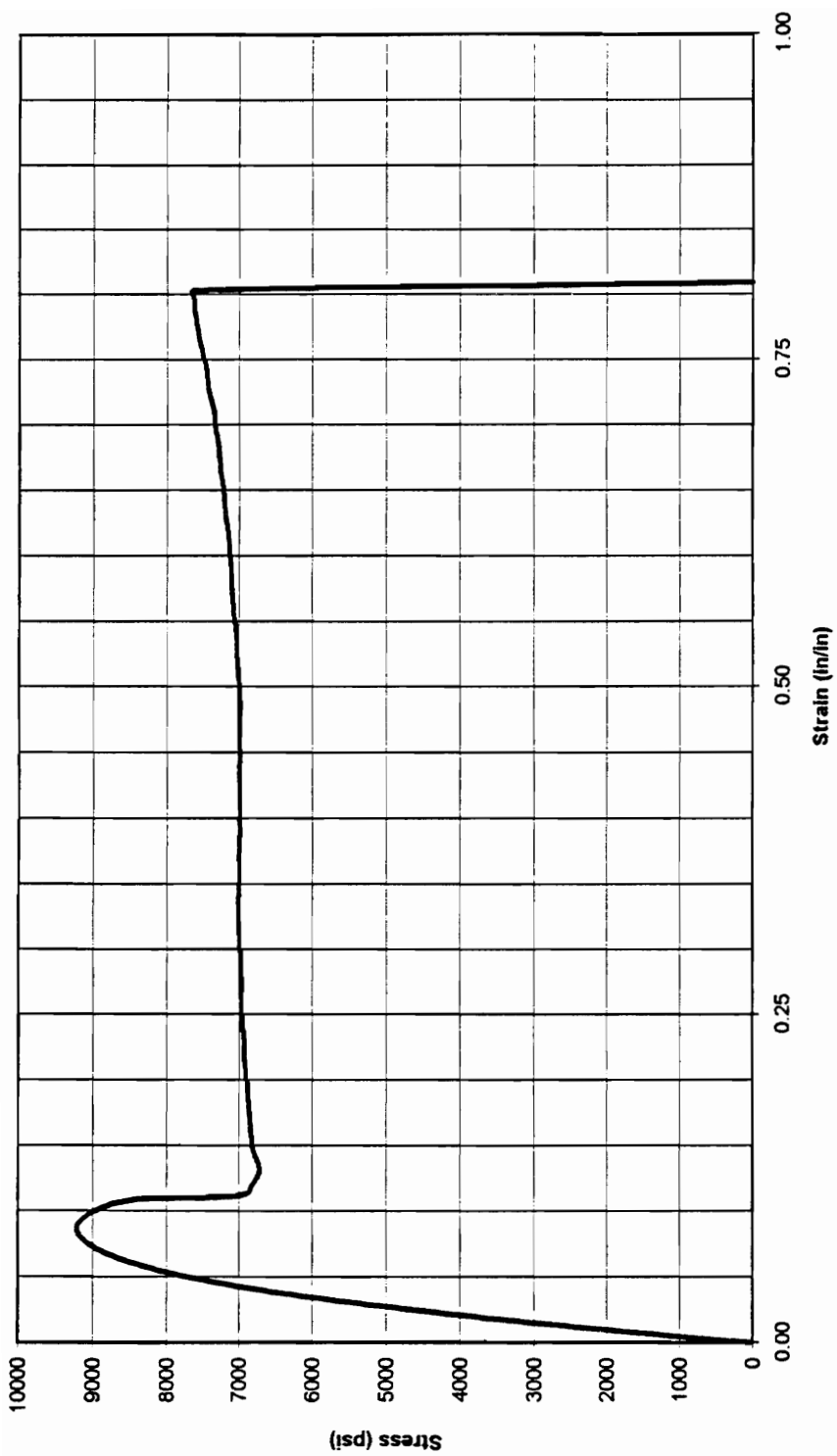


FIGURE 7.10 Stress-strain diagram of polycarbonate exposed to ultraviolet radiation for ten weeks

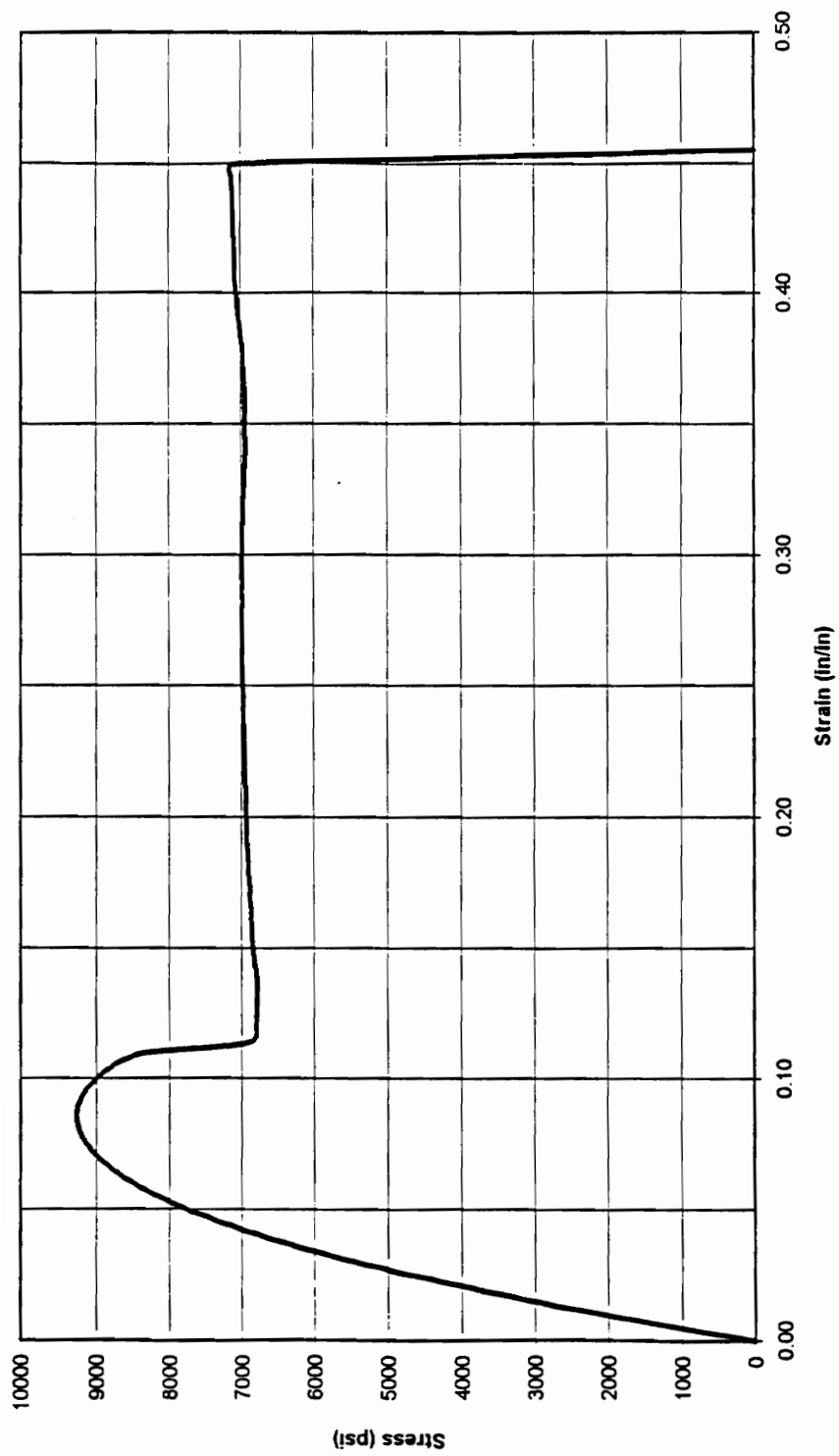


FIGURE 7.11 Stress-strain diagram of polycarbonate exposed to ultraviolet radiation for twenty weeks

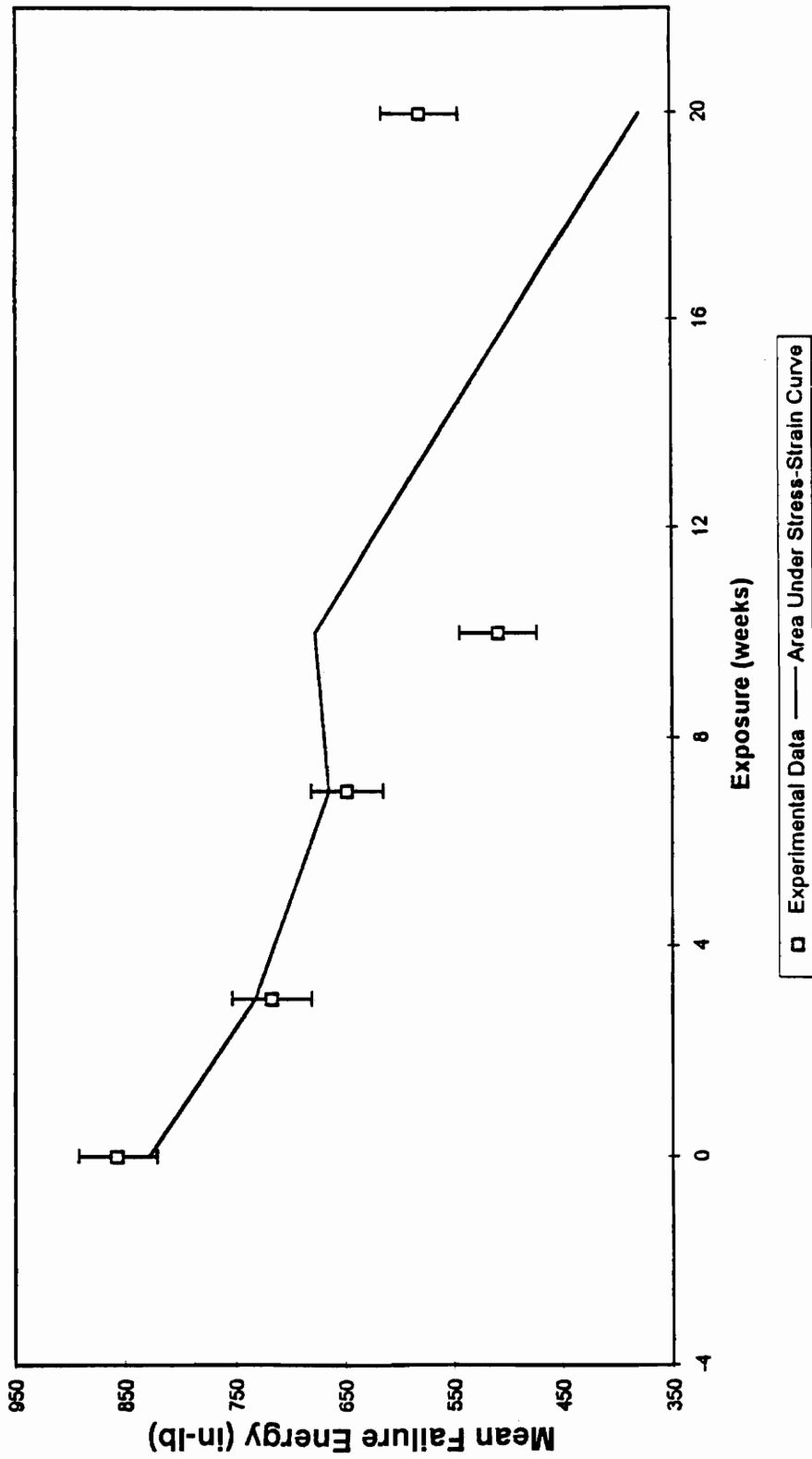


FIGURE 7.12 Mean failure energy and calculated impact energy versus weeks of ultraviolet exposure

CHAPTER 8
CONCLUSIONS AND RECOMMENDATIONS

CONCLUSIONS

- 1) Dynamic mechanical analysis on thin specimens revealed that the storage modulus increased significantly during exposure to ultraviolet radiation indicating an embrittlement or hardening of polycarbonate.
- 2) Exposure of polycarbonate to ultraviolet light caused a reduction in ductility at intermediate levels of exposure followed by a slight increase after the longest exposure periods.
- 3) The true fracture stress of the exposed polycarbonate decreased by about 12% after twenty weeks of exposure to ultraviolet radiation indicating a weakening of the material. This weakening is caused by bonds near the surface of polycarbonate being broken by the energy supplied by ultraviolet radiation.
- 4) The tension specimen surfaces directly exposed to ultraviolet radiation experienced excessive cracking while the surfaces indirectly exposed did not crack. This result indicates that only a thin surface layer of polycarbonate undergoes photodegradation by ultraviolet exposure.
- 5) The average relative molecular weight of polycarbonate decreased by more than 30% after only seven weeks of ultraviolet exposure indicating the occurrence of bond breaking (chain scission).
- 6) The microhardness of the surfaces directly exposed to ultraviolet radiation increased by approximately 27% after exposure to ultraviolet radiation while the microhardness of the indirectly exposed surfaces remained relatively constant. This increase agrees with the previously reported conclusions of surface embrittlement and hardening after exposure to ultraviolet light.

- 7) The mean failure energy measured by drop dart impact tests decreased by almost 42% for samples exposed to ultraviolet radiation for intermediate durations. It then recovered 16% of the impact resistance after longer exposure times. The surface of polycarbonate experienced chain scission causing embrittlement creating an ideal condition for crack initiation which was seen by the reduction in impact resistance at the intermediate levels. After longer exposure periods the thin degraded surface layer became too weak to transmit forces to the undegraded inner material resulting in partial recovery.
- 8) As mentioned briefly in Chapter 7, the specimens that were exposed to ultraviolet light for twenty weeks became opaque. If no other reason exists to remove the transparency from service before loss of transparency occurs then the maximum service life is determined where polycarbonate becomes opaque causing the vision of the pilot to be impaired. This study determined that the loss of transparency occurs at some point between ten and twenty weeks of exposure to ultraviolet radiation in the QUV weathering chamber.

RECOMMENDATIONS FOR FUTURE WORK

- 1) A study should be conducted to correlate the results from artificial laboratory exposure with weathering in the natural service environment of the windshield canopy system.
- 2) Since the main cause for removal of aircraft transparencies is surface scratches then abrasion tests should be performed to determine whether exposure to ultraviolet radiation decreases the scratch resistance of polycarbonate.
- 3) High velocity air gun impact testing could be used to more closely model the impact experienced by high-speed military aircraft.

- 4) Other methods should be investigated to determine the effect of ultraviolet exposure on the glass transition temperature of the surface layer of polycarbonate since the DMA technique possesses too many size limitations on test specimens.
- 5) A fracture mechanics approach should be used to study the fracture of exposed polycarbonate since cracks initiating in the degraded surface layer ultimately determine failure.
- 6) Polymer alloying should be investigating to develop a transparent material with improved ultraviolet stability and impact resistance.
- 7) Positron annihilation lifetime spectroscopy experiments should be conducted to determine the changes in free volume caused by exposure to ultraviolet radiation.

VITA

Stephen Brett Clay was born to Jim and Sharon Clay on December 12, 1969 in Huntington, West Virginia. He graduated from high school in 1988 at Barboursville High School in Barboursville, West Virginia.

Upon graduation from high school, Mr. Clay enrolled at West Virginia Institute of Technology in Montgomery, West Virginia. He graduated Summa Cum Laude with a Bachelor of Science Degree in Mechanical Engineering in 1992. He went on to work at INCO Alloys International in Huntington, West Virginia as a laboratory technician.

In the fall of 1993 Mr. Clay entered the Palace Knight program as a civilian employee of the United States Air Force. His first duty was to enroll as a Master of Science candidate in the Engineering Science and Mechanics Department at Virginia Polytechnic Institute and State University.

Mr. Clay is married to the former Terry Aretta Legg of Barboursville, West Virginia. They plan to live in the Dayton, Ohio area where he will work as a mechanical engineer at Wright Laboratory in Wright Patterson Air Force Base, Ohio. They are expecting their first child in September 1995.

The most important aspect of Mr. Clay's life is God. After he becoming a Christian as a young child he became a member of Antioch Baptist Church in Ona, West Virginia. He is currently attending Gateway Baptist Church in Blacksburg, Virginia where he enjoys helping in the college and bus ministries.